

The UMAP Journal

Publisher
COMAP, Inc.

Executive Publisher
Solomon A. Garfunkel

Editor
Paul J. Campbell
Campus Box 194
Beloit College
700 College St.
Beloit, WI 53511-5595
campbell@beloit.edu

On Jargon Editor
Yves Nievergelt
Department of Mathematics
Eastern Washington University
Cheney, WA 99004
ynievergelt@ewu.edu

Reviews Editor
James M. Cargal
P.O. Box 210667
Montgomery, AL 36121-0667
JMCargal@sprintmail.com

Development Director
Laurie W. Aragón

Production Manager
George W. Ward

Project Manager
Roland Cheyney

Copy Editors
Seth A. Maislin
Pauline Wright

Distribution Manager
Kevin Darcy

Production Secretary
Gail Wessell

Graphic Designer
Daiva Kiliulis

Vol. 20, No. 3

Associate Editors

Don Adolphson
Ron Barnes
Arthur Benjamin
James M. Cargal
Murray K. Clayton
Courtney S. Coleman
Linda L. Deneen
James P. Fink
Solomon A. Garfunkel
William B. Gearhart
William C. Giauque
Richard Haberman
Charles E. Liener
Walter Meyer
Yves Nievergelt
John S. Robertson
Garry H. Rodrigue
Ned W. Schillow
Philip D. Straffin
J.T. Sutcliffe
Donna M. Szott
Gerald D. Taylor
Maynard Thompson
Ken Travers
Robert E.D. ("Gene") Woolsey

Brigham Young University
University of Houston—Downtown
Harvey Mudd College
Troy State University Montgomery
University of Wisconsin—Madison
Harvey Mudd College
University of Minnesota, Duluth
Gettysburg College
COMAP, Inc.
California State University, Fullerton
Brigham Young University
Southern Methodist University
Metropolitan State College
Adelphi University
Eastern Washington University
Georgia College and State University
Lawrence Livermore Laboratory
Lehigh Carbon Community College
Beloit College
St. Mark's School, Dallas
Comm. College of Allegheny County
Colorado State University
Indiana University
University of Illinois
Colorado School of Mines



关注数学模型
获取更多资讯

Subscription Rates for 1999 Calendar Year: Volume 20

MEMBERSHIP PLUS FOR INDIVIDUAL SUBSCRIBERS

Individuals subscribe to *The UMAP Journal* through COMAP's Membership Plus. This subscription includes print copies of quarterly issues of *The UMAP Journal*, our annual collection *UMAP Modules: Tools for Teaching*, our organizational newsletter *Consortium*, on-line membership that allows members to search our on-line catalog, download COMAP print materials, and reproduce for use in their classes, and a 10% discount on all COMAP materials.

(Domestic)	#2020	\$69
(Outside U.S.)	#2021	\$79

INSTITUTIONAL PLUS MEMBERSHIP SUBSCRIBERS

Institutions can subscribe to the *Journal* through either Institutional Plus Membership, Regular Institutional Membership, or a Library Subscription. Institutional Plus Members receive two print copies of each of the quarterly issues of *The UMAP Journal*, our annual collection *UMAP Modules: Tools for Teaching*, our organizational newsletter *Consortium*, on-line membership that allows members to search our on-line catalog, download COMAP print materials, and reproduce for use in **any class taught in the institution, and** a 10% discount on all COMAP materials.

(Domestic)	#2070	\$395
(Outside U.S.)	#2071	\$405

INSTITUTIONAL MEMBERSHIP SUBSCRIBERS

Regular Institutional members receive only print copies of *The UMAP Journal*, our annual collection *UMAP Modules: Tools for Teaching*, our organizational newsletter *Consortium*, **and** a 10% discount on all COMAP materials.

(Domestic)	#2040	\$165
(Outside U.S.)	#2041	\$175

LIBRARY SUBSCRIPTIONS

The Library Subscription includes quarterly issues of *The UMAP Journal* and our annual collection *UMAP Modules: Tools for Teaching* and our organizational newsletter *Consortium*.

(Domestic)	#2030	\$140
(Outside U.S.)		#2031 \$160

To order, send a check or money order to COMAP, or call toll-free
1-800-77-COMAP (1-800-772-6627).

The UMAP Journal is published quarterly by the Consortium for Mathematics and Its Applications (COMAP), Inc., Suite 210, 57 Bedford Street, Lexington, MA, 02420, in cooperation with the American Mathematical Association of Two-Year Colleges (AMATYC), the Mathematical Association of America (MAA), the National Council of Teachers of Mathematics (NCTM), the American Statistical Association (ASA), the Society for Industrial and Applied Mathematics (SIAM), and The Institute for Operations Research and the Management Sciences (INFORMS). The Journal acquaints readers with a wide variety of professional applications of the mathematical sciences and provides a forum for the discussion of new directions in mathematical education (ISSN 0197-3622).

Second-class postage paid at Boston, MA
and at additional mailing offices.

Send address changes to:
The UMAP Journal
COMAP, Inc.

57 Bedford Street, Suite 210, Lexington, MA 02420
© Copyright 1999 by COMAP, Inc. All rights reserved.



关注数学模型
获取更多资讯

Table of Contents

Publisher's Editorial

Mathematics and Its Applications for All

- Solomon A. Garfunkel 185

Modeling Forum

Results of the 1999 Mathematical Contest in Modeling

- Frank Giordano 187

The Asteroid Impact Problem

Deep Impact

- Dominic Mazzoni, Matthew Fluet, and Joel Miller 211

Asteroid Impact at the South Pole: A Model-Based Risk Assessment

- Michael Rust, Paul Sangiorgio, and Ian Weiner 225

Antarctic Asteroid Effects

- Nicholas R. Baeth, Andrew M. Meyers, and Jacob E. Nelson 241

Not an Armageddon

- Mikhail Khlystov, Ilya Shpitser, and Seth Sulivant 253

The Sky is Falling!

- Daniel Forrest, Garrett Aufdemberg, and Murray Johnson 263

Judge's Commentary: The Outstanding Asteroid Impact Papers

- Patrick J. Driscoll 269

The Lawful Capacity Problem

Determining the People Capacity of a Structure

- Samuel W. Malone, W. Garrett Mitchener, and John Alexander Thacker 273

Hexagonal Unpacking

- David Rudel, Joshua Greene, and Cameron McLeman 287

Don't Panic!

- Timothy Jones, Jeremy Katz, and Allison Master 297

Standing Room Only

- Frederick D. Franzwa, Jonathan L. Matthews, and James I. Meye 311

Room Capacity Analysis Using a Pair of Evacuation Models

- Gregg A. Christopher, Orion Lawler, and Jason Tedor 321

Judge's Commentary: The Outstanding Lawful Capacity Papers

- Jerrold R. Griggs 331

Practitioner's Commentary: The Outstanding Lawful Capacity Papers:

The Answer Is Not the Solution

- Richard Hewitt 335

Interdisciplinary Contest in Modeling (ICM)

The Ground Pollution Problem

Pollution Detection: Modeling an Underground Spill through Hydro-Chemical Analysis

- James R. Garlick and Savannah N. Crites 343

Locate the Pollution Source

- Shen Quan, Yang Zhenyu, and He Xiaofei 355

Judge's Commentary: The Ground Pollution Papers

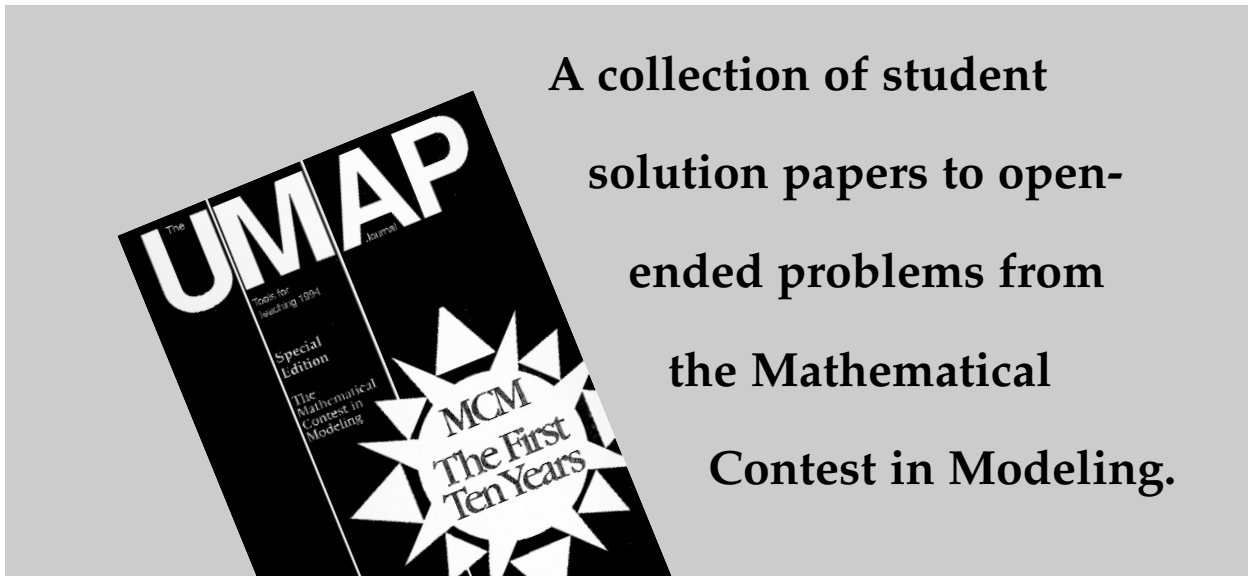
- David L. Elliott 369

Author's Commentary: The Outstanding Ground Pollution Papers

- Yves Nievergelt 369



Our Winners Don't Have All the Answers



A collection of student
solution papers to open-
ended problems from
the Mathematical
Contest in Modeling.

With MCM: The First Ten Years you can:

Build a modeling course

Twenty interesting, open-ended problems

Inspire your students

Creative and eloquent MCM team solution papers

Prepare a team for MCM

Advice from successful advisors and
judges' commentary on winning papers



关注数学模型
获取更多资讯

COMAP ANNOUNCEMENTS

MATHEMATICAL CONTEST IN MODELING

FEBRUARY 4-7, 2000

MCM
2000

The contest offers students the opportunity to compete in a team setting using applied mathematics in the solving of real-world problems.

The sixteenth annual international Mathematical Contest in Modeling will be held February 4-7, 2000. The contest will offer students the opportunity to compete in a team setting, using mathematics to solve real-world problems.

For registration information, contact:

Attn: Clarice Callahan

MCM, COMAP, Inc., Suite 210, 57 Bedford Street, Lexington, MA 02420
email: mcm@comap.com voice: 781/862-7878 ext. 37

Major funding provided by the National Security Agency.

Additional support for this project is provided by the Institute for Operations Research and the Management Sciences, the Society for Industrial and Applied Mathematics, and the Mathematical Association of America.



关注数学模型

获取更多资讯

COMAP



关注数学模型
获取更多资讯

Publisher's Editorial

Mathematics and Its Applications for All

Solomon A. Garfunkel
 Executive Director
 COMAP, Inc.
 57 Bedford St., Suite 210
 Lexington, MA 02420
 s.garfunkel@mail.comap.com

The MCM issue of the UMAP Journal has become an occasion for me to reflect out loud on where COMAP is and where I feel we are going. Like cramming for finals, or preparing for a Board of Trustees meeting, this is a valuable exercise. It is too easy to get caught up in the day-to-day work, answering email, going to meetings, reading brochure copy, and so on, rather than taking a longer view.

Two major new COMAP initiatives were funded this year by the National Science Foundation. They are very closely related and move COMAP in an important new direction. The first of these projects is the Developmental Mathematics and its Applications Project (DevMap) funded through the Advanced Technology Education (ATE) section of the Division of Undergraduate Education (DUE). The goal of this project is to create a new two-semester undergraduate developmental mathematics sequence that embodies the philosophy of reform in the spirit of the NCTM Standards. In other words, we are creating a sequence of developmental courses, which assumes

- graphing calculator use, spreadsheets, and geometric utility programs;
- presents mathematical ideas in the context of their contemporary applications; and
- encourages group activities and a more open pedagogical approach.

Clearly, given our recent high-school efforts in producing *Mathematics: Modeling Our World*, this is a natural direction. But there is much for us to learn.

The UMAP Journal 20(3) (1999) 185–186. ©Copyright 1999 by COMAP, Inc. All rights reserved. Permission to make digital or hard copies of part or all of this work for personal or classroom use is granted without fee provided that copies are not made or distributed for profit or commercial advantage and that copies bear this notice. Abstracting with credit is permitted, but copyrights for components of this work owned by others than COMAP must be honored. To copy otherwise, to republish, to post on servers, or to redistribute to lists requires prior permission from COMAP.



关注数学模型
获取更多资讯

The great majority of students in developmental courses are in two-year colleges. There we find a bimodal distribution of age cohorts—namely, about half of the students coming directly from high school and the other half going back to school frequently after a prolonged absence. Most of these students work and are looking to improve their career options. There is a larger responsibility in courses such as these to use contexts that are immediately relevant to these aspirations.

We have similar concerns in our other major new effort—TechMap. This project's goal is to create a series of modules for use in secondary-school mathematics courses that feature more technically oriented contexts, such as manufacturing, agriculture, finance, and so on. The intent here is to create materials that can serve as replacement units for any core high-school program and at a variety of levels. The important point is that these units are intended for all students, rather than only those students tracked into a vocational course of study. Far too often, important and interesting technical applications of mathematics are considered inappropriate for core curricula. But we all need to learn how the world works and to see the broadest possible range of mathematical models, regardless of whether we know what we want to do when we grow up.

Working in developmental and technical arenas is a new and important direction for COMAP. We look forward to the challenge of serving this large and diverse student population and expanding our mission to include “mathematics and its applications for all.”

About the Author

Sol Garfunkel received his Ph.D. in mathematical logic from the University of Wisconsin in 1967. He was at Cornell University and at the University of Connecticut at Storrs for eleven years and has dedicated the last 20 years to research and development efforts in mathematics education. He has been the Executive Director of COMAP since its inception in 1980.

He has directed a wide variety of projects, including UMAP (Undergraduate Mathematics and Its Applications Project), which led to the founding of this *Journal*, and HiMAP (High School Mathematics and Its Applications Project), both funded by the NSF. For Annenberg/CPB, he directed three telecourse projects: *For All Practical Purposes* (in which he appeared as the on-camera host), *Against All Odds: Inside Statistics*, and *In Simplest Terms: College Algebra*. He is currently co-director of the Applications Reform in Secondary Education (ARISE) project, a comprehensive curriculum development project for secondary school mathematics.



关注数学模型
获取更多资讯

Modeling Forum

Results of the 1999 Mathematical Contest in Modeling

Frank Giordano, MCM Director

COMAP, Inc.

57 Bedford St., Suite 210

Lexington, MA 02420

f.giordano@mail.comap.com

Introduction

A total of 479 teams of undergraduates, from 223 institutions in 9 countries, spent the first weekend in February working on applied mathematics problems. They were part of the 15th annual Mathematical Contest in Modeling (MCM). On Friday morning, the MCM faculty advisor opened a packet and presented each team of three students with a choice of one of two problems. After a weekend of hard work, typed solution papers were mailed to COMAP on Monday. Twelve of the top papers appear in this issue of *The UMAP Journal*.

A new feature this year was the inauguration of the Interdisciplinary Contest in Modeling (ICM), an extension of the MCM designed explicitly to stimulate participation by students from different disciplines and to develop and advance interdisciplinary problem-solving skills. The ICM featured a new kind of problem (Problem C) that in 1999 involved downloading and analyzing data and reflected a situation in which concepts from mathematics, chemistry, environmental science, and environmental engineering were useful. Each year's ICM announcement brochure advises which disciplines are likely to be helpful.

Results and winning papers from the first thirteen contests were published in special issues of *Mathematical Modeling* (1985–1987) and *The UMAP Journal* (1985–1998). The 1994 volume of *Tools for Teaching*, commemorating the tenth anniversary of the contest, contains the 20 problems used in the first ten years of the contest and a winning paper for each. Limited quantities of that volume and of the special MCM issues of the *Journal* for the last few years are available from COMAP.

The UMAP Journal 20 (3) (1999) 187–209. ©Copyright 1999 by COMAP, Inc. All rights reserved. Permission to make digital or hard copies of part or all of this work for personal or classroom use is granted without fee provided that copies are not made or distributed for profit or commercial advantage and that copies bear this notice. Abstracting with credit is permitted, but copyrights for components of this work owned by others than COMAP must be honored. To copy otherwise, to republish, to post on servers, or to redistribute to lists requires prior permission from COMAP.



关注数学模型
获取更多资讯

Problem A: Deep Impact

For some time, the National Aeronautics and Space Administration (NASA) has been considering the consequences of a large asteroid impact on the earth.

As part of this effort, your team has been asked to consider the effects of such an impact were the asteroid to land in Antarctica. There are concerns that an impact there could have considerably different consequences than one striking elsewhere on the planet.

You are to assume that an asteroid is on the order of 1,000 m in diameter, and that it strikes the Antarctic continent directly at the South Pole.

Your team has been asked to provide an assessment of the impact of such an asteroid. In particular, NASA would like an estimate of the amount and location of likely human casualties from this impact, an estimate of the damage done to the food production regions in the oceans of the southern hemisphere, and an estimate of possible coastal flooding caused by large-scale melting of the Antarctic polar ice sheet.

Problem B: Unlawful Assembly

Many facilities for public gatherings have signs that state that it is "unlawful" for their rooms to be occupied by more than a specified number of people. Presumably, this number is based on the speed with which people in the room could be evacuated from the room's exits in case of an emergency. Similarly, elevators and other facilities often have "maximum capacities" posted.

Develop a mathematical model for deciding what number to post on such a sign as being the "lawful capacity." As part of your solution, discuss criteria—other than public safety in the case of a fire or other emergency—that might govern the number of people considered "unlawful" to occupy the room (or space). Also, for the model that you construct, consider the differences between a room with movable furniture such as a cafeteria (with tables and chairs), a gymnasium, a public swimming pool, and a lecture hall with a pattern of rows and aisles. You may wish to compare and contrast what might be done for a variety of different environments: elevator, lecture hall, swimming pool, cafeteria, or gymnasium. Gatherings such as rock concerts and soccer tournaments may present special conditions.

Apply your model to one or more public facilities at your institution (or neighboring town). Compare your results with the stated capacity, if one is posted. If used, your model is likely to be challenged by parties with interests in increasing the capacity. Write an article for the local newspaper defending your analysis.



关注数学模型
获取更多资讯

Problem C: Ground Pollution

Background

Several practically important but theoretically difficult mathematical problems pertain to the assessment of pollution. One such problem consists in deriving accurate estimates of the location and amount of pollutants seeping inaccessibly underground, and the location of their source, on the basis of very few measurements taken only around, but not necessarily directly in, the suspected polluted region.

Example

The data set (an Excel file at <http://www.comap.com/mcm/proedata.xls>, downloadable into most spreadsheets) shows measurements of pollutants in underground water from 10 monitoring wells (MW) from 1990 to 1997. The units are micrograms per liter ($\mu\text{g/l}$). The location and elevation for eight wells are known and given in **Table 1**. The first two numbers are the coordinates of the location of the well on a Cartesian grid on a map. The third number is the altitude in feet above Mean Sea Level of the water level in the well.

Table 1.
Locations for eight wells in Problem C.

Well Number	<i>x</i> -Coordinate (ft)	<i>y</i> -Coordinate (ft)	Elevation (ft)
MW-1	4187.5	6375.0	1482.23
MW-3	9062.5	4375.0	1387.92
MW-7	7625.0	5812.5	1400.19
MW-9	9125.0	4000.0	1384.53
MW-11	9062.5	5187.5	1394.26
MW-12	9062.5	4562.5	1388.94
MW-13	9062.5	5000.0	1394.25
MW-14	4750.0	2562.5	1412.00

The locations and elevations of the other two wells in the data set (MW-27 and MW-33) are not known. In the data set, you will also see the letter T, M, or B after the well number, indicating that the measurements were taken at the Top, Middle, or Bottom of the aquifer in the well. Thus, MW-7B and MW-7M are from the same well, but from the bottom and from the middle. Also, other measurements indicate that water tends to flow toward well MW-9 in this area.

Problem One

Build a mathematical model to determine whether any new pollution has begun during this time period in the area represented by the data set. If so, identify the new pollutants and estimate the location and time of their source.



关注数学模型
获取更多资讯

Problem Two

Before the collection of any data, the question arises whether the intended type of data and model can yield the desired assessment of the location and amount of pollutants. Liquid chemicals may have leaked from one of the storage tanks among many similar tanks in a storage facility built over a homogeneous soil. Because probing under the many large tanks would be prohibitively expensive and dangerous, measuring only near the periphery of the storage facility or on the surface of the terrain seems preferable. Determine what type and number of measurements, taken only outside the boundary or on the surface of the entire storage facility, can be used in a mathematical model to determine whether a leak has occurred, when it occurred, where (from which tank) it occurred, and how much liquid has leaked.

The Results

The solution papers were coded at COMAP headquarters so that names and affiliations of the authors would be unknown to the judges. Each paper was then read preliminarily by two “triage” judges at Southern Connecticut State University (Problem A), Carroll College (Montana) (Problem B), or University of New Hampshire (Problem C). At the triage stage, the summary and overall organization were important for judging a paper. If the judges’ scores diverged for a paper, the judges conferred; if they still did not agree on a score, a third judge evaluated the paper.

Final judging took place at Harvey Mudd College, Claremont, California. The judges classified the papers as follows:

	Outstanding	Meritorious	Honorable Mention	Successful Participation	Total
Asteroid Impact	5	34	61	112	212
Lawful Capacity	5	39	72	91	207
Ground Pollution	<u>2</u>	<u>9</u>	<u>17</u>	<u>32</u>	<u>60</u>
	12	82	150	235	479

The twelve papers that the judges designated as Outstanding appear in this special issue of *The UMAP Journal*, together with commentaries. We list those teams and the Meritorious teams (and advisors) below; the list of all participating schools, advisors, and results is in the **Appendix**.



关注数学模型
获取更多资讯

Outstanding Teams

Institution and Advisor

Team Members

Asteroid Impact Papers

"Deep Impact"

Harvey Mudd College
Claremont, CA
Michael Moody

Dominic Mazzoni
Matthew Fluet
Joel Miller

**"Asteroid Impact at the South Pole:
A Model-Based Risk Assessment"**

Harvey Mudd College
Claremont, CA
Michael Moody

Michael Rust
Paul Sangiorgio
Ian Weiner

"Antarctic Asteroid Effects"

Pacific Lutheran University
Tacoma, WA
Rachid Benkhalti

Nicholas R. Baeth
Andrew M. Meyers
Jacob E. Nelson

"Not an Armageddon"

University of California–Berkeley
Berkeley, CA
Rainer K. Sachs

Mikhail Khlystov
Ilya Shpitser
Seth Sulivant

"The Sky Is Falling"

University of Puget Sound
Tacoma, WA
Perry Fizzano

Daniel Forrest
Garrett Aufderberg
Murray Johnson

Lawful Capacity Papers

**"Determining the People Capacity of a
Structure"**

Duke University
Durham, NC
David P. Kraines

Samuel W. Malone
W. Garrett Mitchener
John Alexander Thacker

"Hexagonal Unpacking"

Harvey Mudd College
Claremont, CA
Ran Libeskind-Hadas

David Rudel
Joshua Greene
Cameron McLeman



关注数学模型
获取更多资讯

“Don’t Panic!”

North Carolina School
of Science and Mathematics
Durham, NC
Dot Doyle

Timothy Jones
Jeremy Katz
Allison Master

“Standing Room Only”

Rose-Hulman Institute of Technology
Terre Haute, IN
Aaron D. Klebanoff

Frederick D. Franzwa
Jonathan L. Matthews
James I. Meyer

“Room Capacity Analysis Using a Pair of
Evacuation Models”

University of Alaska Fairbanks
Fairbanks, AK
Chris Hartman

Gregg A. Christopher
Orion Lawler
Jason Tedor

Ground Pollution Papers

“Pollution Detection: Modeling an
Underground Spill Through
Hydro-Chemical Analysis”

Earlham College
Richmond, IN
Mic Jackson

James R. Garlick
Savannah N. Crites

“Locate the Pollution Source”

Zhejiang University
Hangzhou, China
Zhang Chong

Shen Quan
Yang Zhenyu
He Xiaofei

Meritorious Teams

Asteroid Impact Papers (34 teams)

Asbury College, Wilmore, KY (Kenneth P. Rietz)
Beijing University of Post and Telecommunications, Beijing, China (He Zuguo)
Beloit College, Beloit, WI (Philip D. Straffin)
Brandon University, Brandon, Manitoba, Canada (Doug Pickering)
California Polytechnic State University, San Luis Obispo, CA (two teams)
(Thomas O’Neil)
College of Wooster, Wooster, OH (Reuben Settergren)
Governor’s School for Government and International Studies, Richmond, VA
(two teams) (Crista Hamilton)
Greenville College, Greenville, IL (Galen R. Peters)
Harbin Institute of Technology, Harbin, Heilongjiang, China (Wang Yong)
Hefei University of Technology, Hefei, Anhui, China (Jie Bao)



关注数学模型
获取更多资讯

Lewis and Clark College, Portland, OR (Robert W. Owens)
 Montclair State University, Upper Montclair, NJ (Mary Lou West)
 North Carolina School of Science and Mathematics, Durham, NC (Dot Doyle)
 Nanjing University of Science and Technology, Nanjing, Jiangsu, China
 (Wu Xing Min)
 National U. of Defence Technology, Chang Sha, Hunan, China (Wu MengDa)
 National University of Ireland, Galway, Ireland (Martin Meere)
 Pacific Lutheran University, Tacoma, WA (Rachid Benkhalti)
 Rose-Hulman Institute of Technology, Terre Haute, IN (Frank Young)
 South China University of Technology, Guangzhou, Guangdong, China
 (Xie Lejun)
 Trinity College Dublin, Dublin, Ireland (Timothy G. Murphy)
 Trinity University, San Antonio, TX (Jeffrey Lawson)
 U.S. Air Force Academy, USAF Academy, CO (Dawn Stewart)
 U.S. Military Academy, West Point, NY (Charles C. Tappert)
 University of Alaska Fairbanks, Fairbanks, AK (Chris Hartman)
 University of Colorado, Colorado Springs, CO (Holly Zullo)
 University of South Carolina, Aiken, SC (Nieves A. McNulty)
 Virginia Western Community College, Roanoke, VA (Ruth Sherman)
 Western Washington University, Bellingham, WA (Igor Averbakh)
 Westminster College, New Wilmington, PA (Barbara Faires)
 Wuhan University of Hydraulics and Engineering, Wuhan, Hubei, China
 (Huang Chongchao)
 Zhejiang University, Hangzhou, Zhejiang, China (Qifan Yang)
 Zhong Shan University, Guonmgzhou, Guong, China (Wang Shousong)

Lawful Capacity Papers (39 teams)

Abilene Christian University, Abilene, TX (David Hendricks)
 Asbury College, Wilmore, KY (Kenneth P. Rietz)
 Baylor University, Waco, TX (Frank H. Mathis)
 Beijing University of Chemical Technology, Beijing, China (Zhao Baoyuan)
 Beloit College, Beloit, WI (Philip D. Straffin)
 China University of Mining and Technology, Xuzhou, Jiangsu, China
 (Zhang Xingyong)
 Drake University, Des Moines, IA (Alexander F. Kleiner)
 Eastern Mennonite University, Harrisonburg, VA (John L. Horst)
 Gettysburg College, Gettysburg, PA (two teams) (James P. Fink)
 Grinnell College, Grinnell, IA (Marc Chamberland)
 Grinnell College, Grinnell, IA (William Case)
 Hefei University of Technology, Hefei, Anhui, China (Youdu Huang)
 Indiana University, Bloomington, IN (Russell Lyons)
 James Madison University, Harrisonburg, VA (James S. Sochacki)
 Macalester College, St. Paul, MN (Daniel Kaplan)
 Michigan State University, E. Lansing, MI (C.R. MacCluer)
 National University of Defence Technology, Chang Sha, Hunan, China
 (Cheng LiZhi)
 National University of Ireland, Galway, Ireland (Michael P. Tuite)
 Rose-Hulman Institute of Technology, Terre Haute, IN (Aaron D. Klebanoff)
 Seattle Pacific University, Seattle, WA (Steven D. Johnson)



关注数学模型
获取更多资讯

Shanghai Jiaotong University, Shanghai, China (Song Baorui)
Shanghai Jiaotong University, Shanghai, China (Zhou Gang)
Trinity University, San Antonio, TX (Jeffrey Lawson)
U.S. Military Academy, West Point, NY (Ed Connors)
University of California, Berkeley, CA (Rainer K. Sachs)
University of Dayton, Dayton, OH (Ralph C. Steinlage)
University of New South Wales, Sydney, Australia (James Franklin)
University of Puget Sound, Tacoma, WA (Robert A. Beezer)
University of Richmond, Richmond, VA (Kathy W. Hoke)
University of Science and Technology of China, Hefei, Anhui, China
(Zhou Jingren)
University of Washington, Seattle, WA (Randall J. LeVeque)
Wake Forest University, Winston-Salem, NC
(Stephen B. Robinson and Edward Allen)
Western Washington University, Bellingham, WA (Igor Averbakh)
Wheaton College, Wheaton, IL (Paul Isihara)
Wisconsin Lutheran College, Milwaukee, WI (Marvin C. Papenfuss)
Worcester Polytechnic Institute, Worcester, MA (Bogdan Vernescu)
Xidian University, Xian, Shaanxi, China (Mao Yongcai)
Youngstown State University, Youngstown, OH (Thomas Smotzer)

Pollution Detection Papers (9 teams)

East China University of Science and Technology, Shanghai, China
(Shao Nianci)
Eastern Oregon State College, LaGrande, OR (Jenny Woodworth)
Harvey Mudd College, Claremont, CA (Michael Moody)
Humboldt State University, Arcata, CA (Margaret Lang)
South China University of Technology, Guangzhou, Guangdong, China
(He Chunxiong)
Tsinghua University, Beijing, China (Ye Jun)
University of Science and Technology of China, Hefei, Anhui, China (Du Zheng)
Xian Jiaotong University, Xian, Shaanxi, China (two teams) (Dai YongHong)

Awards and Contributions

Each participating MCM advisor and team member received a certificate signed by the Contest Director and the appropriate Head Judge.

INFORMS, the Institute for Operations Research and the Management Sciences, gave a cash award and a three-year membership to each member of the teams from the University of Puget Sound (Asteroid Impact Problem), Duke University (Lawful Capacity Problem), and Zhejiang University (Ground Pollution Problem). Moreover, INFORMS gave free one-year memberships to all members of Meritorious and Honorable Mention teams.

The Society for Industrial and Applied Mathematics (SIAM) designated as SIAM Winners two teams from Harvey Mudd College—Mazzoni et al. (Aster-



oid Impact Problem) and Rudel et al. (Lawful Capacity Problem)—and the team from Earlham College (Ground Pollution Problem). Each of the team members was awarded a \$300 cash prize. Their school was given a framed certificate hand-lettered in gold leaf. The Harvey Mudd team presented its results at a special Minisymposium of the SIAM Annual Meeting in Atlanta, GA in May.

The Mathematical Association of America (MAA) designated as MAA Winners the teams from the University of Alaska Fairbanks (Lawful Capacity Problem) and Earlham College (Ground Pollution Problem). Both teams presented their solutions at a special session of the MAA Mathfest in Providence, RI in August. Each team member was presented a certificate by MAA President-Elect Thomas Banchoff.

Judging

Director

Frank R. Giordano, COMAP, Lexington, MA

Associate Directors

Robert L. Borrelli, Mathematics Dept., Harvey Mudd College,
Claremont, CA

William Fox, Chair, Dept. of Mathematics, Francis Marion University,
Florence, SC

Asteroid Impact Problem

Head Judge

Patrick Driscoll, Dept. of Mathematical Sciences, U.S. Military Academy
(INFORMS)

Associate Judges

Ron Barnes, University of Houston–Downtown, Houston, TX (MAA)

Paul Boisen, Defense Dept., Ft. Meade, MD

Courtney Coleman, Mathematics Dept., Harvey Mudd College,
Claremont, CA

Lisette de Pillis, Mathematics Dept., Harvey Mudd College, Claremont, CA

Patrick Driscoll, Dept. of Mathematical Sciences, U.S. Military Academy,
West Point, NY (INFORMS)

Ben Fusaro, Mathematics Dept., Florida State University, Tallahassee, FL
(SIAM/MAA)

Richard Haberman, Mathematics Dept., Southern Methodist University,
Dallas, TX (SIAM)

Mario Juncosa, RAND Corporation, Santa Monica, CA

Mark Levinson, Edmonds, WA (SIAM)

Keith Miller, National Security Agency, Ft. Meade, MD



关注数学模型
获取更多资讯

Jack Robertson, Head, Mathematics and Computer Science, Georgia College
and State University, Milledgeville, GA (MAA)

Lee Seitelman, Glastonbury, CT

Robert M. Tardiff, Dept. of Mathematical Sciences,
Salisbury State University, Salisbury, MD

Daniel Zwillinger, Zwillinger & Associates, Arlington, MA

Lawful Capacity Problem

Head Judge

Maynard Thompson, Mathematics Dept., University of Indiana,
Bloomington, IN

Associate Judges

John Boland, Center for Industrial and Applied Mathematics (CIAM),
University of South Australia, Australia

Karen Bolinger, Dept. of Mathematics, Clarion University of Pennsylvania,
Clarion, PA

Doug Faires, Dept. of Mathematics and Statistics, Youngstown State
University, Youngstown, OH

Jerry Griggs, Dept. of Mathematics, University of South Carolina,
Columbia, SC (SIAM)

Jeff Hartzler, Dept. of Mathematics, Penn State University,
Middletown, PA (MAA)

Karla Hoffman, Chair, Dept. of Operations Research, George Mason University,
Fairfax, VA (INFORMS)

Daphne Liu, Mathematics Dept., California State University, Los Angeles, CA

Veena Mendiratta, Lucent Technologies, Naperville, IL

Don Miller, Dept. of Mathematics, St. Mary's College, Notre Dame, IN

Peter Olsen, Charles Stark Draper Lab, Arlington, VA (INFORMS)

Mark Parker, Dept. of Mathematical Sciences,
U.S. Air Force Academy, CO (SIAM)

Catherine Roberts, Northern Arizona University, Flagstaff, AZ (SIAM)

Michael Tortorella, Lucent Technologies, Holmdel, NJ

Marie Vanisko, Carroll College, Helena, MT (Triage)

Martin Wildberger, Electric Power Research Institute, Palo Alton, CA (SIAM)

Ground Pollution Problem

Head Judge

David C. Arney, Dept. of Mathematical Sciences, U.S. Military Academy

Associate Judges

Kelly Black, Mathematics Dept., University of New Hampshire,
Durham, NH (Triage)

James Case, Baltimore, Maryland (SIAM)



关注数学模型
获取更多资讯

David L. Elliott, Institute for Systems Research, University of Maryland,
College Park, MD (SIAM)

John Kobza, Industrial and Systems Engineering, Virginia Polytechnic
Institute and State University, Blacksburg, VA (INFORMS)

John L. Scharf, Carroll College, Helena, MT

Kathleen M. Shannon, Salisbury State University, Salisbury, MD (MAA)

Triage Session

Asteroid Impact Problem

Head Triage Judge

Theresa M. Sandifer, Southern Connecticut State University, New Haven, CT

Associate Judges

Therese L. Bennett, Southern Connecticut State University, New Haven, CT

Cynthia B. Gubitose, Western Connecticut State University, Danbury, CT

David Hahn

Ronald E. Kutz, Western Connecticut State University, Danbury, CT

Val Pinciu, Mathematics Dept., SUNY at Buffalo, Buffalo, NY

C. Edward Sandifer, Western Connecticut State University, Danbury, CT

Lawful Capacity Problem

(all from Mathematics Dept., Carroll College, Helena, MT)

Head Triage Judge

Marie Vanisko

Associate Judges

Peter Biskis, Terence J. Mullen, and Jack Oberweiser

Ground Pollution Problem

(all from Mathematics Dept., University of New Hampshire, Durham, NH)

Head Triage Judge

Kelly Black

Associate Judges

A.H. Copeland, John B. Geddes, Loren D. Meeker, Kevin Short, Lee L. Zia

Sources of the Problems

Contributors of the problems were as follows:

- **Asteroid Impact Problem:** Jack Robertson, Mathematics Dept., Georgia College and State University.
- **Lawful Capacity Problem:** Joe Malkevitch, Mathematics Dept., York College, City University of New York.



- **Ground Pollution Problem:** Yves Nievergelt, Mathematics Dept., Eastern Washington University.

Acknowledgments

The MCM was funded this year by the National Security Agency, whose support we deeply appreciate. The ICM received major funding also from the National Science Foundation. We thank Dr. Gene Berg of NSA for his coordinating efforts. The MCM is also indebted to INFORMS, SIAM, and the MAA, which provided judges and prizes.

I thank the MCM judges and MCM Board members for their valuable and unflagging efforts. Harvey Mudd College, its Mathematics Dept. staff, and Prof. Borrelli were gracious hosts to the judges.

Cautions

To the reader of research journals:

Usually a published paper has been presented to an audience, shown to colleagues, rewritten, checked by referees, revised, and edited by a journal editor. Each of the student papers here is the result of undergraduates working on a problem over a weekend; allowing substantial revision by the authors could give a false impression of accomplishment. So these papers are essentially *au naturel*. Light editing has taken place: minor errors have been corrected, wording has been altered for clarity or economy, and style has been adjusted to that of *The UMAP Journal*. Please peruse these student efforts in that context.

To the potential MCM Advisor:

It might be overpowering to encounter such output from a weekend of work by a small team of undergraduates, but these solution papers are highly atypical. A team that prepares and participates will have an enriching learning experience, independent of what any other team does.



Appendix: Successful Participants

KEY:

P = Successful Participation	A = Asteroid Impact Problem
H = Honorable Mention	B = Lawful Capacity Problem
M = Meritorious	C = Ground Pollution Problem
O = Outstanding (published in this special issue)	

INSTITUTION	CITY	ADVISOR	A	B	C
ALASKA					
Univ. of Alaska Fairbanks	Fairbanks	Chris Hartman	M	O	
ARIZONA					
Northern Arizona Univ.	Flagstaff	James W. Swift		H	
CALIFORNIA					
California Lutheran Univ.	Thousand Oaks	Cynthia J. Wyels	P		
Calif. Poly. State Univ.	San Luis Obispo	Thomas O'Neil	M,M		
California State Univ. Seaside	Bakersfield Seaside	Maureen E. Rush Daniel M. Fernandez	P P		H
Northridge		Gholam-Ali Zakeri	P	P	
Fullerton		Mario U. Martelli	P	P	
Harvey Mudd College	Claremont	Michael Moody Ran Libeskind-Hadas	O,O O		M
Humboldt State Univ.	Arcata	Margaret Lang			M
Loyola Marymount Univ.	Los Angeles	Thomas M. Zachariah	P,P		
Pepperdine University	Malibu	Jane Ganske		P	
Pomona College	Claremont	Richard Elderkin			H
Shasta College	Redding	Cathy Anderson		P	
Sonoma State University	Rohnert Park	Clement E. Falbo	P		
Univ. of California	Berkeley	Rainer K. Sachs	O	M	
COLORADO					
Colorado College	Colorado Springs	Steven Janke	P		
Mesa State College	Grand Junction	Edward Bonan-Hamada	H,P		
Metro. State College	Denver	Thomas E. Kelley		P	
Regis University	Denver	Linda Duchrow		P	
U.S. Air Force Academy	USAF Academy	Jeff Boleng Capt Kirsten Messer Dawn Stewart	P H M		
Boulder		Anne Dougherty	H		
Colorado Springs		Holly Zullo Shannon Michaux	M P		
Univ. of Southern Colo.	Pueblo	Bruce N. Lundberg Paul R. Chacon	P P		



关注数学模型

获取更多资讯

INSTITUTION	CITY	ADVISOR	A	B	C
CONNECTICUT					
Connecticut College	New London	Kathy McKeon		P	
Sacred Heart Univ.	Fairfield	Antonio Magliaro	P		
Southern Conn. State Univ.	New Haven	Ross Gingrich	H		
		Theresa Sandifer	H		
Western Conn. State Univ.	Danbury	Ed Sandifer		H	
		Paul Hines		H	
DISTRICT OF COLUMBIA					
Georgetown University	Washington	Andrew Vogt	P	H	
FLORIDA					
Florida Southern College	Lakeland	Allen Wuertz	P		
Jacksonville University	Jacksonville	Lucinda B. Sonnenberg		P	
		Paul R. Simony	H		
		Robert A. Hollister		P	
Stetson University	Deland	Daniel R. Plante		H	
University of North Florida	Jacksonville	Peter A. Braza	P		
GEORGIA					
Georgia College & State Univ.	Milledgeville	Craig Turner	P		
State Univ. of West Georgia	Carrollton	Scott Gordon	P		
IDAHO					
Boise State University	Boise	Stephen Brill	P	P	
Idaho State University	Pocatello	Jim Hoffman		H	
ILLINOIS					
Greenville College	Greenville	Galen R. Peters	M,P		
Illinois Wesleyan University	Bloomington	Zahia Drici	P		
Northern Illinois University	Dekalb	Hamid Bellout		P	
Wheaton College	Wheaton	Paul Isihara	P	M	
INDIANA					
Earlham College	Richmond	Charlie Peck	P		
		Mic Jackson		O	
Goshen College	Goshen	David Housman	P		
		Patricia Oakley	P	H	
Indiana University	Bloomington	Russell Lyons		M,H	
	South Bend	Morteza Shafii-Mousavi	P		
		Steven Shore	P		
Rose-Hulman Inst. of Tech.	Terre Haute	Frank Young	M	P	
		Aaron D. Klebanoff		O,M	
Saint Mary's College	Notre Dame	Joanne Snow	H	H	
Wabash College	Crawfordsville	Esteban Poffald	P,P		



关注数学模型
获取更多资讯

INSTITUTION	CITY	ADVISOR	A	B	C
IOWA					
Drake University	Des Moines	Alexander F. Kleiner Luz M. De Alba		M P	
Grinnell College	Grinnell	William Case Marc Chamberland	H	M H	M,P
Iowa State University	Ames	Stephen J. Willson			H,H
Luther College	Decorah	Reginald D. Laursen	P	H	
Marycrest Int'l Univ.	Davenport	Jeff Dickerson	P		
Mt. Mercy College	Cedar Rapids	Kent Knopp	P,P		
Simpson College	Indianola	David Olsgaard M.E. Murphy Waggoner	H H	P H	
Univ. of Northern Iowa	Cedar Falls	Gregory M. Dotseth Timothy L. Hardy	P P		
Wartburg College	Waverly	Mariah Birgen			P
KANSAS					
Baker University	Baldwin City	Bob Fraga	P		P
Bethel College	North Newton	Monica Meissen	P,P		
KENTUCKY					
Asbury College	Wilmore	Kenneth P. Rietz	M	M	
Brescia College	Owensboro	Chris A. Tiahrt		P	
LOUISIANA					
McNeese State Univ.	Lake Charles	Karen Aucoin Robert Doucette	P		P
MAINE					
Colby College	Waterville	Tom Berger		H	P
MARYLAND					
Loyola College	Baltimore	John Hennessey		P	P
Mt. St. Mary's College	Emmitsburg	Fred J. Portier		P	
		John August	P		
Salisbury State Univ.	Salisbury	Michael Bardzell	P		
MASSACHUSETTS					
Holy Cross College	Worcester	John Anderson			P
Simon's Rock College	Great Barrington	Allen B. Altman	P,P		
Smith College	Northampton	Yung Pin-Chen	P		
		Yung-Pin Chen and Cristina Suarez			P
Univ. of Massachusetts	Lowell	James Kiwi Graham-Eagle Lou Rossi		H P	
		Eric Haffner	P		
W. New England Coll.	Springfield	Stewart Johnson		P	
Williams College	Williamstown	Arthur C. Heinricher	P		
Worcester Poly. Inst.	Worcester	Bogdan Vernescu		M	



关注数学模型
获取更多资讯

INSTITUTION	CITY	ADVISOR	A	B	C
MICHIGAN					
Albion College	Albion	Scott Dillary	P	P	
Eastern Michigan University	Ypsilanti	Christopher E. Hee	P,P		
Hillsdale College	Hillsdale	John P. Boardman		H,P	
Kettering University	Flint	Craig Andres	P		
Lawrence Technological Univ.	Southfield	Howard Whitston	H		
		Ruth G. Favro		H	
		Scott Schneider	H		
Michigan State University	E. Lansing	C. R. MacCluer		M,H	
		George Stockman			P
Siena Heights College	Adrian	Rick Trujillo	P		
Univ. of Michigan–Dearborn	Dearborn	David A. James	H		
MINNESOTA					
Augsburg College	Minneapolis	Rebekah Valdivia	P	P	
Macalester College	St. Paul	Susan Fox		P	
		Daniel Kaplan		M	
University of Minnesota	Morris	Peh Ng		H,P	
Winona State University	Winona	Barry A. Peratt		P	
MISSOURI					
Missouri Southern State Coll.	Joplin	Patrick Cassens	P	H	
Northeast Missouri State Univ.	Kirksville	Steven J. Smith		P	
Northwest Missouri State Univ.	Maryville	Russell N. Euler	P	P	
Southeast Missouri State Univ.	Cape Girardeau	Robert W. Sheets	P		
Univ. of Missouri	Rolla	Michael G. Hilgers		H	
Wentworth Military Academy	Lexington	Jacque Maxwell		P,P	
MONTANTA					
Carroll College	Helena	Terence J. Mullen		H	
		Jack Oberweiser	P		
		Kevin Wolka	P		
NEBRASKA					
Nebraska Wesleyan Univ.	Lincoln	P. Gavin LaRose		H	
NEVADA					
University of Nevada	Reno	Mark M. Meerschaert	H		
NEW JERSEY					
Kean University	Union	Pablo Zafra			P
Montclair State University	Upper Montclair	Mary Lou West	M		
		Michael Jones		P	
NEW MEXICO					
New Mexico State University	Las Cruces	Marcus S. Cohen	H		



关注数学模型
获取更多资讯

INSTITUTION	CITY	ADVISOR	A	B	C
NEW YORK					
Ithaca College	Ithaca	John C. Maceli	P		
Nazareth College	Rochester	Kelly M. Fuller	H,P		
		Joe Lanzafame		P	
Niagara University	Niagara	Steven L. Siegel		P	
St. Bonaventure Univ.	St. Bonaventure	Maureen P Cox		P	
		Albert G. White		P	
U.S. Military Academy	West Point	Ed Connors		M	
		James S. Rolf		H	
		Charles C. Tappert	M		
		Joanne E. Walser		P	
Wells College	Aurora	Carol C. Shilepsky		H	
Westchester Comm. Coll.	Valhalla	Rowan Lindley	P		
		Sheela Whelan	P		
NORTH CAROLINA					
Appalachian State Univ.	Boone	Holly Hirst	H		
Duke University	Durham	David P. Kraines		O	
Elon College	Elon College	Todd Lee	P	P	
Mount Olive College	Mt Olive	Ollie J Rose		P	
N.C. School of Sci. & Math	Durham	Dot Doyle	M	O	
North Carolina State Univ.	Raleigh	Joyce Hatch		H	
		Robert T. Ramsay		P	H
Salem College	Winston-Salem	Paula G. Young		P	P
Univ. of N. Carolina	Wilmington	Russell L. Herman	H	P	
Wake Forest University	Winston-Salem	Stephen B. Robinson and Edward Allen		M	
Western Carolina Univ.	Cullowhee	Julie Barnes	H		
		Kathy Ivey	H,	P	
OHIO					
Baldwin-Wallace College	Berea	Susan D Penko	P		
College of Wooster	Wooster	Reuben Settergren	M		
Hiram College	Hiram	Brad Gubser	A	P	
Miami University	Oxford	Doug Ward		H	
University of Dayton	Dayton	Ralph C. Steinlage		M	
Wright State University	Dayton	Thomas P. Svobodny	H		
Youngstown State Univ.	Youngstown	Stephen Hanzely	H		
		Robert Kramer		H	
		Scott Martin		P	
		Thomas Smotzer	H	M	H



关注数学模型
获取更多资讯

INSTITUTION	CITY	ADVISOR	A	B	C
OKLAHOMA					
Southeastern Okla. State Univ.	Durant	John McArthur Karla Oty	P P		
OREGON					
Eastern Oregon State College	LaGrande	David Allen John Thurber Anthony Tovar Jenny Woodworth	P P	H	
Lewis and Clark College	Portland	Robert W. Owens	M		M
Southern Oregon State College	Ashland	Kemble R. Yates		H	P
PENNSYLVANIA					
Carnegie Mellon University	Pittsburgh	Walker	P		
Clarion Univ. of Pennsylvania	Clarion	Michael Barrett Jon Beal	P P		
Dickinson College	Carlisle	Bill Krugh		H	
Gettysburg College	Gettysburg	Lorelei Koss			P
Haverford College	Haverford	James P. Fink		M,M	
Messiah College	Grantham	Stephanie Singer		P	
Shippensburg University	Shippensburg	Lamarr C. Widmer			H
Westminster College	New Wilmington	Cheryl Olsen Barbara Faires Richard Sprow	P M,P		
SOUTH CAROLINA					
Charleston Southern Univ.	Charleston	Stan Perrine	P		
Francis Marion University	Florence	C. Abbott	P		
Univ. of South Carolina	Aiken	Laurene Fausett Nieves A. McNulty	M	H	
SOUTH DAKOTA					
Northern State University	Aberdeen	A.S. Elkharder			P
TENNESSEE					
Carson-Newman College	Jefferson City	Catherine Kong	H		
Christian Brothers University	Memphis	Cathy W. Carter		P	
Lipscomb University	Nashville	Mark A. Miller		H	
TEXAS					
Abilene Christian University	Abilene	David Hendricks	M		
Baylor University	Waco	Frank H. Mathis	M		
Southwestern University	Georgetown	T. Shelton	P		
Trinity University	San Antonio	Jeffrey Lawson	M	M	
		Fred Loxom		H	
University of Dallas	Irving	Pete McGill	P		
University of Houston	Houston	Barbara Lee Keyfitz	P		
University of Texas at El Paso	El Paso	Michael D. O'Neill	P		



关注数学模型
获取更多资讯

INSTITUTION	CITY	ADVISOR	A	B	C
UTAH					
University of Utah	Salt Lake City	Don H. Tucker	H		
VERMONT					
Johnson State College	Johnson	Glenn D. Sproul	P	P	
VIRGINIA					
College of William & Mary	Williamsburg	Michael Trosset	H		
Eastern Mennonite Univ.	Harrisonburg	John L. Horst		P	
Governor's School for Gov. & Int'l Studies	Richmond	John Barnes Crista Hamilton	M,M	H	
James Madison University	Harrisonburg	Donna Fengya James S. Sochacki	P	M	
Thomas Jefferson H.S. for Sci. & Tech.	Alexandria	John Dell	H		
University of Richmond	Richmond	Kathy W. Hoke	M		
Virginia Western Comm. Coll.	Roanoke	Ruth Sherman	M,P		
WASHINGTON					
Pacific Lutheran University	Tacoma	Rachid Benkhalti	O,M		
Seattle Pacific University	Seattle	Steven D. Johnson	M		
University of Puget Sound	Tacoma	Robert A. Beezer	M,H		
Univ. of Washington	Seattle	Perry Fizzano	O,P		
Washington State Univ.	Pullman	Randall J LeVeque	M		
Western Washington Univ.	Bellingham	Richard Gomulkiewicz Igor Averbakh	P	M	P
		Saim Ural	P	P	
WISCONSIN					
Beloit College	Beloit	Philip D. Straffin	M	M	
Northcentral Technical Coll.	Wausau	Frank J. Fernandes	P		
		Robert J. Henning	P		
Univ. of Wisconsin	Madison	David Moulton	P		
	Platteville	Mike Penn		P	
		Sheryl Wills	H		
	Stevens Point	Nathan Wetzel	H		
		Robert Kreczner	P		
Wisconsin Lutheran College	Milwaukee	Marvin C. Papenfuss	M		
AUSTRALIA					
Curtin University of Tech.	Perth	Yong Hong Wu	P		
Univ. of New South Wales	Sydney	Dr James Franklin	M		
Univ. of Southern Queensland	Toowoomba	Christopher J. Harman	H		
		Tony Roberts	P		



关注数学模型
获取更多资讯

INSTITUTION	CITY	ADVISOR	A	B	C
CANADA					
Brandon University	Brandon, MB	Doug Pickering	M		
Memorial Univ. of Nfld	St. John's, NF	Andy Foster	P		
University of Calgary	Calgary, AB	David R. Westbrook		P	
University of Saskatchewan	Saskatoon, SK	Prof. Raj Srinivasan	H		
Univ. of Western Ontario	London, ON	C. Lindsay Dennison			P
		Peter H. Poole	H		P
York University	Toronto, ON	Juris Steprans		H,P	
CHINA					
Anhui University	Hefei, Anhui	Sjyang Shangjun	H		
		Wang Haixian		H	
Anhui University	Hefei, Anhui	Zhang Quanbin	P		
Beijing Institute of Tech.	Beijing	Yang Guoxiao	P		
		Xiao Di Cui		H	
Beijing Union University	Beijing	Ren KaiLong	H		
		Wang Xinfeng	H		
		Xing Chun Feng		P	
		Zeng Qingli		P	
Beijing U. of Aero. & Astro.	Beijing	Peng Linping	P		
Beijing Univ. of Chem. Tech.	Beijing	Liu Damin	P		
		Shi Xiaoding		H	
		Zhao Baoyuan		M	
Beijing U. of Post & Telecomm.	Beijing	He Zuguo	M	H	
		Luo Shoushan		P,P	
Central-South Inst. of Techn.	Hengyang, Hunan	Liu Yachun		P,P	
China Univ. of Mining & Techn.	Xuzhou, Jiangsu	Zhang Xingyong		M	
		Zhou Shengwu		H	
Chongqing University	Chongqing	Fu Li		H	
		Gong Qu	P		
		He Zhongshi		H	
		Liu Qiongsen		P	
		Yang DaDi		H	
Dalian University of Tech.	Dalian, Liaoning	He Mingfeng	P	P	
		Yu Hongquan		H,H	
		Zhao Lizhong	H		P
E. China Univ. of Sci. and Tech.	Shanghai	Liu Zhaohui		H	
		Lu Xiwen			H
		Shao Nianci	H		M
		Lu Xiwen		P	
		Lu Yuanhong	H		



关注数学模型
获取更多资讯

INSTITUTION	CITY	ADVISOR	A	B	C
Exp'l H.S. Beijing U. Normal	Beijing	Han Leqing Zhangjilin		P	
First Middle School of Jiading District	Jiading, Shanghai	Xiexilin Xurong		H H	
Fudan University	Shanghai	Wan Huiling Zhou Xi Cai Zhijie	P H	P	
Harbin Engineering Univ.	Harbin, Heilongjiang	Luo Yuesheng Shen Jihong Shi Jiuyu Zhang Xiaowei		P,P H	H
Harbin Inst. of Technology	Harbin, Heilongjiang	Liu Jin Shang Shouting Wang Yong Yu Xiujuan	H H M	P	H
Hefei University of Tech.	Hefei, Anhui	Bao Jie Du Xueqiao Zhou Yongwu Huang Youdu	M P H		
JianPing Senior High School	Shanghai	Huang Liangfu Zhu Weizheng		H H	
Jilin University	Changchun, Jilin	Lu Xian Vui	P		
Jilin University of Tech.	Changchun, Jilin	Fang Peichen Liu Xiaoyu Zhang Peiyuan	P H H		
Jinan University	Guangzhou, Guangdong	Ye Shiqi Fan Suohai	P H		
Mechanical Eng'ng Coll.	Shijiazhuang	Yang Pinghua Zhao Ruiqing	H H		
Nanjing Univ. of Sci. & Tech.	Nanjing, Jiang Su	Wu Xing min Yang Xiaoping	M P		
Nankai University	Tianjin	Wang Bin Huang Wuqun Zhou XingWei Chen Zenzqiang		P H P P	
National U. of Defence Tech.	Chang Sha, HuNan	Cheng LiZhi Wu MengDa	M		
Northwestern Polytech. Univ.	Xian, Shaanxi	Lu Xiao Dong Nie Yu Feng Wang MingYu		H H	
		Xu Wei	H		



关注数学模型
获取更多资讯

INSTITUTION	CITY	ADVISOR	A	B	C
Peking University	Beijing	Lei Gongyan Deng Minghua	H,P P,P		P P
Shandong University	Jinan, Shandong	Cui Yuquan		P	
Shanghai Jiaotong Univ.	Shanghai	Huang Jianguo Song Baorui Yang Bing Zhou Gang		H M	
Shanghai Maritime Univ.	Shanghai	Ding Songkang Sheng Zining	P		P
Shanghai Normal Univ.	Shanghai	Zhu Detong Guo Shenghuan		P,P P	
South China Univ. of Tech.	Guangzhou, Guangdong	Fu Hongzhuo Hao Zhifeng He Chunxiong Xie Lejun Zhu Fengfeng		H M	H
Southeast University	Jiangsu, Nanjing	He Lin and Wei Fangfang Huang Jun Zhou Jianhua Zhu Dao-Yuan		P	
Tsinghua University	Beijing	Hu Zhiming Ye Jun		P,P H,P	P M
Univ. of Elec. Sci. & Tech.	Chengdu	Du Hongfei Wang Jianguo Xu Quanzhi Zhong Erjie	P		H P
U. of Sci. and Tech. of China	Hefei, Anhui	Gao Jie Xu Qingqing Du Zheng Guo Quji Lai Junwen Zhou Jingren		H	H M
Wuhan U. of Hydraul. & Eng'ng	Wuhan, Hubei	Cheng Guixing Huang Chongchao Peng Zhuzeng	H M,H		
Xian Jiaotong University	Xian, Shaanxi	He Xiaoliang Zhou Yicang Dai YongHong	H	P H,P	
Xidian University	Xian, Shaanxi	Hu Yupu Li Junmin Mao Yongcai	H		M,M H M



关注数学模型
获取更多资讯

INSTITUTION	CITY	ADVISOR	A	B	C
Zhejiang University	Hangzhou, Zhejiang	Yang Qifan He Yong Zhang Chong	M H	P H	O
Zhengzhou Electr. Power Coll.	Zhengzhou, Henan	Cheng Ruizhong Cui Yingjian	H		P
Zhengzhou Univ. of Tech.	Zhengzhou, Henan	Wang Jinling Wang Shubin		H	P
Zhong Shan Univ.	Guonmgzhou, Guong	Jiang Xiaolong Wang Shousong Wang Yuan Shi Yang Yin Zhao		H	P
FINLAND					
Paivola College	Valkeakoski	Merikki Lappi		P,P	
HONG KONG					
Hong Kong Baptist Univ.	Kowloon	Chong Sze Tong		P,P	
IRELAND					
National Univ. of Ireland	Galway	Michael P. Tuite Martin Meere		M	
Trinity College Dublin	Dublin	Timothy G. Murphy	M,H		
University College Cork	Cork	Patrick Fitzpatrick Jim Grannell Michael Quinlan	P P		H
University College Dublin	Belfield, Dublin	Ted Cox Maria Meehan		H	P
LITHUANIA					
Vilnius University	Vilnius	Ricardas Kudzma Antanas Mitasiunas Saulius Ragaisis Algirdas Zabulionis		P P P	
SOUTH AFRICA					
University of Stellenbosch	Matieland	J.H. Van Vuuren		P	

Acknowledgment

The editor wishes to thank Chia Tzun Goh '01 of Beloit College for his help in identifying family names of team advisors from China, for whom the family name is listed first.



关注数学模型
获取更多资讯



Deep Impact

Dominic Mazzoni

Matthew Fluet

Joel Miller

Harvey Mudd College

Claremont, CA 91711

Advisor: Michael Moody

Abstract

We consider the impact of a 1,000 m-diameter asteroid with the South Pole. Impacts of this magnitude can have substantial effects, including earthquakes and tsunamis on a regional scale and the possibilities of global climatic change and catastrophic agricultural damage from dust ejected into the atmosphere.

Luckily, an Antarctic collision would result in a far less disastrous scenario. By modeling the possible trajectories of the asteroid, we determined that the angle of incidence would be relatively small, resulting in a smaller, more shallow crater. Since Antarctica is covered by a thick ice cap, very little dust would be ejected into the atmosphere. The heat of the collision would melt an insignificant amount of ice. The worst scenario would be if the shock wave created by the impact resulted in a large tsunami, so we predict which coastal areas would be flooded.

Initial Assumptions

1. The asteroid is spherical, is 1,000 m in diameter, has a typical composition and density, and strikes the Earth at the South Pole.
2. The asteroid originated in our solar system and so before the collision was orbiting the Sun in the same plane as the Earth [Transcript—Plane of the Solar System 1996].
3. The only bodies significantly affecting the trajectory of the asteroid are the Sun, the Earth, and the Moon. The trajectories of the four bodies can be predicted using a Newtonian model of gravitation.

The UMAP Journal 20 (3) (1999) 211–224. ©Copyright 1999 by COMAP, Inc. All rights reserved. Permission to make digital or hard copies of part or all of this work for personal or classroom use is granted without fee provided that copies are not made or distributed for profit or commercial advantage and that copies bear this notice. Abstracting with credit is permitted, but copyrights for components of this work owned by others than COMAP must be honored. To copy otherwise, to republish, to post on servers, or to redistribute to lists requires prior permission from COMAP.



关注数学模型
获取更多资讯

4. Near the South Pole, the Antarctic ice cap is uniformly 2 km deep, has roughly constant density, and is at -76° C everywhere.

Properties of the Asteroid

Location, Angle, and Velocity of Impact

We investigate the relative probability of impacting at the South Pole vs. elsewhere. So we simulate the motions of the Sun, Earth, Moon, and asteroid, based on the Newtonian model of gravitation, in which

$$F = \frac{Gm_1m_2}{d^2}$$

describes the magnitude of the force F exerted on two masses, m_1 and m_2 separated by a distance d . The direction of the force is along a straight line connecting the center of mass of each object. The universal gravitational constant G has the value $6.67259 \times 10^{-20} \text{ km}^3 \text{ s}^{-2} \text{ kg}^{-1}$. Gravitational force accelerates a body according to $\vec{a} = \vec{F}/m$. This acceleration changes the body's velocity \vec{v} , which in turn affects the body's position \vec{x} .

We use a time-discretized numerical simulation. The location $\vec{x}_{i,t+\Delta t}$ of a body i at time $t + \Delta t$ is calculated using the locations and masses of the other planetary bodies in addition to the location, velocity, and mass of body i at time t . In particular, we perform the following calculations on each body in the system:

$$\begin{aligned}\vec{F} &= \sum_{j,j \neq i} \frac{Gm_i m_j}{|\vec{x}_{i,t} - \vec{x}_{j,t}|^2} \times \frac{\vec{x}_{i,t} - \vec{x}_{j,t}}{|\vec{x}_{i,t} - \vec{x}_{j,t}|} \\ \vec{a}_{i,t+\Delta t} &= \frac{\vec{F}}{m_i} \\ \vec{v}_{i,t+\Delta t} &= \vec{v}_{i,t} + \vec{a}_{i,t+\Delta t} \times \Delta t \\ \vec{x}_{i,t+\Delta t} &= \vec{x}_{i,t} + \vec{v}_{i,t+\Delta t} \times \Delta t + \frac{1}{2} \vec{a}_{i,t+\Delta t} \times (\Delta t)^2.\end{aligned}$$

The Sun, Earth, and Moon initially have the characteristics in **Table 1** [Lide 1992, 14–26, 14–27].

We choose our coordinate system with the Sun at the origin and both the Earth and the Moon in the xy -plane. By Assumption 1, the asteroid is spherical with diameter 1,000 m. Thus, it has volume of $V_{\text{ast}} = \frac{4}{3}\pi(0.5 \text{ km})^3$, or 0.524 km^3 . A typical asteroid has density $\rho_{\text{ast}} = 2.5 \times 10^{12} \text{ kg km}^{-3}$ [Toon et al. 1997, 44]. Thus, the asteroid has mass of $m_{\text{ast}} = 1.31 \times 10^{12} \text{ kg}$.

We distinguish between asteroids that approach the Earth from within the solar system plane (such as ones from the asteroid belt of the solar system) and those that approach from outside that plane. Would an asteroid approaching



Table 1.
Mass, radius, position, and speed of the Sun, Earth, and Moon.

	Sun	Earth	Moon
m_i	1.99×10^{30} kg	5.97×10^{24} kg	7.35×10^{23} kg
r_i	6.96×10^5 km	6.38×10^3 km	1.74×10^3 km
\vec{x}	(0, 0, 0) km	$\vec{x}_{\text{Sun}} + (1.50 \times 10^8, 0, 0)$ km	$\vec{x}_{\text{Earth}} + (0, 3.84 \times 10^5, 0)$ km
\vec{v}	(0, 0, 0) km s ⁻¹	$\vec{v}_{\text{Sun}} + (0, 29.8, 0)$ km s ⁻¹	$\vec{v}_{\text{Earth}} + (-1.02, 0, 0)$ km s ⁻¹

from outside the plane be more likely to hit the South Pole? To find out, we simulate both kinds of asteroids.

We place the asteroid at a random location 1.54×10^6 km (about four lunar distances away) from the Earth. We give the asteroid the same velocity that the Earth has relative to the Sun, as though the asteroid were falling through an orbit that coincides with that of the Earth. We put the asteroid on a collision course with the Earth by adding 10 km s⁻¹ to the asteroid's velocity in a direction towards a random point no more than 9.57×10^3 km from the center of the Earth (i.e., the asteroid is approaching a point contained within a sphere centered on the Earth with a radius 1.5 times that of the Earth).

We ran the simulation with $\Delta t = 10$ s. A collision occurred if the distance between the asteroid and the Earth was less than the sum of their radii. We calculate the latitude of the impact from the vector. The angle that the vector $\vec{x}_{\text{ast}} - \vec{x}_{\text{Earth}}$ makes with the xy -plane determines the latitude of the impact:

$$\begin{aligned} \Delta \vec{x} &= \vec{x}_{\text{ast}} - \vec{x}_{\text{Earth}} \\ \text{latitude} &= \arctan \left(\frac{\Delta \vec{x} \times (0, 0, 1)}{\sqrt{(\Delta \vec{x} \times (1, 0, 0))^2 + (\Delta \vec{x} \times (0, 1, 0))^2}} \right). \end{aligned}$$

Similarly, we calculate the angle of incidence and the velocity of the impact from the vectors $\vec{x}_{\text{ast}} - \vec{x}_{\text{Earth}}$ and $\vec{v}_{\text{ast}} - \vec{v}_{\text{Earth}}$, since the angle that the vector makes with the tangent plane of the Earth's surface at the point of impact is the angle of the impact, and the magnitude of this vector is the speed of impact:

$$\begin{aligned} \Delta \vec{x} &= \vec{x}_{\text{ast}} - \vec{x}_{\text{Earth}} \\ \Delta \vec{v} &= \vec{v}_{\text{ast}} - \vec{v}_{\text{Earth}} \\ \text{angle} &= -\arcsin \left(\frac{\Delta \vec{x}}{|\Delta \vec{x}|} \times \frac{\Delta \vec{v}}{|\Delta \vec{v}|} \right) \\ \text{speed} &= |\Delta \vec{v}| \end{aligned}$$

We ran 20,000 simulations of the asteroid, half for an asteroid approaching from within the solar system plane and half for an asteroid approaching from outside the plane. In both cases, slightly under one-fourth of the asteroids avoided colliding with the Earth. **Figure 1** shows the distribution by latitude of those hitting the Earth. For either approach, there is about a 1% chance of an asteroid impacting above 80° S.



关注数学模型
获取更多资讯

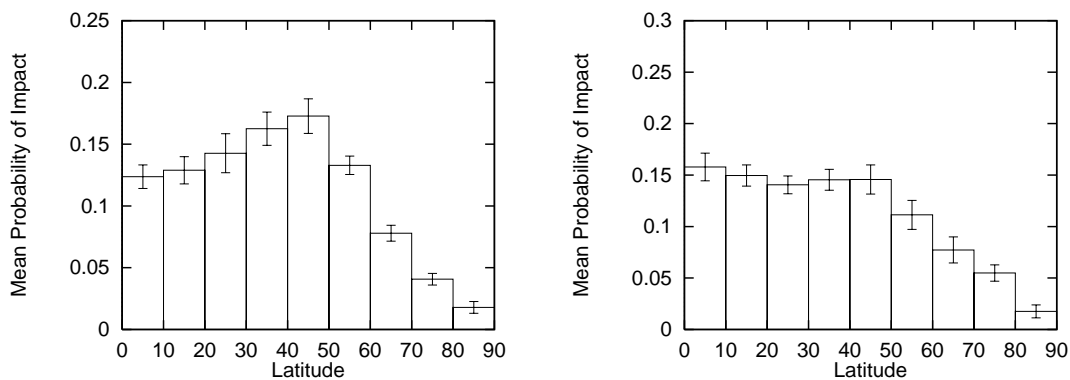


Figure 1. Probability of impact for asteroid from within the solar system plane (left) and from outside (right).

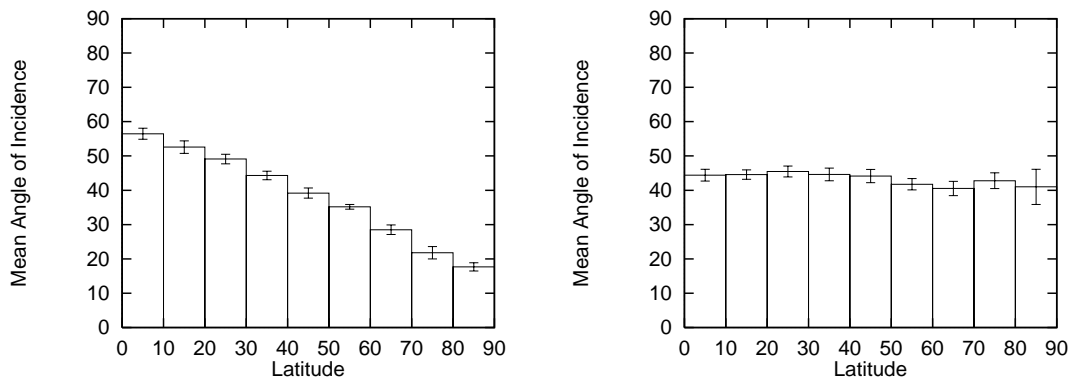


Figure 2. Angle of incidence for asteroid from within the solar system plane (left) and from outside (right).

However, an asteroid from within the solar system plane impacting in the highest latitude ranges is more likely to impact at a shallower angle: $18^\circ \pm 1^\circ$ vs. $41^\circ \pm 5^\circ$ (see **Figure 2**).

For asteroids with radii exceeding 100 m, air resistance is negligible; such asteroids hit the ground with most of their original kinetic energy [Hills and Mader 1995]. Our simulations show impact at a relative speed of 15 km/s, consistent with the literature [Chapman and Morrison 1994, 34].

The calculations do not take into account the Earth's tilt relative to the *xy*-plane (about 22°), since we have no information about the time of year of the collision. Hence, the probability of impact at the South Pole cannot be taken simply by reading the height of the bar in **Figure 1**, nor can the expected angle of incidence be read directly from **Figure 2**.



Dynamics of Collision

Using the calculated mass of 1.31×10^{12} kg and the velocity of 15 km/s, we find that the energy of the asteroid reaching the Earth's atmosphere is

$$E = \frac{mv^2}{2} = \frac{(1.31 \times 10^{12} \text{ kg})(15 \text{ km/s})^2}{2} = 1.5 \times 10^{20} \text{ Joules.}$$

This is equivalent to 3.5×10^4 megatons (MT) of TNT. (If the collision were with a comet rather than an asteroid, the speed of impact would be 50 km/s; but because of the comet's lesser density of 1 g/cm, the energy of impact would be slightly less [Toon et al. 1997, 44].)

The ice cover over Antarctica makes predicting the size of the crater problematic. For impacts on land, Toon gives the following two formulas for the expected value of the diameter of the crater (km):

$$D = 0.64 \left(\frac{Y}{\rho_t} \right)^{1/3.4} \left(\frac{20000}{v_i} \right)^{0.1} (\cos \theta)^{0.5} \left(\frac{\rho_i}{\rho_t} \right)^{0.083},$$

$$D = 0.53 c_f \left(\frac{Y}{\rho_t} \right)^{1/3.4} (\cos \theta)^{2/3},$$

where

Y is the energy in megatons,

ρ_t is the density of the target,

ρ_i is the density of the impactor,

v_i is the speed of the impactor,

c_f is a correction factor with value approximately 1.37, and

θ is the angle of impact [1997, 45].

The value $\theta = 18^\circ$ from our model for an asteroid from within the plane of the solar system is probably a little low, because asteroids are likely to have some perturbation from the plane. Hence we use $\theta = 30^\circ$. With a density of 0.9 g/cm³ for ice, both formulas give a crater diameter of about 15 km.

Since a crater for a "typical" asteroid has a depth-to-diameter ratio of about 1:5 or 1:7 [Terrestrial Impact Craters 1999], a crater of this diameter would have a depth of 2.5 to 3 km. However, a "typical" asteroid does not hit at as shallow an angle as the asteroid of our model, which plows through a large swath of the ice to create a crater that is wider but not as deep. If, despite its reduced downward momentum, the asteroid were to break through the ice, it would encounter a much denser bedrock 2 to 2.5 km deep; so we do not expect the crater to be much deeper than 2 km.



关注数学模型
获取更多资讯

Since ice melts more readily than the rock, we could be underestimating the size of the crater. Ice around the South Pole has a depth of 2 km and an average temperature of -76°C . A crater of diameter 15 km and average depth just 1 km would displace about 175 km^3 of ice. However, melting so much ice is unlikely. Also, the collision would send a large amount of ice/water, and some bedrock, into the atmosphere, but less rock than if the asteroid hit another continent.

Effects on Antarctica

The effects of an asteroid hitting Antarctica would be profoundly different from those of a collision elsewhere. Although Antarctica is far from most centers of population, the melting of the ice cap is a concern. Our calculations use the data of **Table 2**.

Table 2.
Data on the Antarctic ice cap.

Feature	Size	Source
Volume	$30 \times 10^6 \text{ km}^3$	Virtual Antarctica [1999]
Area	$14 \times 10^6 \text{ km}^2$	World Factbook [1998]
Avg. thickness	2 km	Computerworld Antarctica [1999]
Avg. temperature	-76°C	Assumption 4

In theory, a large-enough collision could melt the entire ice cap, raising the water level of the world's oceans by 70 m [Computerworld Antarctica 1999]. Assume for the moment that all of the energy produced in the collision were converted to heat. To calculate the volume of ice that could be melted by the collision, we need some thermal properties of water (see **Table 3**).

Table 3.
Thermal properties of water, from Lide [1992, 6-172, 6-174].

Phase	Conductivity ($\text{Wm}^{-1}\text{K}^{-1}$)	Specific Heat c ($\text{J K}^{-1}\text{kg}^{-1}$)	$k/c\rho$ (m^2s^{-1})
Ice	1.88	2030	9.26×10^{-7}
Water	0.61	4810	1.27×10^{-7}
Vapor	0.027	2020	1.34×10^{-8}
Enthalpy of Fusion		$3.33 \times 10^5 \text{ J kg}^{-1}$	
Enthalpy of Vaporization		$2.26 \times 10^6 \text{ J kg}^{-1}$	

Let us suppose that all of the $1.5 \times 10^{20} \text{ J}$ of collision energy raised the temperature of mass M_{ice} of ice to 0°C and melted the ice, without heating the resulting water. Then we have:

$$1.5 \times 10^{20} \text{ J} = (273.2 \text{ K} - 197.2 \text{ K}) \times 2030 \text{ J K}^{-1} \text{ kg} \times M_{\text{ice}} + 3.33 \times 10^5 \text{ J kg}^{-1} \times M_{\text{ice}}.$$



Solving gives $M_{\text{ice}} = 3.1 \times 10^{14}$ kg of ice. Using a density of 0.9 g/cm^3 for ice, the impact would melt 340 km^3 of ice, slightly more than $1/100,000$ of the total volume of the Antarctic ice cap! If all of the water could reach the ocean, it would raise the levels of the oceans by less than 1 mm. However, since the South Pole is over 500 km from the nearest Antarctic coast, it is unlikely that *any* of the water would reach the ocean.

For a more accurate model of the heat in the Antarctic ice cap, let us suppose that all 1.5×10^{20} J of the energy raises the temperature of the ice beneath the asteroid, which we approximate by a cylinder of diameter 1 km. The mass of ice under a circle 1 km in diameter would be 1.5×10^{12} kg.

- The energy to heat the ice by 76° C (to its melting point) would be the mass times the temperature change times the specific heat of ice, giving 2.31×10^{17} J.
- The enthalpy of fusion of ice is $3.33 \times 10^5 \text{ J/kg}$, so the energy to melt the ice would be 5.00×10^{17} J.
- Raising the ice another 100° C would expend 7.2×10^{17} J.
- Vaporizing the water at boiling point would expend 3.39×10^{18} J (the enthalpy of vaporization is $2.26 \times 10^6 \text{ J/kg}$).

Subtracting these four numbers from the initial energy still would leave 1.46×10^{20} J. If we assume that all of the remaining energy would be used to heat the water vapor, we find (by applying the specific heat of water vapor) that the water vapor could be raised to $48,000^\circ \text{ C}$.

It is unlikely that all of the energy of the impact would go into heating the ice, and some of the water vapor would escape before passing on its heat to the surrounding ice, so this model gives a huge overestimate of the effects of the collision.

The Heat Equation

We model the spread of the temperature distribution by using the heat equation. Since the ice sheet is an average of only 2 km thick but more than 6,000 km wide, we model it using just two dimensions. Let $u(x, y, t)$ represent the temperature ($^\circ \text{C}$) of the ice sheet at position (x, y) (meters) at time t (seconds). Set the coordinate system so that $u(0, 0, 0)$ is the temperature of the center of the impact location at the time of impact. In the heat equation

$$\frac{\partial u}{\partial t} = \frac{k}{c\rho} \left(\frac{\partial^2 u}{\partial x^2} + \frac{\partial^2 u}{\partial y^2} \right),$$

the constant k is the thermal conductivity of the substance, c is the specific heat, and ρ is the density. Because all three values change as the ice turns to water and then to vapor, the only way to solve this equation is numerically. We use a



关注数学模型
获取更多资讯

method based on an algorithm given in Burden and Faires [1997]. Let the time step between successive iterations be Δt and let the physical distances between temperature readings be Δx and Δy . To derive the method of finite differences, first consider the Taylor series approximations of u in t , x , and y :

$$\begin{aligned}\frac{\partial}{\partial t} u(x, y, t) &= \frac{u(x, y, t + \Delta t) - u(x, y, t)}{\Delta t} - \frac{\Delta t}{2} \frac{\partial^2}{\partial t^2} u(x, y, \tau), \\ \frac{\partial^2}{\partial x^2} u(x, y, t) &= \frac{u(x + \Delta x, y, t) - 2u(x, y, t) + u(x - \Delta x, y, t)}{(\Delta x)^2} - \frac{(\Delta x)^2}{12} \frac{\partial^4}{\partial x^4} u(\chi, y, t), \\ \frac{\partial^2}{\partial y^2} u(x, y, t) &= \frac{u(x, y + \Delta y, t) - 2u(x, y, t) + u(x, y - \Delta y, t)}{(\Delta y)^2} - \frac{(\Delta y)^2}{12} \frac{\partial^4}{\partial y^4} u(x, \psi, t),\end{aligned}$$

for some $\tau \in (t, t + \Delta t)$, $\chi \in (x - \Delta x, x + \Delta x)$, and $\psi \in (y - \Delta y, y + \Delta y)$. Let us assume that $\Delta x = \Delta y$, so that we can combine more terms. Substituting these into the partial differential equation, and separating out the error terms as $E(x, y, t)$, yields the following relations:

$$\begin{aligned}\frac{u(x, y, t + \Delta t) - u(x, y, t)}{\Delta t} &= \\ \frac{k}{c\rho} \left(\frac{u(x + \Delta x, y, t) + u(x - \Delta x, y, t) + u(x, y + \Delta y, t) + u(x, y - \Delta y, t) - 4u(x, y, t)}{(\Delta x)^2} \right), \\ E(x, y, t) &= \frac{\Delta t}{2} \frac{\partial^2}{\partial t^2} u(x, y, \tau) - \frac{k}{c\rho} \frac{(\Delta x)^2}{12} \left(\frac{\partial^4}{\partial x^4} u(\chi, y, t) + \frac{\partial^4}{\partial y^4} u(x, \psi, t) \right).\end{aligned}$$

The constants can be grouped into a single term K :

$$K = \frac{k}{c\rho} \frac{\Delta t}{(\Delta x)^2}.$$

Then solving the first equation for $u(x, y, t + \Delta t)$ yields the following equation, which allows us to solve for the temperature distribution at time $t + \Delta t$ given the distribution at time t :

$$\begin{aligned}u(x, y, t + \Delta t) &= u(x, y, t) (1 - 4K) + K (u(x + \Delta x, y, t) + u(x - \Delta x, y, t) \\ &\quad + u(x, y + \Delta y, t) + u(x, y - \Delta y, t) - 4u(x, y, t)).\end{aligned}$$

Simulation Results

We wrote a computer program in C to solve this equation for an initial temperature distribution of -76° C everywhere except for a circular region of diameter 1 km, to which we gave an initial temperature of $48,000^\circ$ C. We discovered that if all of the hot water vapor remained in place (instead of rising into the atmosphere, as we would expect), it could at most melt 5.7×10^7 m 3 of ice (enough to raise the ocean level by 2×10^{-7} m), and melting this much would take more than 10 days! Long before then, one would expect everything



to cool off. Even the water that would melt would have a difficult time reaching the ocean, because much of the surface of Antarctica has been pushed below sea level by the enormous weight of the ice [Virtual Antarctica 1999].

The results of the simulation are not too surprising once one considers the order of magnitude difference in the thermal conductivities of ice and water. The initial heat melts a large amount of ice fairly quickly, but the rate of temperature increase slows rapidly as the temperature rises, reaching almost an equilibrium at less than 100° C. The process provides a layer of insulation between the hot vapor that was supposed to transfer the heat and the surrounding ice, which is now adjacent to just very warm water. As that ice melts, it does not transmit much heat to the next layer of ice.

Conclusion: The last thing that we need to worry about is any significant amount of ice melting.

Antarctic Ecosystem

The waters around Antarctica are inhabited by small crustaceans called krill, which are central to the food chain in this region. Small differences in water temperature, or any natural disaster that upsets the balance of nature, could affect their population, with global repercussions. However, since little ice would melt and there would be no other significant long-term effects of the collision, our best estimate is that nature would repair itself over time.

Effects on a Global Scale

Tsunami

One of the most significant things we need to worry about is the possibility that the collision would cause an earthquake large enough to start a tsunami (tidal wave), which tends to be more severe if caused by a disturbance near the surface. Tsunamis can measure 10 to 30 m in height but extend 4 to 5 km from front to back [Monastersky 1998b], and they typically travel at about 800 km/hr [Monastersky 1998a]. (Technically, the word “tsunami” refers to a large wave that has slowed down and increased in height as it hits a continental shelf before a coastline, but we use the term in a broader sense to refer to any large wave with the potential of becoming a tsunami.)

Tsunamis are extremely hard to forecast. It is not the magnitude of the earthquake that determines the height of the wave, but rather the frequency; in particular, the cause is long-period vibrations over time that drive the wave up higher and higher [Monastersky 1998a]. When the waves hit the coastline, they rise up even higher and flood the land with a wall of water, causing mass destruction. Between 1992 and 1997, 1,200 lives were lost as a result of tsunamis in the Pacific; and the July 1998 tsunami in Papua New Guinea claimed at least



关注数学模型
获取更多资讯

2,500 more. A primary reason for loss of life is little to no warning of the tsunami's approach.

A tsunami caused by an asteroid impact in Antarctica would take more than an hour to reach the southernmost tip of South America, and we would know far in advance of the approach of an asteroid of that size (within 10 years, 90% of Earth-orbit-crossing asteroids of this size should be identified and their orbits should be plotted [Asteroid Comet Impact Hazards 1999].) Therefore, human casualties could be almost completely avoided by evacuating coastal areas.

The maximum distance that a tsunami travels inland can be determined from its height when it hits the shore, the depth of the water at the shoreline, the roughness of the terrain, and the slope of the shore away from the coast. As an example, for a terrain corresponding to a typical developed area, a 40-m tsunami could travel inland about 9 km, and a 100-m one could travel inland about 100 km [Hills and Mader 1995].

An accurate simulation of a tsunami on a global scale would require complicated fluid-dynamics equations, but these simulations would be meaningless without extremely good initial data. Instead, we created a much simpler model. Assume that the shock wave caused by the asteroid collision would travel through the Antarctic continent quickly enough that it would reach the coastline at all places at approximately the same time. Then the initial wave-front would take on the shape of Antarctica and travel north. Consider a two-dimensional grid of lattice points representing the surface of the Earth. Label each point initially as either water or land. Points that represent water are given two variables: a height (a scalar) and a direction of wave motion (a vector). Initially, all points representing water are given zero height and no direction, except for a wavefront at the border of Antarctica directed away from the continent at all points. Each time step, the waves propagate in the direction of motion and interfere constructively or destructively with other parts of the wave. Unless acted upon by another wavefront, water above sea level falls back towards the ocean.

This model of a tsunami is limited, but it is about as much as can be expected without more information on the type of earthquake that might cause the tsunami to start. **Figure 3** shows the output of our computer simulation of the tsunami at various moments in time.

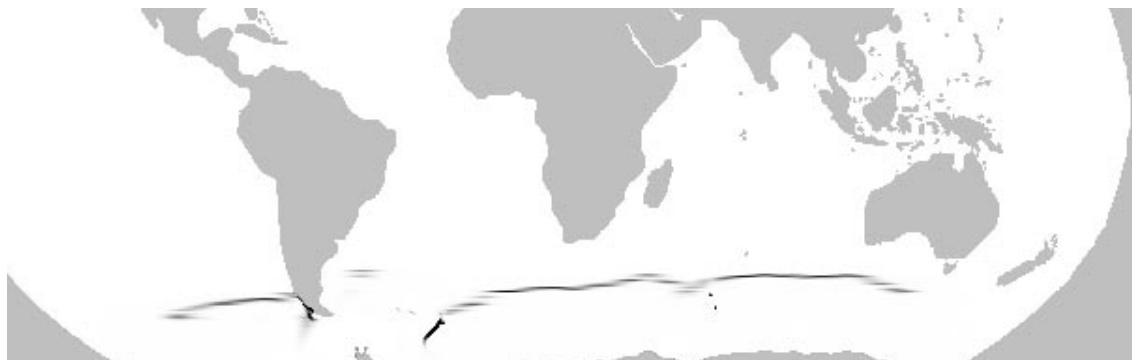
While the exact locations of coastal flooding are unpredictable, some general trends can be observed:

- The west coast of South America is more likely to be flooded than the east coast, mostly because of the shape of the Antarctic Peninsula.
- The southern-facing borders of Africa, Madagascar, India, and Australia have nothing in their way, so they are likely to be flooded.
- Both the east coast of North America and most of Europe are shielded from the tsunami and need not evacuate.





One hour after impact. The shape of the Antarctic Peninsula has caused the wave to avoid hitting the southeastern coast of South America.



One hour later. The tsunami has struck South America.



Hours later. The tsunami has flooded parts of Africa and Australia.



Final image, showing all flooded coastlines in black.

Figure 3. Computer-generated model of tsunami waveform.



关注数学模型
获取更多资讯

Dust and Ice Loading

To the person living in Tibet, a tsunami doesn't much matter. But if huge amounts of dust were released into the atmosphere, Tibetans would find the weather unusually cold, and the plants that they depend on for food would stop photosynthesizing and die. This effect worldwide could destroy all traces of civilization.

We can see from volcanic activity what dust can do. On 15 June 1993, Mt. Pinatubo in the Philippines erupted. It had the largest effect on the particulate levels in the atmosphere of any event this century [McCormick et al. 1995, 399]. An asteroid hitting land with energy of 10^4 MT of TNT would send up about the same amount of dust; with energy of 10^5 MT of TNT, it would produce results similar to the eruption in Tambora in 1815 [Toon et al. 1992, 59]. Pinatubo lowered global temperatures by about 0.5°C [McCormick et al. 1995] and Tambora by 0.75°C [Tambora, Indonesia, 1815 1999].

This gives us a rough bracketing of what to expect from our asteroid with energy 3.4×10^4 MT of TNT, though hitting the thick ice sheet at a shallow angle should produce less dust than striking another continent.

The dust put into the atmosphere would not have sufficient energy to go into orbit and so would spread around through the atmosphere [Toon et al. 1992, 57]. We expect the spread of dust to be restricted by the prevailing winds, which create bands blowing in opposing directions. To cross from the South Pole to the Northern Hemisphere by following prevailing winds, the dust would have to change altitude significantly several times. It took 2 to 3 months for the dust from the Pinatubo eruption to spread from the equator to the Northern and Southern Hemispheres. We would expect a similar (if not greater) time lag for transporting dust from the South Pole to the Northern Hemisphere.

While the dust from the impact would have consequences to the global climate, it is unlikely to be of a magnitude to damage civilization significantly. It would have moderate and temporary effects on agriculture, particularly in the Southern Hemisphere.

In addition to the dust, a significant amount of ice would be put into the atmosphere. A substantial part of this would become rain or snow and fall back to Earth, possibly removing some of the dust from the atmosphere. Increased water vapor would lower the temperature in the upper atmosphere, because water is a strong infrared radiator, causing more water vapor to condense and precipitate out [Toon et al. 1992, 68–69].

An impact in the ocean with energy of 10^4 MT of TNT would about double the amount of water in the ambient upper atmosphere. This would have a minor greenhouse effect that would be somewhat canceled by ice clouds blocking the sun. It would not have any significant impact unless it lasted longer than the 10-year response time of the oceans to temperature change [Toon et al. 1992, 69].



关注数学模型
获取更多资讯

Conclusions

An asteroid 1000 m in diameter could cause a serious global disaster. An impact near a heavily populated area could cause mass destruction and loss of life, and an ocean collision could create a tremendous tsunami. If an asteroid were to strike a continent not near the poles, it could send up enough dust into the atmosphere to cause long-term environmental damage. Compared to any of these scenarios, an Antarctic collision would be far less disastrous.

The angle of incidence would likely be small for an asteroid originating in our solar system, creating a wider, shallower crater than if it hit perpendicularly. Because the ice cap is 2 km thick at the South Pole, most of what would get thrown into the atmosphere is shards of ice, not dust. Escaping dust would not travel north to more populated areas, because of the prevailing wind currents. The ice that would reach the atmosphere could cause a greenhouse effect, but only if it remained for many years; it is likely that much of it would fall in the form of rain.

The possibility of a tsunami is real but impossible to predict. Our model predicts the possible flood locations, but these simulations would need to be done in greater detail with a more accurate model of the world and a more sophisticated model of a tsunami. In any event, because of advance warning, coastal areas could be evacuated. Serious flooding could damage millions of square kilometers of food production regions, but these effects would be short-term.

One would hope for enough warning to evacuate the 4,000 people on Antarctica doing exploration and scientific research.

References

- Asteroid Comet Impact Hazards. 1999. <http://impact.arc.nasa.gov/index.html>.
- Burden, Richard L., and J. Douglas Faires. 1997. *Numerical Analysis*. New York: Brooks/Cole.
- Chapman, R.C., and D. Morrison. 1994. Impacts on the Earth by asteroids and comets: Assessing the hazard. *Nature* 367 (1994): 33–40.
- Computerworld Antarctica. 1999. <http://antarctica.computerworld.com/>.
- Hills, Jack G., and Charles L. Mader. 1995. Tsunami produced by the impacts of small asteroids. *Proceedings of the Planetary Defense Workshop*. Livermore, CA. Available at <http://www.llnl.gov/planetary>.
- Lide, David R., editor. 1992. *CRC Handbook of Chemistry and Physics*. 73rd ed. Boca Raton, FL: Chemical Rubber Company Press. Thermal properties of water: 6–172, 6–174.



关注数学模型
获取更多资讯

- McCormick, M.P., L.W. Thomason, and C.R. Trepte. 1995. Atmospheric effects of the Mt. Pinatubo eruption. *Nature* 373: 399–404.
- Monastersky, Richard. 1998a. How a middling quake made a giant tsunami. *Science News* 154 (1 August 1998): 69.
- _____. 1998b Waves of death: Why the New Guinea tsunami carries bad news for North America. *Science News* 154 (3 October 1998): 221–223.
- Montgomery, Carla W. 1995. *Environmental Geology*. 4th ed. Dubuque, IA: Wm. C. Brown Communications, Inc.
- Tambora, Indonesia, 1815. 1999. <http://volcano.und.nodak.edu/vwdocs/Gases/tambora.html>.
- Terrestrial Impact Craters.
<http://www.cpk.lv/hata/solarsys/solar/tercrate.htm>.
- Toon, O.B., R.P. Turco, and C. Covey. 1997. Environmental perturbations caused by the impacts of asteroids and comets. *Reviews of Geophysics* 35: 41–78.
- Transcript—Plane of the Solar System (October 20, 1996). 1996. <http://www.earthsky.com/1996/es961020.html>.
- Virtual Antarctica.
<http://www.terraquest.com/va/science/snow/snow.html>.
- World Factbook. 1998. <http://www.odci.gov/cia/publications/factbook/ay.html>.



关注数学模型
获取更多资讯

Asteroid Impact at the South Pole: A Model-Based Risk Assessment

Michael Rust
 Paul Sangiorgio
 Ian Weiner
 Harvey Mudd College
 Claremont, CA 91711

Advisor: Michael Moody

Introduction

We consider approximate upper bounds for the magnitude of various environmental consequences of a spherical iron asteroid with a diameter of 1,000 m impacting at the South Pole.

The increase in worldwide ocean levels would be on the order of a millimeter, except for the possibility of an unstable ice sheet being dislodged into the ocean. There would be global warming effects, though they would not be much greater than those caused by human-based industrial emissions. Significant amounts of acidic water vapor would likely be produced, and the subsequent precipitation of this acid rain in nearby fishing areas would disrupt ecosystems and lead to decreased fish harvests.

Simplifying Assumptions and Modeling

A Worst-Case Scenario

The possible consequences of the impact of a comparatively large asteroid on the Earth are immense in number and in potential impact. A practical model would treat quantitatively only those effects that can be characterized by well-understood physical processes. For each effect, we consider the upper limit of potential environmental impact. This method estimates the “worst-case scenario.”

The UMAP Journal 20 (3) (1999) 225–240. ©Copyright 1999 by COMAP, Inc. All rights reserved. Permission to make digital or hard copies of part or all of this work for personal or classroom use is granted without fee provided that copies are not made or distributed for profit or commercial advantage and that copies bear this notice. Abstracting with credit is permitted, but copyrights for components of this work owned by others than COMAP must be honored. To copy otherwise, to republish, to post on servers, or to redistribute to lists requires prior permission from COMAP.



关注数学模型
获取更多资讯

The Size and Composition of the Asteroid

We assume that the asteroid is spherical and made of iron. Although many near-Earth asteroids are composed of other materials [Kieffer 1980], an iron asteroid would pose the gravest threat, due to its high density, which implies a higher kinetic energy and hence a greater capacity to induce seismic shocks.

Velocities and Energies

We offer a celestial mechanics model to estimate the incident velocity of an asteroid on the Earth's outer atmosphere. To consider the descent of the asteroid, we present a detailed dynamical model to calculate impact velocities as well as to estimate the energy transferred to the atmosphere.

Ice Melting, Vaporization, and Ejection

The asteroid would impact in the heart of the largest reservoir of frozen water on the planet. How much ice would be liberated from the continent? We consider three likely routes by which ice may be affected directly:

- direct heating from the impact kinetic energy,
- melting and vaporization from the pressure wave released, and
- ice fragments breaking off the continent and entering the ocean.

To place upper bounds on these effects, we consider the cases of maximum possible energy transfer to each of these reservoirs. For the pressure wave and the ice fracturing, the bounds are less exact, since empirical estimates must be made of quantities such as the seismic efficiency.

Seismic Shocks and Ice

There is potential for the unstable western ice sheet to become dislodged, partially slip into the ocean, and melt, possibly having dramatic consequences for ocean levels. The calculation is accomplished using a simple wave-equation model for the shock wave and is sensitive to the empirically determined proportion of kinetic energy that goes into the pressure wave.

Climatic Changes from Atmospheric Water Vapor

A large asteroid impact into the ice would transfer much water vapor into the atmosphere, possibly creating an effect similar to the increased greenhouse gases that have raised the mean surface temperature of the Earth. We analyze these potentialities, treating the Earth as a blackbody radiator with a varying albedo.



Chemical Effects and Acid Rain

A final consideration is the production of chemicals in the atmosphere such as nitrous oxides, which can undergo later reactions to produce nitric acids and result in acid rain. Using empirical data for the rate of production of these compounds and the modeled atmospheric energy transfer, we estimate upper bounds on the acidity of rain in the region and for its effects.

Celestial Dynamics of the Asteroid

Gravity

By Newton's Law of Gravitation, the force of attraction between the asteroid and any body is

$$\mathbf{F} = -\frac{Gm_a M}{r^2} \hat{\mathbf{r}},$$

where G is the gravitational constant, m_a is the mass of the asteroid, M is the mass of the other body, and \mathbf{r} is a vector directed from the other body to the asteroid. Being a central force, \mathbf{F} may be written as the gradient of a scalar function ϕ :

$$\mathbf{F} = -\nabla\phi = -\nabla\left(-\frac{Gm_a M}{r}\right).$$

An integral of F over a path depends only on the endpoints of integration and not on the path itself. Because of this feature, ϕ is known as the *gravitational potential energy*. The work-energy theorem of classical mechanics implies the following relationship between the change in the kinetic energy T of the asteroid and the changes in gravitational potential energy for any physical process [Marion and Thornton 1995]:

$$\Delta T = \Delta\left(\frac{1}{2}m_a v^2\right) = \sum_i \Delta(\phi_i),$$

where the sum is over all bodies with which the asteroid is interacting.

A Lower Estimate of Asteroid Velocity

To obtain a lower estimate of the asteroid's impact velocity, we follow the approach of Melosh in using Earth's escape velocity [Melosh 1989]. The *escape velocity* for a planet is the velocity required for a body to escape completely from the planet's gravitational field. That is, the escape velocity corresponds to



the change in gravitational potential energy in bringing an object from infinity to the surface of the planet. We have

$$\frac{1}{2}m_a v^2 = \lim_{R \rightarrow \infty} Gm_a m_e \left(\frac{1}{r_e} - \frac{1}{R} \right),$$

where m_e and r_e are the mass and radius of the Earth. The asteroid does not come from infinity but more plausibly from the asteroid belt, perhaps 3 au from the Sun (1 au [“astronomical unit”] = mean radius of the orbit of the Earth).

This is a lower bound because we neglect both the previous kinetic energy of the asteroid in its orbit and its gravitational interaction with the Sun. We obtain 11.2 km/s for the speed of the asteroid (terminal velocity) upon impacting the outer atmosphere, using 32,000 m as the height of the atmosphere. This result is independent of the mass of the asteroid.

A More Realistic Estimate of Asteroid Velocity

A more realistic model of the asteroid’s incident velocity would include its interaction with the Sun and the kinetic energy of its orbit. We assume that the asteroid occupies a pre-collision orbit that is totally determined by its interaction with the Sun.

The Virial Theorem

The total energy of the asteroid’s orbit may be determined from the geometry of its orbit and the classical virial theorem. A result of the general equations of motion, the virial theorem states [Marion and Thornton 1995]:

$$T = -\frac{1}{2} \langle F \cdot r \rangle.$$

The right-hand side of the equation, called the *virial*, reduces in the case of a circular orbit in a central gravitational field to

$$-\frac{1}{2} \langle F \cdot r \rangle = -\frac{1}{2} \left(\frac{Gm_a m_{\text{Sun}}}{r^2} \hat{r} \cdot r \right) = -\frac{1}{2} \frac{Gm_a m_{\text{Sun}}}{r} = -\frac{1}{2} \phi.$$

Though the asteroid’s orbit is almost certainly not circular if it is to collide with Earth, we make the approximation of circularity to obtain a simple velocity estimate.

Total Energy of the Asteroid’s Orbit

Using the virial, we can write the total energy as

$$E = T + \phi = \frac{1}{2} \phi.$$



When the asteroid reaches the Earth, it is at a distance 1 au from the Sun. In this model, conservation of energy requires that the change in potential must be absorbed as kinetic energy of the asteroid.

$$\frac{1}{2}m_a v^2 = \frac{1}{2}\phi - \phi_{\text{at Earth}}$$

Again, the mass of the asteroid cancels out, since it appears in both ϕ and ϕ_{atEarth} . If the asteroid is from the midst of the asteroid belt, so that the average radius in the circular-orbit approximation is, say, 2.6 au [Gehrels 1979], we get a velocity of $v = 23.5$ km/s.

We have neglected the interaction with the gravitational field of the Earth. To obtain a total estimate, we add on the energy from the calculation of the Earth's terminal velocity. Our best estimate for the incident velocity is $v = 26$ km/s, in good agreement with impact data [Gehrels 1994; Kieffer 1980].

From Atmosphere to Impact

What would happen to the asteroid as it descended through the atmosphere? This question is of interest in determining both the kinetic energy on impact and the energy transferred to the atmosphere during the descent. This latter aspect is important because energy transfer plays a significant role in atmospheric chemistry [Melosh 1989].

Dynamical Equations

In describing the dynamics of the asteroid descent, we follow the approach of Melosh [1989]. By considering the physics of the descent, we acquire a simplified model consisting of four coupled nonlinear differential equations. We begin by introducing coordinates to specify the state of the system:

$v(t)$ is the speed of the asteroid;

$\theta(t)$ is the instantaneous angle that the trajectory makes with the horizon;

$m(t)$ is the mass of the asteroid, which changes in time due to ablation caused by heat generated by friction with the atmosphere; and

$Z(t)$ is the vertical altitude of the asteroid.

We also consider the following functions of the state variables:

$\rho_g(Z)$ is the density of air at the altitude of the asteroid, and

$A(m)$ is the cross-sectional area of the asteroid.



关注数学模型
获取更多资讯

The $v(t)$ Equation

The only forces that change the speed of the asteroid act along the line of motion. There is a component of gravity $g \sin \theta$ acting in the direction of motion, as well as a drag force retarding the motion. To calculate the drag force, we assume with Melosh that the air immediately behind the asteroid is at effectively zero pressure and that the air immediately in front is at the *stagnation pressure* $\rho_g v^2$ [Melosh 1989]. This pressure differential produces a force equal to $A \rho_g v^2$, where A is the cross-sectional area of the asteroid. Combining these forces with Newton's Second Law, we obtain the differential equation for $v(t)$:

$$v' = -\frac{A \rho_g v^2}{m} + g \sin \theta.$$

The $\theta(t)$ Equation

We approximate the surface of the Earth as flat. This assumption does not have significant consequences as long as θ is not particularly small, since the horizontal displacement is thus smaller than the curvature scale of the Earth's surface.

We assume that the only force acting perpendicular to the direction of motion is gravity. This neglects possible lift forces, but Melosh's analysis suggests that lift is small compared to the force of gravity [1989]. Suppose that the velocity vector of the asteroid undergoes a small perpendicular displacement denoted Δv_{\perp} . Then the change in the angle made with the horizontal $\Delta\theta$ is

$$\Delta\theta = \tan \left(\frac{\Delta v_{\perp}}{v} \right).$$

As we allow the size of the displacements to become infinitesimally small, we can neglect all but the first term in the Taylor series expansion of this function:

$$\Delta\theta \approx \frac{\Delta v_{\perp}}{v}.$$

But Δv_{\perp} for small changes is just the acceleration of the asteroid perpendicular to its motion times Δt . Since we assume that gravity is the only significant component to this acceleration, we obtain

$$\frac{\Delta\theta}{\Delta t} \approx \frac{g \cos \theta}{v}.$$

In the limit, we obtain the differential equation for θ

$$\theta' = \frac{g \cos \theta}{v}.$$



关注数学模型
获取更多资讯

The $m(t)$ Equation

The issue of ablation due to heating is less straightforward. Our approach follows that of Melosh [1989]. A calculation of the available energy due to the pressurized heating of the atmosphere tells us how much ablation could occur. Two dimensionless empirical parameters are involved: C_h , which is an *ablation efficiency*, and a term involving the velocity squared, $1 - (v_{\text{cr}}/v)^2$, which accounts for a critical speed v_{cr} below which ablation does not occur. The resulting differential equation is

$$m' = -\frac{C_h \rho_g A v}{2\zeta} \left(1 - \left(\frac{v_{\text{cr}}}{v}\right)^2\right),$$

where ζ is the heat of ablation for the material. For reasonable values of C_h and v_{cr} , Melosh gives empirically determined values of about 0.02 and 3,000 m/s.

The $Z(t)$ Equation

The equation for $Z(t)$ is particularly simple, resulting from purely kinematic considerations. We need only project the total speed v into its velocity component in the vertical direction. Since we approximate the surface of the Earth as a plane, this component is simply

$$Z' = -v \sin \theta.$$

Air Density and Cross-Sectional Area

To obtain $A(m)$, the cross-sectional area, we must presume a shape for the asteroid. Though many asteroids have large eccentricities [Gehrels 1979], modeling the impactor as a solid uniform ball has the advantage of being mathematically tractable as well as not too far from reality. From the geometric formula for the volume of a ball, the expression for the asteroid radius R in terms of its mass m and its density ρ is

$$R = \left(\frac{3}{4\pi} \frac{m}{\rho}\right)^{1/3}.$$

From this, the cross-sectional area $A = \pi R^2$ becomes

$$A = \left(\frac{9\pi}{16}\right)^{1/3} \left(\frac{m}{\rho}\right)^{2/3}.$$

To find an expression for $\rho_g(Z)$, we use a simple model in which the density decreases exponentially as altitude increases. A good value for the characteristic height scale of the atmosphere is 10 km [Melosh 1989]. Thus, we have

$$\rho_g = \rho_0 e^{Z/10},$$

where ρ_0 is the atmospheric density at sea level and Z is measured in kilometers.



关注数学模型
获取更多资讯

Numerical Solution

As promised, we have obtained a coupled set of nonlinear ordinary differential equations. Substituting the algebraic relations from the previous section removes dependence on A and ρ_g . With a given set of initial values for the height, angle, speed, and mass, we have an initial-value problem that completely specifies the physics of the asteroid descent.

Though some of the equations have simple cascade relationships to the other state variables, the nonlinearities make an analytic approach intractable. We solved the system using the fourth-order Runge-Kutta integration method in the software package ODE Architect, published by Intellipro.

Results

To obtain numerical results, we must take another step away from the world of theory toward empiricism, imposing additional constraints on the composition of the asteroid. We presume that the asteroid is composed of iron with approximate density $\rho = 2,600 \text{ kg/m}^3$. Many asteroids are largely iron [Gehrels 1979]; impacting on ice, iron creates some of the most severe pressure effects of any common asteroid composition [Kieffer 1980].

A solid iron ball of radius $R = 500 \text{ m}$ has a mass of approximately $1.4 \times 10^{12} \text{ kg}$. We use the estimated velocity of 26 km/s for an asteroid at a distance of $Z = 32,000 \text{ km}$ away from the Earth's surface.

Impact Velocity

Using the above parameter values, we consider the dynamics of an asteroid with initial angles of 30° , 45° , 60° , and 90° from the horizontal. Because the mass of the asteroid is comparatively large, we do not expect a large fraction of the asteroid's energy to be given up during the descent.

For all four trajectories, the final velocity decreases to $2.58 \times 10^4 \text{ m/s}$ and the mass to $1.38 \times 10^{12} \text{ kg}$, though, as shown in **Figures 1** and **2**, the incident angle has a significant effect on the flight time.

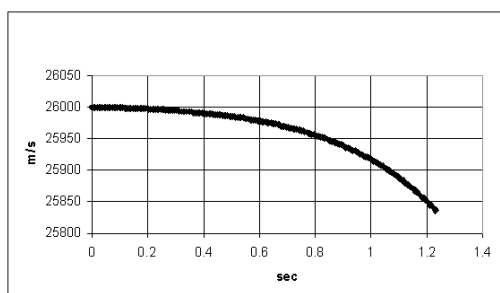


Figure 1. Initial angle of 90° .

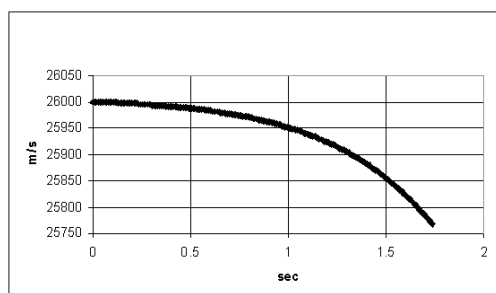


Figure 2. Initial angle of 45° .



关注数学模型
获取更多资讯

Atmospheric Energy Transfer

To obtain an upper bound on the energy transfer to the atmosphere, we again appeal to the tools of energy conservation. Neglecting the energy retained by ablated asteroid material, we obtain

$$E_{\text{to atm}} = \Delta T - mgZ = \frac{1}{2}m_f v_f^2 - \frac{1}{2}mv^2 - mgZ.$$

That is, whatever kinetic energy is lost by the asteroid must go somewhere, so that gravity, the only conservative force in effect, can be accounted for. Since Melosh finds 45° to be the most probable incident angle [1989], we take our calculations for 45° as representative.

With these data, we obtain an energy transfer of $E = 1.57 \times 10^{19}$ J, a figure which later has relevance to the treatment of environmental effects.

Effects on the Earth's Oceans

Introduction

Since the global-warming crisis came to the forefront of environmental thought in the mid-1980s, scientists have warned of the possibility of melting an Antarctic ice sheet and the inevitable catastrophic consequences. With regard to ice melting, the impact of a high-velocity asteroid with Antarctica could have two potentially disastrous results:

- the sheer amount of kinetic energy could vaporize a large amount of ice, which would eventually rain down into the ocean; or
- the collision could act as a pseudo-earthquake, generating seismic waves strong enough to break apart and move above-ground ice sheets, forcing large amounts of ice into the ocean.

Either of these events could potentially raise the water level by a significant amount. In addition, whenever there is a large seismic event, there is the possibility of a tsunami, which could have deadly consequences.

Vaporization of Ice

If we assume that all of the asteroid's kinetic energy is converted directly into thermal energy that is used solely for melting and vaporizing the ice, we can estimate an upper bound — however unrealistic — on the amount of water deposited into the Earth's atmosphere.

For ease of calculation, we first calculate the number of moles of H_2O vaporized by the impact. We assume that the ice is initially at -40° C . The amount



of energy needed to vaporize the ice is

$$\Delta H = \Delta H_{\text{H}_2\text{O at } -40^\circ} \rightarrow \text{H}_2\text{O at } 0^\circ + \Delta H_{\text{fusion}} + \Delta H_{\text{H}_2\text{O at } 0^\circ} \rightarrow \text{H}_2\text{O at } 100^\circ \\ + \Delta H_{\text{vaporization.}}$$

Using the values [Atkins and Jones 1997] specific heat of ice = $2.03 \text{ J}\cdot\text{C}^{-1}\cdot\text{g}^{-1}$, latent heat of fusion = $6.01 \text{ KJ}\cdot\text{mol}^{-1}$, specific heat of water = $4.18 \text{ J}\cdot\text{C}^{-1}\cdot\text{g}^{-1}$, and the latent heat of vaporization = $40.7 \text{ KJ}\cdot\text{mol}^{-1}$, we calculate the most that could be vaporized would be 5.03×10^{15} moles, or 9.05×10^{13} kg, of water. If this water were spread around the water-covered surface of the Earth—given that the radius of the Earth is approximately 6.4×10^6 m and the surface area covered by water is approximately 3.6×10^{14} m²—it would change the water level by only $\Delta h \approx 0.4$ mm. This amount is insignificant in comparison with seasonal changes, so we conclude that melting of the ice would have almost no effect on sea level.

Breaking Up of Ice Sheets

Given the very complex nature of the ice sheets on Antarctica, it is beyond the scope of this paper to give a detailed model of the amount of damage that a seismic wave generated by the impact could bring about. Melosh claims that based on geological evidence from previously studied asteroid impacts, the seismic efficiency, or fraction of impact energy converted into seismic energy, is on the order of 10^{-4} [1989]. Given an impact energy of 4×10^{20} J, the approximate seismic energy, as measured on the Richter scale, is $M \approx 7.9$. This is a significant earthquake, but Melosh also points out that this would produce mainly p-waves, while s-waves—the transverse waves created by the slipping of plates in an earthquake—are far more destructive. Therefore, he suggests that the damage of the pseudo-earthquake would be comparable to an actual earthquake of an order of magnitude less, in this case, an earthquake of magnitude 6.9.

Although a magnitude 6.9 earthquake is very large, we must consider that the nearest floating ice sheet to the South Pole, the Ross Ice Shelf, is nearly 400 km away. If we assume that all of the seismic energy radiates in a hemispherical pattern, then from the point of view of conservation of energy, we can say that at a distance r from the South Pole, the energy density, J , is

$$J = \frac{E_{\text{initial}}}{2\pi r^2}.$$

For $r = 400$ m and the initial seismic energy of a magnitude 6.9 earthquake, we find an energy density of 1.5 KJ/m^2 . This amount is equivalent to a large man falling five or six feet to the ground, which, considering the density of the ice, should not be that significant. This rough estimate is in agreement with observed impacts with the moon. Melosh claims that “few surface features on the moon or other planets can be directly attributed to impact-induced seismic



关注数学模型
获取更多资讯

shaking”[1989]. Still, the possibility that large chunks of ice could fall into the ocean is not negligible but is beyond the scope of this model.

Tsunami Generation

The generation of tsunamis by underground seismological events is poorly understood; their generation by land-based seismological events is even less understood. Many people have attempted to calculate the size of the water wave that would be created by a near-shore nuclear blast, yet the strength of the tsunami is always overestimated [Murty 1977]. If we also consider that by the time the shock wave would reach the ocean, over 1,000 km away, the energy density would be around 250 J/m^2 , then the chances of a dangerous oceanic shock wave are negligible.

Potential Impact on the Earth’s Climate

Introduction/General Modeling Concept

Many models of asteroid impact on land masses predict that a large dust cloud would be released into the atmosphere, causing massive global warming due to greenhouse effects. An asteroid’s impact on Antarctica would be substantially different in this respect. Antarctica is covered by an average of 2 km of ice, so little or no dust would be released. However, the rapid release of a large amount of water vapor into the Earth’s atmosphere has the potential to significantly alter climate, much as the release of greenhouse gases has stimulated global warming. We present here a simple climatic model of the Earth based on the assumption that the Sun and the Earth behave as blackbody radiators. This model allows us to determine a reasonable upper bound on potential global warming due to vapor injection.

The two defining characteristics of a blackbody radiator are:

- All radiation incident upon it is absorbed.
- Energy is re-radiated over the entire spectrum of wavelengths.

Through quantization of the radiation field, quantum theory tells us that the *radiancy*, or power per area, radiated by a blackbody is given by Stefan’s law:

$$R_T = \sigma T^4 \quad [\text{Eisberg and Resnick 1985}],$$

where σ is experimentally determined to be $5.67 \times 10^{-8} \text{ W/m}^2\cdot\text{K}^4$. We treat both the Sun and the Earth as ideal blackbody radiators; this treatment is commonly accepted as an accurate assumption for the purposes of global climate studies [Toon and Pollack 1980]. The majority of the light incident upon the Earth from the Sun is in the visible spectrum, while the light radiated from the Earth is



mostly in the infrared. For this reason, we model the atmosphere as a shell of particles with two distinct albedos: one for visible light, the other for infrared light. We denote the percentage of the Sun's light that is transmitted through to the Earth by K_{visible} and the percentage of the Earth's light transmitted out into space by K_{IR} . For the Earth to be in thermal equilibrium, the power entering the atmosphere must equal the power leaving, that is,

$$P_{\text{from Sun}} = P_{\text{reflected sunlight}} + P_{\text{transmitted from Earth}}.$$

The power that reaches the atmosphere from the Sun is just

$$\sigma T_{\text{Sun}}^4 \pi R_{\text{atm}}^2 R_{\text{Sun}}^2 / d^2,$$

where d is the distance from the Sun to the Earth's atmosphere and R_{atm} represents the radius of the Earth's atmosphere. The R_{Sun}^2/d^2 term in the equation accounts for the fact that the power from the Sun that actually reaches the Earth is determined by the solid angle subtended by the Earth. The πR_{atm}^2 term accounts for the effective area of the atmosphere that is exposed to the radiation, characterized by the cross section of the Earth. Using Stefan's law, we have the following relation for thermal equilibrium:

$$\sigma K_{\text{visible}} T_{\text{Sun}}^4 \pi R_{\text{atm}}^2 \frac{R_{\text{Sun}}^2}{d^2} = \sigma K_{\text{IR}} T_{\text{Earth}}^4.$$

Worst-Case Heating of the Atmosphere

Upon injection of water vapor into the upper atmosphere, the values of K_{visible} and K_{IR} can be expected to change significantly. We first concern ourselves with the worst-case heating of the atmosphere due to water vapor. In this case, the vapor would act to reflect the Earth's infrared radiation back to the surface, causing a greenhouse effect corresponding to a decrease in K_{IR} and/or an increase in K_{visible} . From our general equation for equilibrium, we see that

$$T_{\text{Earth}} \propto \left(\frac{K_{\text{visible}}}{K_{\text{IR}}} \right)^{1/4},$$

which follows from the fact that all other quantities of interest would remain constant. To place an upper bound on potential global heating, we make the simplifying assumption that $K_{\text{visible}}/K_{\text{IR}}$ is directly proportional to the amount of water vapor in the atmosphere. This is not a completely unreasonable assumption; Toon and Pollack note that "the radiation budget of the Earth is dominated by water vapor and clouds" [1980]. For an upper bound on the effects, we take the vapor released to be the maximal amount, roughly 9×10^{13} kg, calculated in the previous section. According to Trewartha, the average moisture in the atmosphere is about 1.31×10^{16} kg, yielding an increase of about 0.69% [1954]. Using Trewartha's value for the mean global blackbody temperature of 287 K, we find that the equilibrium value for the temperature of the



关注数学模型
获取更多资讯

Earth after water injection is 287.50 K, an increase of half a degree. Such climatic changes are roughly equivalent to the already observed increase in global mean temperature due to global warming [Oppenheimer 1998]; and while it is not a totally insignificant consequence of impact, the effects would merely accelerate the global warming that is already underway.

Worst-Case Cooling of the Atmosphere

Although it is less likely that the injection of water into the atmosphere could exhibit a cooling effect, it has been suggested by some sources that, below a certain threshold droplet size, and high enough in the atmosphere, water could act to reflect the Sun's light, thus causing a trend of overall cooling [Toon and Pollack 1980]. We can show, using our simple atmospheric model, that the worst-case cooling effect is negligible. Returning to our general equilibrium expression, we see that

$$T_{\text{Earth}} \propto \left(\frac{K_{\text{visible}}}{K_{\text{IR}}} \right)^{1/4}.$$

Using the simplifying assumption this time that $K_{\text{visible}}/K_{\text{IR}}$ is *inversely* proportional to the amount of vapor in the atmosphere, we find once again, that there is roughly a decrease of half a degree in global mean temperature. Not only would such an effect be negligible, but it would actually work to counteract the global warming process underway.

Conclusions/Limitations of Climatic Model

The predictions of our model suggest that the worst-case climatic changes to the atmosphere would be a change in global mean temperature of roughly $\pm 1/2$ K. We state a few limitations of this simple model.

- First, the calculations are based on water that is vaporized by the energy of the asteroid. In actuality, there would likely be some ice ejecta mechanically propelled into the atmosphere by the impact. However, this effect should fit within our upper bound, because the ratio of energy to mass of water required to overcome the Earth's gravity, in addition to the energy expended by the damping effect of traversing the atmosphere itself (which would likely vaporize the ice particles), is substantially higher than the ratio for merely vaporizing the water. In addition, somewhat less than the maximum possible amount of water would be vaporized, since much of the asteroid's energy would be dissipated elsewhere.
- The model offers only an equilibrium value for the temperature of the Earth; the climatic changes are gradual, not sudden. Due to the large thermal mass of the Earth's oceans, temperature effects on the scale of global warming could take more than a decade to reach equilibrium [Toon and Pollack 1980].



关注数学模型
获取更多资讯

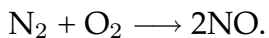
- Finally, the model assumes that the percentages of light transmitted are proportional to the amount of water vapor in the atmosphere. Ignoring other particles in the atmosphere has the effect of making the predicted climatic changes worse than they might be in reality, which is acceptable, given the modest climatic changes predicted. The assumption that the percentages are merely proportional, however, is somewhat simplistic, given the complex nature of the atmosphere. This assumption is the most severe limitation on the model.

Nitric Acid Contamination

Generation of Nitrous Oxide

As the asteroid passes through the atmosphere, it is likely that the heat generated would cause nitric oxide to be generated. The nitric oxide would subsequently form nitric acid, possibly leading to severe acid rain in the vicinity of the impact.

A reaction that forms nitric oxide in the air is



The energy required for this reaction is 173.1 kJ per mole of NO generated [Atkins and Jones 1997]. The theoretical maximum amount of NO that can be generated is therefore about 1.73×10^{-7} kg/J. However, according to Melosh, the actual amount generated is closer to 7×10^{-9} kg/J [1989]. Using the amount of energy released into the atmosphere calculated previously, we find that 1.1×10^{11} kg, or 3.66×10^{13} moles, of NO would be produced. This NO would react in the atmosphere to produce nitric acid, HNO₃.

A Simple Lower Bound on Acid Rain Damage

We can get an idea of the minimum amount of damage that this nitric oxide production could cause by assuming that each mole of NO produced becomes a mole of nitric acid and that the nitric acid is homogeneously distributed into five years' worth of rain throughout the globe. The estimate of five years is based on Toon's assertion that it would take about five years to remove the nitric acid generated by a large impact from the atmosphere [Gehrels 1994]. The average yearly rainfall over the Earth is 5×10^{20} g of H₂O/year [Gehrels 1994]. This corresponds to 5×10^{17} L of water, yielding a molarity of 14.6 micromolar. Toon notes that many regions in Europe and the eastern United States receive acid rain at more than 100 micromolar [Toon and Pollack 1980]. Therefore, the effects of such a minimum damage scenario would be negligible.



关注数学模型
获取更多资讯

Upper Bound on Acidification of the Earth's Oceans

If we assume that the nitric acid would find its way into the surface layers of the Earth's oceans, we can predict what percentage of the world's oceans would be rendered corrosively acidic. We define "corrosively acidic" as a 600 micromolar solution of nitric acid in water; this is the nitric-acid concentration necessary to dissolve calcite [Gehrels 1994]. We take the depth of "surface layers" to be 75 m, as suggested by Toon [Gehrels 1994]. Using the surface area of the Earth covered by water, we find the total volume of surface layer water to be $2.7 \times 10^{16} \text{ m}^3$. The density of water is $5.5 \times 10^4 \text{ mol/m}^3$; so 0.23% of the Earth's oceans could, in principle, be rendered corrosively acidic, corresponding to an area of about $8.2 \times 10^{11} \text{ m}^2$ of ocean, or a cylinder of water with a radius of about 510 km. For a relatively strong acid such as HNO₃, we expect the pH of the water to be close to the negative log of the molarity, which yields a pH value of 3.2. The actual value, however, is likely to be higher because of the buffering effect of the salt in ocean water. According to Howells, a pH of 3.5 to 4.0 will kill almost any fish [1995].

Conclusions

A large quantity of nitric acid would likely be released into the oceans surrounding Antarctica. This release would likely devastate the fish population of the region, including Australia and the southernmost parts of South America. It is difficult to determine the exact effects because of the lack of data regarding acid rain pollution of seawater environments.

Conclusions and Limitations of the Models

The models that we developed are focused on placing an upper-bound estimate on the damage that could occur if a 1,000 m-diameter asteroid were to impact the South Pole. Using Newtonian mechanics, we estimated the probable impact velocity of the asteroid and the energy released from the asteroid onto the Earth. These estimates allow us to place an upper bound on many of the possible destructive consequences of the impact.

The primary concern associated with impact is the potential raising of the water levels of the Earth's oceans. A simple argument based on energy conservation demonstrates that the water vapor created by the impact would not substantially raise the level of the Earth's oceans. Another argument demonstrates that the seismic shock waves generated would likely have little effect on the ice sheets near the Antarctic coast, although there is always the possibility of instabilities in the ice sheet structure, which is not accounted for by the model.

Another significant cause for concern is the long-term climatic impact of the asteroid. While very little dust is expected to be released into the atmosphere, a large quantity of water vapor almost certainly would be. Calculations show,



关注数学模型
获取更多资讯

however, that the upper bound on climatic changes amounts to, at most, the same climatic changes of about 0.5 K that are a consequence of current global warming. Therefore, while global warming would be accelerated somewhat, it is not a primary concern. The model implicitly assumes that the albedo of the Earth's atmosphere is simply proportional to the amount of water vapor it holds.

The major cause for concern, according to our model, is the large quantities of nitric acid that would be released on the oceans surrounding Antarctica. These waters would be contaminated with enough nitric acid to completely destroy their food-production capabilities.

References

- Atkins, P., and Loretta Jones. 1997. *Chemistry: Molecules, Matter, and Change*. New York, NY: W.H. Freeman and Co.
- Eisberg, Robert, and Robert Resnick. 1985. *Quantum Physics of Atoms, Molecules, Solids, Nuclei, and Particles*. New York, NY: John Wiley and Sons.
- Gehrels, Tom, editor. 1979. *Asteroids*. Tucson, AZ: University of Arizona Press.
- _____, editor. 1994. *Hazards Due to Comets and Asteroids*. Tucson, AZ: University of Arizona Press.
- Howells, G. 1995. *Acid Rain and Acid Waters*. Great Britain: Ellis Horwood Limited.
- Kagan, Boris A. 1995. *Ocean-Atmosphere Interaction and Climate Modelling*. New York, NY: Cambridge University Press.
- Kieffer, Susan Werner. 1980. The role of volatiles and lithology in the impact cratering process. *Reviews of Geophysics and Space Physics* 18 (1): 143–181.
- Marion, Jerry B., and Stephen T. Thornton. 1995. *Classical Dynamics of Particles and Systems*. Fort Worth, TX: Saunders College Publishing.
- Melosh, H.J. 1989. *Impact Cratering*. New York, NY: Oxford University Press.
- Murty, T.S. 1977. *Seismic Sea Waves: Tsunamis*. Canada: Ministry of Supply and Services.
- Oppenheimer, Michael. 1998. Global warming and the stability of the west Antarctic ice sheet. *Nature* 393: 325–332.
- Toon, Owen B., and James B. Pollack. 1980. Atmospheric aerosols. *American Scientist* 68: 268–277.
- Trewartha, Glenn T. 1954. *An Introduction to Climate*. New York, NY: McGraw-Hill Book Company.



关注数学模型
获取更多资讯

Antarctic Asteroid Effects

Nicholas R. Baeth

Andrew M. Meyers

Jacob E. Nelson

Pacific Lutheran University

Tacoma, WA 98447

Advisor: Rachid Benkhalti

Motivation for the Model

The only type of energy expansion relatively similar in scale to an asteroid impact is a nuclear explosion. The National Research Council (NRC) assessed the impacts of nuclear war on the atmosphere [Press et al. 1985], and their report details the potential for major atmospheric effects for blasts of various sizes. Our model extrapolates these effects for much higher yields.

We calculate the energy yield of the asteroid impact using Newtonian mechanics. We then use the NRC findings to estimate the impacts of such a yield. Finally, we assess human casualties from the impact in terms of food production, rising sea levels, and atmospheric fluctuations.

Initial Assumptions

- The asteroid is 1 km in diameter at impact.
- The asteroid is approximately spherical. A different shape would affect air drag and thus impact velocity but little else. Hence, a nonspherical asteroid is equivalent to a spherical asteroid with a different velocity.
- The asteroid has a density of between 2 and 8 g/cm³, typical of a stony meteorite or asteroid [Wasson 1974].
- The asteroid's velocity when striking the earth is between 11 and 70 km/s [Wasson 1974].
- The Earth-asteroid collision is inelastic.

The UMAP Journal 20 (3) (1999) 241–252. ©Copyright 1999 by COMAP, Inc. All rights reserved. Permission to make digital or hard copies of part or all of this work for personal or classroom use is granted without fee provided that copies are not made or distributed for profit or commercial advantage and that copies bear this notice. Abstracting with credit is permitted, but copyrights for components of this work owned by others than COMAP must be honored. To copy otherwise, to republish, to post on servers, or to redistribute to lists requires prior permission from COMAP.



关注数学模型
获取更多资讯

- The crater produced by the impact has a parabolic shape. This is consistent with models in King [1976].
- There is no great difference in effect due to the angle of impact. We assume that pieces of the asteroid burnt away during descent are significantly less important than the impact itself; an asteroid reduced in this way should be equivalent to a spherical asteroid of a different velocity.
- The explosion of impact is similar to a nuclear blast.

Table 1.
Symbols used in equations.

Symbol	Description	Units
α	Nitric oxide constant	0.8×10^{32} (molecules NO)/MT
C	Initial amount of nitric oxide post-impact	mol
D	Diameter of crater	m
d	Density of asteroid	kg/m ³
ΔT	Change in temperature	°C/yr
G	Greenhouse constant	0.007°C/yr
k	Joule-kiloton proportion constant	4.2×10^{12} J/kT
KE	Kinetic energy of asteroid at impact	Joules (= kg·m ² /s ²)
M	Mass of asteroid	kg
ω	Percentage of ozone lost	—
ρ	Ratio of diameter to depth	—
V_{asteroid}	Volume of asteroid	m ³
V_{crater}	Volume of crater	m ³
v	Velocity of asteroid at impact	m/s
w	Ejecta of H ₂ O into atmosphere	mol

Impact

Diameter of the Crater

The diameter of the crater depends on the kinetic energy of the asteroid. A basic Newtonian formula gives the kinetic energy of the asteroid as

$$\text{KE} = \frac{1}{2} Mv^2.$$

The mass is simply the volume multiplied by the density, giving

$$\text{KE} = \frac{1}{2} V_{\text{asteroid}} dv^2.$$

For a spherical asteroid, the volume is

$$V_{\text{asteroid}} = \frac{4}{3} \pi r^3.$$



The diameter of the crater, according to Wasson [1974], is

$$D = 49W^{0.294},$$

where W is the total work done by the asteroid on the Earth, in kilotons of TNT. Thus, to find the diameter, we substitute kinetic energy for total work:

$$D = 49 \left(\frac{1}{2} V dv^2 k \right)^{0.294},$$

where k is a proportionality constant that converts Joules to kilotons of TNT:

$$k = \frac{1}{4.2 \times 10^{12}} \frac{\text{kT}}{\text{J}}.$$

Thus, the diameter depends on the volume of the asteroid, its density, and the velocity at which it impacts the South Pole. See **Table 2** for different scenarios for varying densities (2, 3, 5, and 8 g/cm³) and velocities.

Table 2.
Scenarios.

Scenario	Asteroid			Crater			
	Velocity v km/s	Mass M $\times 10^{12}$ kg	Energy $\times 10^4$ MT	Diameter $\times 10^3$ m	ρ	Volume $\times 10^{10}$ m ³	Depth $\times 10^3$ m
A	11	1.05	1.51	8.27	5	4.44	1.67
		2.62	3.76				
		4.14	6.02				
	20	2.62	7.48				
B	20	1.57	12.5	10.1	7	9.22	1.44
	30	1.57	16.8				
C	30	2.62	28.1	11.8	7	18.6	1.69
	50	1.57	46.7				
D	50	2.62	78.1	20.2	8	12.9	2.53

Volume of the Crater

Let the crater have a diameter-to-depth ratio of ρ ; according to King [1976], $5 \leq \rho \leq 8$. Thus the crater has radius of $D/2$ and depth D/ρ .

We assume that the crater is a paraboloidal cap with cross-sectional parabola

$$y = Ax^2.$$

Algebraic manipulation gives

$$y = \frac{4}{\rho D} x^2.$$



关注数学模型
获取更多资讯

We rotate the parabola around the y -axis and use circular disks to find the volume of the paraboloidal cap:

$$V_{\text{crater}} = \int_0^{D/\rho} \pi x^2 y \, dy = \int_0^{D/\rho} \frac{\pi \rho D}{4} y \, dy = \frac{\pi D^3}{8\rho}.$$

For a density of 3.0 g/cm^3 and an impact velocity of 20 km/sec , we find that the crater has volume $9.22 \times 10^{10} \text{ m}^3$.

Effects of Impact

We first look at how much water would be ejected by the impact and then consider the effects of the shock wave created by impact.

Ejecta

We assume that due to the depth of the ice at the South Pole, the amount of dust ejected from the crater would be minimal. However, the amount of ice ejected is a different matter. For this, we look at the effects of nuclear blasts and ejections of dust with diameter less than one micrometer.

In nuclear blasts, about 1% of the volume of the crater is ejected into the stratosphere [Press et al. 1985]. We assume that ice would eject at a higher rate than dust because instead of rock, this asteroid would vaporize ice—a much easier task. So we use 5% of the volume of the crater as the total amount of ejecta (water as vapor, water, and ice) into the stratosphere.

The amount of dust vapor from a nuclear blast of 1 MT or less is between 0.2 and $0.5 \times 10^{12} \text{ g/MT}$ [Press et al. 1985]. For Scenario B (an average case), with energy 7.5×10^4 megatons, a yield of 5% of volume gives $0.06 \times 10^{12} \text{ g/MT}$.

Some dust would be ejected into the atmosphere, some would come from the asteroid itself, and some could even from Antarctic soil if the depth of the crater exceeds the depth of the ice (2,800 m)—but this last does not occur in any of our scenarios (see last column of **Table 2**).

Shock Waves

At impact, a spherical shock wave would be emitted, affecting both land and air but at different rates. Most effects of the impact would come from the shock wave rather than from the ejecta. We discuss the effects of the shock wave in terms of overpressurization, a thermal radiation contour, and the making of nitric oxide.



关注数学模型
获取更多资讯

Overpressurization

According to Press et al. [1985], an area is “overpressurized” if the shock wave creates a 5 psi (pounds per square inch) increase over normal atmospheric pressure.

Table 3 provides sample radii of overpressurization, given certain energy levels. The Ross Ice Shelf is 600 km, and the West Ice Shelf is 2600 km, from the impact site. Overpressurization past these points would overstress the respective ice shelves, possibly causing massive volumes of ice to break off and float into the ocean.

In addition to the ice shelves, there are more massive ice sheets that hold the vast majority of water in the continent. The Western Ice Sheet may be unstable [Glacier . . . 1999; Is Global Warming . . . 1999], and overpressurization of the sheet could cause much of it to break off from the continent.

Table 3.

Shock wave effect radii in km, from regression on the yield x in kilotons.

Scenario	Overpressure radius $r_o = 8.62010 + 0.132189x$ ($\times 10^3$ km)	Incineration radius $r_i = 2.50300 + 0.247767x$ ($\times 10^3$ km)
A	1.26	1.72
B	1.77	2.43
C	3.44	4.71
D	5.73	7.85

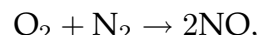
Thermal radiation contour

The shock wave also would create a 30 cal/cm^2 thermal radiation contour. This is essentially a heat wave; there is little on the Antarctic plain that would incinerate, but the heat would instantaneously melt the surface ice. Much of the water would refreeze as quickly as it melted, but water that doesn’t refreeze quickly could account for additional water vapor in the air.

At higher energy levels, the incineration radius encompasses large portions of South America and could lead to forest fires (see **Table 3**).

Nitric Oxide Emission

From Press et al. [1985], we know that large blasts create and release large volumes of nitric oxide (NO) into the stratosphere. The chemical reaction is



and NO is produced at a rate of

$$\alpha = 0.8 \times 10^{32} \text{ molecules NO/MT}.$$

Table 4 uses this rate to give the amounts of NO that would result from explosions of various megatonnage.



Table 4.
Quantities of H₂O and NO (in moles) lofted by explosion.

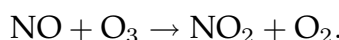
Scenario	H ₂ O	NO
A	1.22×10^{14}	5.0×10^{12}
B	2.56×10^{14}	9.93×10^{12}
C	5.16×10^{14}	3.74×10^{13}
D	3.58×10^{14}	1.04×10^{14}

Atmospheric Effects

The impact would have major consequences in the upper levels of the atmosphere, including a significant decline in stratospheric ozone. Also, some nitric oxide would convert into nitric acid and cause acid rain.

Ozone

The atmosphere currently contains 3.3×10^{15} g of ozone. With the emission of nitric oxide caused by the heat created by the impact, a significant amount of stratospheric ozone would decompose into nitrogen dioxide and oxygen, according to the reaction



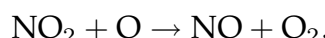
From how much nitric oxide is put into the air and the rate at which it reacts with ozone, we can find how much ozone would decompose and how fast.

The amount of nitric oxide emitted by the shockwave is αE , where E is the energy of the explosion given in megatons.

Normally in the atmosphere, 99% of the nitric oxide reacts with ozone to form nitrogen dioxide and oxygen. However, given the substantial amount of water displaced into the stratosphere by the asteroid, we predict that only 97% of the NO would react with O₃. Thus, the rate at which NO is lost over time due to reaction is given by

$$\frac{d(\text{NO})}{dt} = -0.03(\text{NO}). \quad (1)$$

The nitrogen dioxide produced by the reaction is reconverted into nitric oxide (NO) according to



Thus, nitric oxide is replenished naturally after reacting with ozone.

Solving (1), we get

$$\text{NO} = Ce^{-0.03t}, \quad (2)$$

where C is the initial amount of nitric oxide after the explosion. The normal amount of NO in the atmosphere is 10^{10} moles. To judge the effects of additional



NO in the atmosphere, we need the time for the NO levels to return to normal (see **Table 5**).

Table 5.
NO normalization time.

Scenario	Time (days)
A	207
B	230
C	274
D	308

Since ozone reacts with NO in a one-to-one ratio of molecules, the area under the curve of (2) yields the mass of ozone (in moles) that is decomposed:

$$\int_0^t C e^{-0.03t} dt.$$

Solving, we find that all of the ozone would be depleted long before NO levels return to normal. **Table 6** shows estimates of ozone depletion from nuclear blasts. Regression on **Table 6** gives a fairly linear fit, which produces results similar to our own.

Table 6.
Nuclear war ozone depletion estimates, from Press et al. [1985].

Scenario	Yield (MT)	Maximum Ozone Depletion (%)
Baseline	6,500	17
Excursion	8,500	43
Chang Case A	10,600	51
Chang Case B	5,300	32
Chang Case C	5,670	42
Chang Case D	4,930	16
Chang Case E	6,720	39
Chang Case F	3,890	20
<i>Ambio</i> excursion	10,000	65
Turco et al. (1983)	10,000	50

Acid Rain

The other 3% of NO reacts in the stratosphere first to form NO_2 and then with water to form nitric acid:



Only 3% of NO converts to HNO_3 , and only 3.8% of HNO_3 turns into a cloud form [Walker 1977]. Therefore, only 0.114% of the NO turns into acid rain.



关注数学模型
获取更多资讯

However, this concentration is much higher than that of normal acid rain. The usual concentration of HNO_3 in water vapor is 30 ppb [Walker 1977]. **Table 7** shows the different concentrations of HNO_3 in water vapor after varying scenarios.

Table 7.

Acid rain; the usual $\text{HNO}_3/\text{H}_2\text{O}$ is 30 parts per *billion*.

Scenario	$\text{HNO}_3/\text{H}_2\text{O}$ (ppm)
A	46
B	44
C	83
D	330

Environmental Impacts

Global Warming

With the complete loss of the ozone, it is safe to say that catastrophic events would occur, especially with respect to global climate. Let ω stand for the percentage loss of ozone. Let G stand for the “greenhouse constant,” which is the amount of temperature increase given no ozone depletion. Thus, our model equation is given by

$$\Delta T = G + \zeta\omega,$$

where ζ is a proportionality constant. By experimentation (of others), we find that $G \approx 0.007^\circ \text{C}/\text{yr}$. Earth’s climate has increased approximately 4°C over a twenty-year period. In that time, the ozone level decreased by 4%, giving $\omega \approx 0.04$. Solving for ζ gives $\zeta \approx 4.83$. Thus, our equation for the change in temperature in $^\circ\text{C}/\text{year}$ given ω is

$$\Delta T = 0.007 + 4.83\omega.$$

This model works nicely but only for small values of ω . When $\omega \geq 0.2$, as in our scenarios, the model loses most of its usefulness. The temperature increase due to a lack of ozone would be large and pose a threat to human existence.

Sea Levels

One of the major concerns of global warming theorists is the effect of polar melting and a change in sea level. A rise of 1 cm in sea level would salinize coastal rivers up to 1 km inland [Glacier . . . 1999]. The melting of the Western Ice Sheet of Antarctica would cause a 6 m rise. Having no ozone would



关注数学模型
获取更多资讯

eventually lead to these events. Besides the Western Ice Sheet, there are many other ice formations in Antarctica that could be affected by global warming. If all of Antarctica's ice melted, sea level would rise 60 m. Other possible causes of a rise in sea level are the overpressurization of Antarctic ice and the thermal radiation contour created by the blast. The thermal radiation contour might weaken the ice, and the overpressurization would then break the ice off the continent.

Our model predicts that the oceans would rise 7 to 10 m within 10 years. This would cause most small island countries to become uninhabitable. Coastal seaports would be flooded all over the world. With no ozone in the atmosphere, this rise would surely continue over the following years.

Food Supplies

The impact would significantly decrease crop yields, because of the rise in sea level, the rise in temperature, and the overabundance of ultraviolet radiation.

The rise in the sea level would wipe out all crops in coastal regions, especially in Brazil, southeastern China, the Mediterranean, and India. Salinization of coastal rivers would significantly reduce the amount of irrigation that can be done, thus affecting the midwestern United States along with interior Africa.

The desalinization of the ocean due to the melting of polar ice caps would significantly affect the South Atlantic, South Pacific, and Indian Oceans. This desalinization would pose serious health risks to shallow-water fish and other sea life that relies on salt water. Thus, fishing would significantly decrease off the coasts of South America, Africa, the Indian Peninsula, and Southeast Asia.

The rise in temperature and the overabundance of UV would also greatly affect all plant and animal life. Since this change is so rapid, the threat of extinction of multiple species would be imminent.

Impacts to Humans

Crops highly affected would be ones requiring lots of fresh water, such as rice, corn, grain, bananas, coffee, sugar, and other staples. The regions most affected would be those that grow enough just to support their own nations, not those that export these staples. Nations such as Brazil, China, India, and much of the non-industrialized world would find a severe lack of food. Countries like the United States, which have enough grain and corn to export, would barely be able to sustain themselves, much less export food to other countries. Much of North Africa, the Middle East, Central Asia, and central South America, which have little natural arable land, would indubitably starve. The impact of this alone could cause the population in those areas to suffer tremendous losses.

For example, "soybean yield may drop one percent for each one percent drop in ozone" [Hidore 1996]. By extrapolation, a complete loss of the ozone



关注数学模型
获取更多资讯

layer would result in the complete loss of soybean crops. The same holds true for many other crops. Even if the loss were not this drastic, most of the world's crop production would be lost.

The severe increase in ultraviolet radiation would significantly impact the entire planet. According to Hidore [1996], "models show that a 16% reduction in ozone will result in a 44% increase in UVB radiation. A 30% global reduction in ozone will produce a doubling of surface UVB radiation." A 100% loss of ozone would more than sextuple the amount of radiation, given a linear model. "The EPA forecasts that for every 1% decrease in the ozone layer, there will be a 3% increase in non-melanoma skin cancer." Hence non-melanoma skin cancer cases would triple under our scenario.

A rise of sea levels of 7 to 10 m would displace the half of the world's population that resides near coastlines. Most of this would occur in India and Southeast Asia. Other major seaports such as New York, Tampa, Rio, Bangladesh, Cape Town, and Cairo would also be affected. This major relocation of people would lead to massive overcrowding in the rest of the world and impose on land designated for the growing of crops and the raising of livestock.

Although less likely, a very serious threat that could threaten the population of southern Chile and Argentina is a large-scale earthquake. The shock wave, if large enough (Scenario D), would overpressurize the Tierra del Fuego and surrounding areas. This could also create tsunamis that would ravage the coasts in this area.

Other Effects

Our model concentrates mostly on atmospheric effects of the asteroid's impact, but focuses little on two areas of possible importance: severe cloud cover and tsunami. Severe cloud cover caused by the tremendous amount of water vapor and/or dust ejected into the stratosphere could cover the earth for several months. However, since the average water cloud lasts for only an hour, the probability of long-term cloud cover is minimal. The force of the impact itself and the shockwaves from the explosion, or even ice shelves falling into the ocean, might cause enough seismic disturbance to create a tsunami. Such a tsunami could immediately threaten coastal areas in the Southern Hemisphere, resulting in severe flooding along the coasts of South America, Southern Africa, India, and Southeast Asia.

Strengths and Weakness of the Analysis

Strengths

The greatest strength of the model is the ease with which the equations are derived and can be recalculated given different scenarios, such as a smaller or



larger asteroid. The model also incorporates the significant parameters of the impact, including velocity and density of the asteroid.

Weaknesses

The greatest weakness is the model's simplicity. Our model does not take into account carbon dioxide effects in terms of global warming, deal with desalinization of the ocean currents, nor calculate the pH difference due to a significant amount of HNO_3 being displaced due to acid rain.

In basing our modeling on smaller-scale detonations, we extrapolate into uncharted territory, which could very easily lead us to overestimate or underestimate the impacts of the asteroid.

Conclusions

Since our model suggests that the environment would be ravaged by such an impact, that sea levels would rise due to global warming and the breaking off of Antarctic ice sheets, and that a severe loss of food due to flooding and salinization of previously freshwater coastal river would occur, the probability of a substantial number of deaths is quite high.

Our model shows significant damage done to staple crops (such as soybeans) and a significant increase in ocean temperature, along with desalinization due to ice melting and rain. In the short term, we predict a 7 to 10 m rise in sea level, with a long term forecast of a 60 m rise with the complete melting of the Antarctic ice sheets.

Human deaths would result from multiple factors:

- Flooding would destroy much of the coastal regions of the earth. Half of the Earth's population would be displaced to higher and less arable ground.
- The tripling of UV-B radiation would certainly shorten the life expectancy of humankind.
- There would be an intense increase in the world's mean temperature, which has not happened since the dawn of man.

It is hard to picture the drastic conclusions that we have reached because we have no experience with events of this nature. We certainly hope that science can find a way to prevent such an event.

References

Asteroid and Comet Impact Hazards: Spaceguard Survey. 1991.

http://impact.arc.nasa.gov/reports/spaceguard/sg_2.html.



关注数学模型
获取更多资讯

- Congressional Testimony. 1993.
http://impact.arc.nasa.gov/congress/1993_mar/dmorrison.html.
- Evans, Daniel J., et al. 1992. *Policy Implications of Greenhouse Warming*. Washington DC: National Academy Press.
- Glacier: The Ice Sheet Today. 1999.
http://glacier.rice.edu/land/5_antarcticicesheetparts.html.
- Hidore, John J. 1996. *Global Environmental Change: Its Nature and Impact*. Upper Saddle River, NJ: Prentice Hall.
- Hills, Jack G., and Charles L. Mader. 1995. Tsunami produced by the impacts of small asteroids. In *Proceedings of the Planetary Defense Workshop*. Livermore, CA. Available at <http://llnl.gov/planetary>.
- Is Global Warming Melting Antarctica? 1999.
<http://livingearth.com/Home/Antarctica.html>.
- Isobe, Syuzo, and Makoto Yoshikawa. 1995. Colliding asteroids with very short warning time. In *Proceedings of the Planetary Defense Workshop*. Livermore, CA. Available at <http://llnl.gov/planetary>.
- King, Elbert A. 1976. *Space Geology: An Introduction*. New York: John Wiley & Sons.
- Litvinov, B.V., et al. 1995. Investigation of cavities and craters formed as the result of nuclear explosions for the purpose of solving the problem of Earth protection against near-Earth objects. In *Proceedings of the Planetary Defense Workshop*. Livermore, CA. Available at <http://llnl.gov/planetary>.
- Nemtchinov, I.V., et al. 1995. Historical evidence of recent impacts on the Earth. In *Proceedings of the Planetary Defense Workshop*. Livermore, CA. Available at <http://llnl.gov/planetary>.
- Press, Frank, et al. 1985. *The Effects on the Atmosphere of a Major Nuclear Exchange*. Washington DC: National Academy Press, 1985.
- Sea Level Rise. 1999.
<http://fao.org/waicent/faoinfo/sustdev/Eldirect/Elre0046.htm>.
- Shapley, Deborah. 1985. *The Seventh Continent: Antarctica in a Resource Age*. Washington, DC: Resources for the Future.
- Toon, Owen B., et al. Environmental perturbations caused by the impacts of asteroids and comets. In *Proceedings of the Planetary Defense Workshop*. Livermore, CA. Available at <http://llnl.gov/planetary>.
- Walker, James C.G. 1977. *Evolution of the Atmosphere*. New York: Macmillan.
- Ward, Peter D. 1995. Impacts and mass extinctions. In *Proceedings of the Planetary Defense Workshop*. Livermore, CA. Available at <http://llnl.gov/planetary>.
- Wasson, J.T. 1974. *Meteorites: Classification and Properties*. New York: Springer-Verlag.



关注数学模型
获取更多资讯

Not an Armageddon

Mikhail Khlystov

Ilya Shpitser

Seth Sulivant

University of California–Berkeley

Berkeley, CA 94720

Advisor: Rainer K. Sachs

Abstract

We separate the effects of the impact into three periods.

- **Pre-impact** Loss of kinetic energy due to air resistance as the asteroid travels through the atmosphere is less than 0.15%, which is negligible.
- **Short-term**
 - The impact could produce at most 2,940 km³ of liquid water, which is not sufficient to affect sea level.
 - The maximum volume of ice turned to water vapor would be 383 km³, insufficient to cause long-term weather changes.
 - We anticipate global seismic effects on the order of 4 to 6 on the Richter scale, depending on the velocity and composition of the asteroid and the distance from the South Pole.
- **Long-term**
 - Even in the worst case, the water vapor introduced to the atmosphere would condense and precipitate quickly, due to the low dewpoint of the polar air and the presence of iron particles to serve as condensation nuclei. We are uncertain as to the effects of iron fallout on the ecology of the Southern Hemisphere.
 - There would be moderate loss of life and property damage in the southern hemisphere. We remain uncertain as to the ecological effects of such an impact but suspect that they would be negligible. We expect that there would be no threats of coastal flooding due to asteroid impact.

The UMAP Journal 20 (3) (1999) 253–261. ©Copyright 1999 by COMAP, Inc. All rights reserved. Permission to make digital or hard copies of part or all of this work for personal or classroom use is granted without fee provided that copies are not made or distributed for profit or commercial advantage and that copies bear this notice. Abstracting with credit is permitted, but copyrights for components of this work owned by others than COMAP must be honored. To copy otherwise, to republish, to post on servers, or to redistribute to lists requires prior permission from COMAP.



关注数学模型
获取更多资讯

Assumptions

- The asteroid is spherical in shape (this shape maximizes the asteroid's mass, and therefore its kinetic energy and the impact effects).
- The asteroid has an approximate diameter of 1 km.
- The asteroid strikes at the South Pole.
- Since an asteroid that "strikes the earth" does not explode in the atmosphere or rebound off the atmosphere (like a stone skipping on water), we assume that the angle of entry must be greater than 10° .
- The asteroid is primarily composed of iron and nickel. While this assumption is slightly inaccurate (other constituents being varieties of minerals, such as silica and magnesia), it facilitates calculations; because these are the densest materials in an asteroid, this composition results in the greatest mass and thus the greatest energy of impact. The average density of such an asteroid is $5,000 \text{ kg/m}^3$. Moreover, an asteroid composed primarily of iron is significantly less likely to explode before impact.
- The energy of impact of an asteroid is divided between heating the target, heating the asteroid, deformation, and kinetic energy of ejecta. This assumption comes from the 1978 NASA Conference Proceedings on Asteroids [Morrison and Wells 1978, 148].
- The energy of an earthquake is inversely proportional to the square of the distance from the epicenter.
- Seismic waves propagate mainly along the surface of the earth, rather than in a straight line between two points on the surface.
- The depth of ice at the South Pole is approximately 2.5 km.

Model Inputs

- Density of asteroid (depending upon its composition), ρ_{ast}
- Velocity of the asteroid at impact, V_0
- Angle of entry, α
- Initial average temperature of the ice at the South Pole, T_{in}

Other inputs are the percentages of kinetic energy that go into:

- Heating the asteroid, H_{ast}
- Heating the planet (ice), H_{ice}



- Energy of deformation, E_{def} , and
- Kinetic energy of the ejecta, E_{eje} .

Atmospheric Entrance Model

We calculate how much energy is transferred from the kinetic energy of the asteroid to heating the asteroid via air resistance.

$$\text{Mass : } M_{\text{ast}} = \rho_{\text{ast}} \pi d_{\text{ast}}^3 / 6$$

$$\text{Kinetic energy of impact : } KE = M_{\text{ast}} V_0^2 / 2$$

The kinetic energy converted to heating the asteroid, due to air resistance, is

$$KE = \frac{10^5 C A V^2}{6 \ln 10 \sin \alpha},$$

where c is a physical constant based on viscosity and density of air, v is velocity, A is the cross-sectional area of the asteroid, and the rest is a factor corresponding to the changing density of air as the asteroid enters the atmosphere. (We derive this formula in the **Appendix**.)

Entrance Results

The fraction of kinetic energy turned into heat energy by the air resistance would be only 0.02% to 0.15%; therefore, the effect of air resistance would not be significant.

Impact Model

We compute

- the mass of the evaporated water, $M_{\text{H}_2\text{O}}$;
- the size of the impact crater, D_{cra} ;
- the mass of ejected debris from the impact, M_{eje} ; and
- the approximate Richter value of the shock wave generated by the impact and the earthquake intensities felt at certain southern hemisphere cities.

We proceed in the following fashion:

Mass: $M_{\text{ast}} = \rho_{\text{ast}} \pi d_{\text{ast}}^3 / 6$

Kinetic energy of impact: $KE = M_{\text{ast}} V_0^2 / 2$



Crater diameter: $d_{\text{cra}} = (\text{KE}/k)^{2/7}$ [Davies 1986, 103], with $k \approx 10^{15}$. (We estimated this proportionality constant based upon experimental data on size and kinetic energy involved in the formation of craters given in Davies.)

Volume of crater ejecta: Since crater depth is approximately one-tenth of the diameter [Verschuur 1996, 17], we have $\text{Vol}_{\text{cra}} = \pi d_{\text{cra}}^3/40$.

Approximate earthquake forces: These calculations are based on a linear regression (of data gathered from the Cascades Volcanoes Observatory Home-page [1999]) of Joules of energy compared to Richter scale value. For cities distant from the South Pole, we use an inverse-square law to determine how much energy would reach the city and calculate the magnitude of an earthquake with epicenter there to give an approximate “Richter” value. The distance, d , is taken to be the ratio of the distance to the edge of the epicenter (about 1 km) of a quake at the city and the distance from the South Pole to the city. This “Richter” value is an extreme exaggeration and should be taken as the absolute upper bound on the vibration and damage that is done to a given city.

Epicenter Richter value: $R_{\text{epi}} = \log_{10}(E_{\text{def}} \text{KE})/1.4995 - 3.2035$.

Distance “Richter” value: $R_d = \log_{10}(E_{\text{def}} \text{KE}/d^2)/1.4995 - 3.2035$.

Mass and volume of water vapor: We assume that all of the heat that goes toward heating the planet and ice evaporates ice. This assumption gives the worst case in terms of the amount of new water vapor introduced into the atmosphere.

Mass vaporized:

$$M|_{\text{vap}} = \frac{H_{\text{ice}} \text{KE}}{T_{\text{in}} S_{\text{ice}} + \text{HF}_{\text{ice}} + 100^\circ C \times S_{\text{H}_2\text{O}} + \text{HV}_{\text{H}_2\text{O}}},$$

where S_x is the specific heat, HF is the heat of fusion, and HV is the heat of vaporization.

Volume vaporized: $\text{Vol}_{\text{vap}} = M_{\text{vap}}/r_{\text{ice}}$.

Mass and volume of liquid water: We suppose that all of the kinetic energy of the asteroid goes into melting the ice.

Mass melted: $M_{\text{mel}} = \frac{H_{\text{ice}} \text{KE}}{T_{\text{in}} S_{\text{ice}} + \text{HF}_{\text{ice}}}$.

Volume melted: $\text{Vol}_{\text{mel}} = M_{\text{mel}}/\rho_{\text{ice}}$.

Scenarios

We ran a number of scenarios to determine the worst possible global damage, based on unfavorable assumptions about energy distribution upon impact, asteroid densities, and asteroid velocities. We also ran a scenario with relatively more realistic assumptions about the distribution of kinetic energy and with densities and velocities closer to average for an asteroid of the given size.



关注数学模型
获取更多资讯

First we supposed that the impact velocity of the asteroid would be 30 km/s (approximate upper bound for asteroid velocity), with a density of $5,000 \text{ kg/m}^3$, and that all of the energy would go into melting ice near the Pole. Our model calculates that approximately 3.81×10^{14} kg of water vapor would be ejected into the atmosphere. This corresponds to 413 km^3 or 0.0013% of the frozen ice on the Antarctic continent. Even in this exaggerated scenario, we anticipate that there would be no threat to coastal populations from flooding. On the other hand, this amount of water vapor corresponds to a relatively large increase in atmospheric water vapor (0.74%), but mixing with the very cold polar air would lead almost immediately to condensation and then precipitation [Ahrens 1994, 139–141].

If we suppose that all the kinetic energy would merely melt the ice (and leave it at 0° C), we find that 2.94×10^{15} kg of ice would melt, equivalent to $2,940 \text{ km}^3$ of water. But this is only 0.0093% of the ice on Antarctica. This corresponds to an average rise of water level of 7 mm and would not cause any coastal flooding. Moreover, most of this water would remain in the crater, and other water is unlikely to travel the more than 1,200 km to the ocean.

Another extreme scenario is that the kinetic energy would all be converted to deformation energy (and thus earthquakes), that the asteroid has a density of $10,000 \text{ kg/m}^3$, and that the asteroid is traveling at 35 km/s. This seismic worst-case gives an epicenter magnitude of 11.1 on the Richter scale. This is about 230 times(!) as powerful as any recorded earthquake. Vostok Station (about 1,333 km from the South Pole) would feel the shock of a magnitude-7 earthquake, and major Southern Hemisphere cities would feel a shock of magnitude 6. There might be a considerable number of casualties in those cities.

A more reasonable scenario is the energy distribution given by Chapman [Morrison and Wells 1978, 145–160]: An asteroid striking the moon at 5 km/s would contribute 20% of its energy to heating the target, 20% to heating the asteroid, 50% to deformation, and 10% to the kinetic energy of the ejecta.

The 20% of the kinetic energy that would go into heating the asteroid would have the effect of turning part of the asteroid into a super-heated gas. The 20% into heating the ice surrounding the impact site would evaporate 36.8 km^3 of ice and send the resulting water vapor up into the atmosphere. The 10% to ejecta would eject a portion of still-solid ice into the atmosphere and onto Antarctica. A crater 35 km in diameter would be created.

The remaining 50% of the asteroid's kinetic energy would be converted into energy of deformation and produce shock waves, which in turn would cause earthquakes. The earthquake energy at the epicenter would be equivalent to a 10.4-magnitude earthquake, about 20 times as large as any recorded. At Vostok Station, this would feel like a magnitude 6.4 earthquake. Major Southern Hemisphere cities would feel the equivalent of a 5.5-magnitude earthquake.

In any scenario, the net effect of these shocks to Antarctica would probably be severe cracking of ice and the creation of new icebergs all along the coast of Antarctica. Earthquakes would also cause fatalities in polar research stations.



关注数学模型
获取更多资讯

Because the epicenter of the earthquake is at least 1,200 km from the nearest coast, there is no need to worry about the possibility of tsunamis.

Ecology

Since the depth of ice at the south pole is 2.5 km, very little dust from the Earth would be thrown into the atmosphere. Most of the heating would occur in the upper layers of ice, so the rock under the ice would experience fracturing but not vaporize. The air near the impact would be saturated with water vapor [Ahrens 1994, 139–141] and would mix with the very dry and cold polar air. This would produce rapid condensation and formation of clouds. The iron particles thrown into the atmosphere would serve as condensation nuclei, facilitating rain and snow. We can expect the precipitate to settle over much of Antarctica and the Southern Ocean.

Our model does not incorporate the effects of adding up to 2.6×10^{12} kg of iron to the world oceans. Coincidentally, Monastersky [1995] writes that addition of iron to the ocean could be a possible solution to global warming by encouraging the growth of phytoplankton that use carbon dioxide in photosynthesis. But a dramatic increase in phytoplankton could lead to the production of methane. At any rate, the theory is uncertain, as is our knowledge of net ecological effects of the fallout.

Error Analysis

There is no way to verify the accuracy of the model results. While our sources give similar values for the energy imparted to the Earth by asteroid collision, as well as values for the asteroid temperature after impact, the values are not based on observed energy emission at impact but are estimates of the energy released after impact of asteroids millions of years ago. These sources are likely working upon the same assumptions that we are, but we cannot realistically say how accurate such assumptions are.

General Results

Testing our model for various energy distributions leads us to believe that:

- There would be no significant melting of the polar ice cap.
- The seismic effects would be very intense on the Antarctic continent. Nearby major cities should anticipate, at worst, the equivalent shock force of a magnitude-5 earthquake. The force of collision near the impact might cause the ice crust to crack and shift, and ice near the edge of the ice shelves could break off and form icebergs.



- There would be casualties of some polar research scientists, with minimal other casualties elsewhere.
- Water evaporated in the impact would quickly condense and fall out as rain and snow on the Antarctic continent and Southern Ocean. Such condensation would occur relatively quickly, so we do not anticipate a net warming effect such as might occur if another greenhouse gas of the same volume were released into the atmosphere.
- We are uncertain about the effect of iron and nickel fallout on the ecology of the Southern Ocean.

Strengths and Weaknesses

Strengths of the model include a good estimate of an upper bound on physical damage to Earth. It is highly improbable that shock waves or atmospheric effects could be any more severe than we have calculated. The analytic simplicity of the model is another positive feature.

Weaknesses of the model are the lack of long-term weather and ecological analysis, though the first two portions of the model indicate that the net effect in these areas would most likely be relatively small.

Appendix: Derivation of Formula for Air Resistance

The formula for the air resistance force is

$$R = c\rho AV^2,$$

where V is the speed of the object, A is the area of its cross-section, c is a dimensionless constant that depends on the form and the surface structure of the object, and ρ is density of air at sea level. We denote $c\rho$ by C ; at sea level, C should be about 0.2 to 0.4 kg/m³ for a spherical asteroid.

We seek an upper bound for the kinetic energy converted into heat due to air resistance. During the fall from a height of 100 km, the speed of the asteroid would increase by only about 1 km/sec, which is only 4 to 7% of its speed at impact; this small increase would not affect much the trajectory. So we can assume that the asteroid would fall in a straight line and that the speed at impact is the greatest speed reached.

The surface level at the Pole is approximately 3 km above sea level, so the air pressure there is somewhat less than that at sea level. Hence the work done by the air resistance force would be even less than we calculate below.

The density of air changes with height, but according to Davies [1986], we need consider air resistance only in the lowest 100 km of the Earth's atmosphere.



关注数学模型
获取更多资讯

For 0–100 km, the logarithmic fraction of density of air at sea level [Gamow and Cleveland 1976] is approximated well by a linear function, so we take the density to be 10^{ad+b} , where d is height above sea level.

We identify a and b . The 100-km height of the atmosphere is relatively small compared to the Earth's radius of 6,370 km, so we may disregard the Earth's curvature and consider the Earth's surface to be horizontal. Suppose the asteroid enters the atmosphere at an angle α with the horizontal. Then the asteroid must travel $(10^5 / \sin \alpha)$ m from the height of 100 km to sea level, so

- At sea level: $10^0 = 10^{a \cdot 0 + b}$, so $0 = a \cdot 0 + b$, that is, $b = 0$.
- At $(10^5 / \sin \alpha)$ m from impact, the density of air is 10^{-6} of that at sea level, so $10^{-6} = 10^{a \cdot 10^5 / \sin \alpha}$, so $-6 = a \cdot 10^5 / \sin \alpha$, thus $a = -6 \sin \alpha / 10^5$.

Thus, the air density at a distance h from the point of impact is a fraction $10^{-6}h \sin \alpha / 10^5$ of the density at sea level. Air resistance there is

$$R = 10 - \frac{6h \sin \alpha}{10^5} \cdot CAV^2.$$

The work of the air resistance force done on this straight line trajectory is

$$\begin{aligned} W &= - \int_{10^5 / \sin \alpha}^0 R dh \\ &= - \int_{10^5 / \sin \alpha}^0 10^{-6h \sin \alpha / 10^5} CAV^2 dh \\ &= \frac{10^5 CAV^2}{6 \ln 10 \sin \alpha} 10^{-6h \sin \alpha / 10^5} \Big|_{10^5 / \sin \alpha}^0 \\ &= \frac{10^5 CAV^2}{6 \ln 10 \sin \alpha} (10^0 - 10^{-6}) \\ &\approx \frac{10^5 CAV^2}{6 \ln 10 \sin \alpha}. \end{aligned}$$

We estimate $0.2 < C < 0.4$ and $A \leq \pi r^2$, where $r = 500$ m (since the diameter of the asteroid is 1 km). Since both the kinetic energy of asteroid and the work of the air resistance force are proportional to V^2 , the percentage of the kinetic energy that is turned into heat by the resistance force does not depend on the speed of the object.

The angle α cannot be very small, or the asteroid would bounce off the atmosphere like a stone off the surface of water. **Table 1** gives the percentage of kinetic energy of the asteroid that is yielded to air resistance for various values of α less than 1% for any entry angle.



关注数学模型
获取更多资讯

Table 1.

Percentage P of kinetic energy changed into heat by air resistance, for $C = 0.4$, $A = 500$ m, and different values of trajectory angle α (in degrees).

α	10	20	30	40	50	60	70	80	90
P	0.163	0.083	0.057	0.044	0.037	0.033	0.030	0.029	0.028

References

- Ahrens, Donald. *Meteorology Today*. 1994. Los Angeles, CA: West Publishing Company.
- Alaska Seismic Studies Homepage. 1999.
<http://giseis.alaska.edu/Seis/Input/laahr/laahr.html>.
- Barnes-Svarney, Patricia. 1996. *Asteroid*. New York: Plenum Press.
- Benest, Daniel, and Claude Froeschlé, editors. 1998. *Impacts on Earth*. New York: Springer.
- Cascades Volcanoes Observatory Homepage. 1999.
<http://vulcan.wr.usgs.gov/home.html>.
- Davies, John. 1986. *Cosmic Impact*. New York: St. Martin's Press.
- Espenshade, Edward, editor. 1995. *Goode's World Atlas*. New York: Rand McNally.
- Gamow, George, and John Cleveland. 1976. *Physics: Foundations and Frontiers*. Englewood Cliffs, NJ: Prentice Hall.
- Hansom, James, and John Gordon. 1998. *Antarctic Environments and Resources*. New York: Addison Wesley Longman.
- Harte, John. *The Green Fuse*. 1993. Berkeley, CA: University of California Press.
- _____, and Allen Goldstein, editors. 1997. *The Biosphere*. Berkeley, CA: University of California Publishing.
- Kalinin, Yu.D. 1993. *Ulary Gigantskikh Asteroidov i Geomagnitnye Yavleniya*. Krasnoyarsk.
- Monastersky, Richard. 1995. Iron versus the greenhouse. *Science News* (30 September 1995): 220–222.
- Morrison, David, and William C. Wells, editors. 1978. *Asteroids: An Exploration Assessment: A Workshop*. NASA Conference Publication 2053. Washington, DC: NASA, Science and Technology Information Office.
- Resnick, Robert, David Halliday, and Kenneth S. Crane. 1992. *Physics*. New York: John Wiley & Sons.
- Verschuur, Gerrit. 1996. *Impact!* New York: Oxford University Press.



关注数学模型
获取更多资讯



The Sky is Falling!

Daniel Forrest
 Garrett Aufdemberg
 Murray Johnson
 University of Puget Sound
 Tacoma, WA 98416

Advisor: Perry Fizzano

Assumptions

1. The diameter (D) of the asteroid at impact is 1,000 m. Heat and stress while traveling through the Earth's atmosphere would cause some portion to vaporize or burn before impact. However, for an object this large traveling at speeds typical of cosmic objects impacting the earth, one can ignore the deceleration and ablation (loss of mass from the surface of an object due to frictional forces) due to the atmosphere [Steel 1995, 178].
2. The asteroid strikes the earth at the geographic South Pole.
3. The asteroid is spherical.
4. The asteroid is homogeneous with uniform density $\rho = 2.5 \text{ g/cm}^3$; uniform density allows for simple estimates of the mass. The value of ρ is typical of C-type (carbonaceous) asteroids, which make up the majority of the asteroids in the solar system and therefore are the most likely type to strike earth, and also within the typical range of densities of S-type (stony) asteroids, which make up a majority of the asteroids with orbits that cross the Earth's orbit [Morrison and Owen 1996, 103–132].

Preliminary Calculations

Mass of the Asteroid

The mass of the asteroid (M_a) is its density (ρ) multiplied by its volume (V). For a spherical asteroid, the mass is given by

The UMAP Journal 20 (3) (1999) 263–268. ©Copyright 1999 by COMAP, Inc. All rights reserved. Permission to make digital or hard copies of part or all of this work for personal or classroom use is granted without fee provided that copies are not made or distributed for profit or commercial advantage and that copies bear this notice. Abstracting with credit is permitted, but copyrights for components of this work owned by others than COMAP must be honored. To copy otherwise, to republish, to post on servers, or to redistribute to lists requires prior permission from COMAP.



关注数学模型
获取更多资讯

$$M_a = V\rho = \frac{4}{3}\pi \left(\frac{D}{2}\right)^3 \rho.$$

For our asteroid, $D = 1,000$ m and $\rho = 2.5$ g/cm³, thus

$$M_a = 1.3 \times 10^{12} \text{ kg.}$$

Upper and Lower Bounds on Impact Speed

A planet's escape velocity (v_{esc}) is the minimum speed that an object must have to escape the planet. It is calculated by determining the change in potential energy caused by moving an object from the planet's surface to "infinity." To escape the planet, the object's initial kinetic energy must be greater than or equal to the change in potential energy. By symmetry, the escape velocity is also the minimum velocity that an object from beyond the planet can have when it reaches the planet's surface. Thus, the Earth's escape velocity, $v_{\text{esc}} = 11.2$ km/s, is a lower bound on the asteroid's impact speed (v_{imp}).

There is also an upper bound on the impact velocity, "a combination of escape velocity, heliocentric orbital velocity, and the velocity of an object just barely bound to the sun at the planet's orbital position." For Earth, this maximum is 72.8 km/s [Melosh 1989, 205]. Thus, the impact velocity is bounded by

$$11.2 \text{ km/s} \leq v_{\text{imp}} \leq 72.8 \text{ km/s.} \quad (1)$$

Energy Released on Impact

The energy of the collision (E_{imp}), drawn from the kinetic energy of the asteroid, is

$$E_{\text{imp}} = \frac{1}{2} M_a v_{\text{imp}}^2.$$

The impact velocity is bounded and the asteroid's mass is fixed. Applying (1), we have

$$8.2 \times 10^{19} \text{ J} \leq E_{\text{imp}} \leq 3.4 \times 10^{21} \text{ J.} \quad (2)$$

Effects of Impact

Crater Size

The crater from the impact would be roughly parabolic in shape, with a diameter of approximately 10 km and a depth of approximately 1 km [Koeberl and Sharpton 1998]. The pressure is so great in impacts of this sort that the crater



forms partially from the vaporization of the target material. At the South Pole, the asteroid would be impacting in ice about 2,600 m thick. It takes considerably lower energies to vaporize ice than rock or soil, therefore we expect that the impact crater would be larger than similar impact craters in other locations.

Melting and Vaporization of Antarctic Polar Ice Cap

Could an asteroid impact at the South Pole melt the Antarctic polar ice cap and drastically changing global sea levels? The ice cap covers $1.32 \times 10^{13} \text{ m}^2$ with average thickness 2,440 m [Ronne 1997]. Thus, there is $3.2 \times 10^{16} \text{ m}^3$ of ice, with mass $2.9 \times 10^{19} \text{ kg}$.

At most, the asteroid impact could create $3.4 \times 10^{21} \text{ J}$. If all the energy were to melt ice, how much ice could be melted?

Assuming that the ice is at 0° C , it would take $3.33 \times 10^5 \text{ J/kg}$ to melt 1 kg of ice [Wilson and Buffa 1997]. So, at most

$$\frac{3.4 \times 10^{21}}{3.3 \times 10^5} \approx 1 \times 10^{16} \text{ kg}$$

of ice could be melted. This translates to $1 \times 10^4 \text{ km}^3$ of liquid water. The area of the world's oceans is approximately $3.61 \times 10^6 \text{ km}^2$; so if the melted water were evenly distributed across the world's oceans, sea level would rise less than 3 cm. This is not enough to endanger human lives or displace human settlements.

This estimate is an upper bound, since some energy goes into destroying the asteroid on impact; vaporizing part of the asteroid; vaporizing ice; excavating the crater; creating sound, shock, and seismic waves; and heating the air around the impact site. The impact would probably vaporize much of the ice from the impact crater. Assuming that the volume of ice vaporized is equal to the volume of ice in the largest cone that fits in the roughly parabolic crater, the impact would vaporize $2.6 \times 10^{10} \text{ m}^3$ of ice, or $2.4 \times 10^{13} \text{ kg}$ of ice. The energy required to melt a kilogram of ice, heat the kilogram of resulting water to 100° C , and vaporize the water is $3 \times 10^6 \text{ J}$. Vaporizing so much ice would require $7.2 \times 10^{19} \text{ J}$. This value is within the bounds on the impact energy in (2).

Earthquakes and the Risk of Tsunami

We can estimate the magnitude (Q) of the seismic disturbance (as measured on the Richter scale) from the formula [Melosh 1989, 67]

$$Q = 0.67 \log_{10}(E_{\text{imp}}) - 4.87. \quad (3)$$

The seismic disturbance due to a cosmic impact is not the same as from normal seismic activity. The effect of impact-generated seismic waves is estimated to be an earthquake of one magnitude less than the approximate magnitude generated by impact [Melosh 1989, 67].



For our asteroid, equation (3) (using the energy range from (2)) tells us that the impact would generate a seismic disturbance ranging in magnitude from 8.5 to 9.6 on the Richter scale (**Figure 1**). Even if the effects are discounted by one magnitude, such an earthquake would cause many human casualties if located in a more-populated part of the world than the South Pole. However, human casualties are negligible because the continent is mostly uninhabited and because Antarctica is large enough that any damage would be limited to Antarctica.

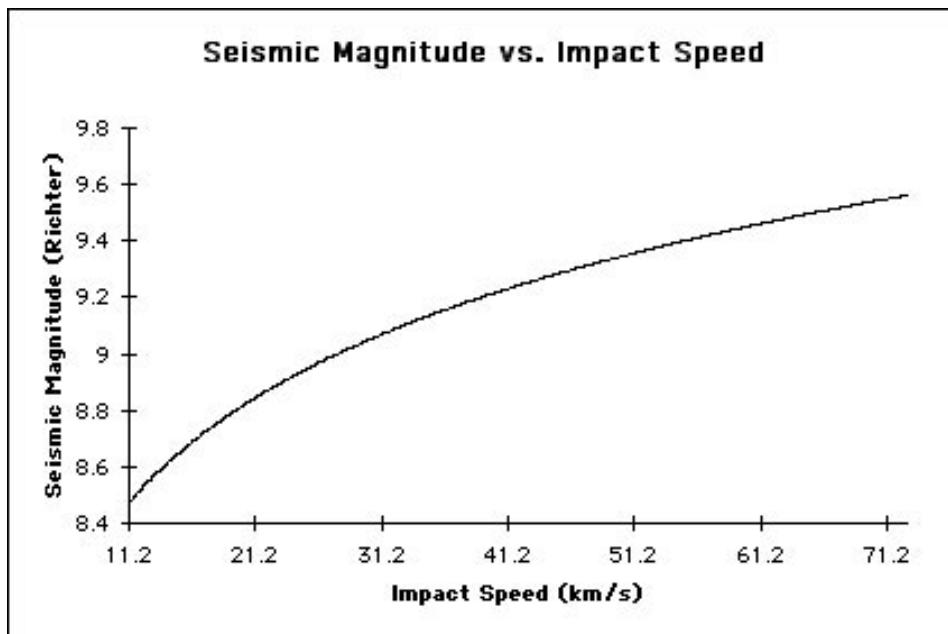


Figure 1. Seismic magnitude vs. impact speed.

Because the impact is at least 500 km from the closest shoreline and 1,500 km from most of the shoreline, the risk of a catastrophic tsunami being generated is negligible. A large percentage of the coast of Antarctica is lined with sheer walls of ice (on the order of 30 m in height). There is indeed a very real danger that the seismic disturbance could cause large fragments to break off, fall into the water, and cause tsunamis. Landslide-generated tsunamis can be large; the 1936 tsunami in Lituya Bay, Alaska, reached a height of 150 m [Hamilton 1998a]. However, they dissipate quickly and are unable to cross the great, transoceanic distances associated with earthquake-generated tsunamis. The greatest risk would be to coastal areas on the southern tip of South America.

Atmospheric Effects

Upon impact, the asteroid would disintegrate. Approximately 10% of the mass, 3.1×10^{11} kg, would be vaporized into submicron particles that would rise to the stratosphere (an altitude of 16 to 48 km) and would remain there for months [Steel 1995, 67]. If dust made up of 1-micron particles were spread



evenly in a 1-micron-thick spherical layer at height H above the surface of the earth, it would cover approximately 10% of the surface area of the imaginary sphere and would block 10% of incoming solar radiation. On a very cloudy day, the intensity of light reaching the surface of the earth is roughly 10% of the intensity of light on a clear day [Steel 1995, 66]. A 10% drop in intensity would allow 9 times the intensity of light to reach earth as on a very cloudy day; but over a period of months, such a drop would be significant enough to cause global temperature change.

The ice vaporized on impact would rise into the atmosphere and form clouds. The water vapor in these clouds would eventually fall to earth as rain, increasing the amount of liquid water on the Earth by $8.1 \times 10^{10} \text{ m}^3$. If it all ended up in the world's oceans, the global sea level would rise about 2 cm.

Conclusions

Fear that the ice cap would melt and cause global flooding is unfounded.

Because the asteroid would impact at the South Pole, the dust levels are far less than if the same asteroid impacted in soil and / or rock. Still, enough dust is lifted into the stratosphere to block up to 10% of the sunlight—enough to impact global temperature but far from the threshold where photosynthesis becomes impossible. Reduced light levels and temperature would affect agricultural production, but the impact on the world's food supply would be small; food surpluses in industrialized countries should be able to make up for agricultural losses in other nations.

The ice vaporized from the crater would form clouds and eventually fall to earth in liquid form. But the volume of the water is not large enough to cause large-scale coastal flooding, unless it all falls in a limited area in a limited amount of time. The dust that is larger than a micron and does not reach the stratosphere could still have detrimental effects, such as acid rain. But our model has no way of estimating the amount, location, or effects of possible acid rain.

Because the asteroid hits in Antarctica, the death toll directly due to impact is limited to the few hundred researchers stationed there. These casualties could be eliminated by evacuation if there is enough advance warning.

Strengths and Weaknesses

Our model is successful in that we have quantitative estimates of many of the effects associated with the impact, such as the range of possible impact velocities, the range of possible impact energies, the size of the impact crater, the effect of dust raised by impact in the atmosphere, and the magnitude of seismic disturbance generated by impact. Our model is simple enough that all calculations were performed without resorting to a computer.



关注数学模型
获取更多资讯

The simplicity of our model also brings about some weaknesses. We have no accurate method to estimate how the total impact energy is distributed. We are also unable to determine long-term environmental consequences. Because of the unpredictable nature of atmospheric dynamics, we are unable to develop a model that would show specific locations and amounts of crops affected by dust raised from the impact. Our model predicts no direct loss of human life, but we are unable to take into account human life lost due to effects on food production.

Our model, while not sophisticated, offers intuitive results. Our estimates of crater size, impact energy, and magnitude of seismic disturbance correlate nicely to other models' predictions, such as those of Hamilton [1998b].

References

- Fishbane, Paul M., Stephen Gasiorowicz, and Stephen T. Thornton. 1993. *Physics for Scientists and Engineers*. Englewood Cliffs, NJ: Prentice Hall.
- Hamilton, Douglas P. 1998a. Notable Tidal Waves of this Century.
<http://janus.astro.umd.edu/astro/Wave.htm>.
- _____. 1998b. Solar System Collisions.
<http://janus.astro.umd.edu/astro/impact.html>.
- Koeberl, Christian, and Virgil L. Sharpton. 1998. Terrestrial Impact Craters.
<http://cass.jsc.nasa.gov/publications/slidesets/impacts.html>.
- Melosh, H.J. 1989. *Impact Cratering: A Geological Process*. New York: Oxford University Press.
- Morrison, David, and Tobias Owen. 1996. *The Planetary System*. Reading, MA: Addison-Wesley.
- Ronne, Finn. 1997. Antarctica. *Encyclopedia Americana*.
- Steel, Duncan. 1995. *Rogue Asteroids and Doomsday Comets*. New York: John Wiley & Sons.
- Wilson, Jerry D., and Anthony J. Buffa. 1997. *College Physics*. Upper Saddle River, NJ: Prentice Hall.



关注数学模型
获取更多资讯

Judge's Commentary: The Outstanding Asteroid Impact Papers

Patrick J. Driscoll

Department of Mathematical Sciences
U.S. Military Academy
West Point, NY 10996
ap5543@exmail.usma.army.mil

Introduction

The A problem has, over time, assumed near mythological association, upon first reading by contestants, with challenging mathematical analysis. Upon further discussion and examination by team members, however, the problem typically succumbs to rather straightforward mathematics combined with innovative thinking. The Asteroid Impact problem continued this trend, providing contestants with an opportunity to wrestle with a sophisticated and challenging real-world problem. Despite the wealth of reference material accessible to contestants in reference libraries and on the Internet, the task of clearly identifying the short- and long-term effects of an asteroid impact in Antarctica left plenty of ideas for contestants to explore.

In past years, the diverse backgrounds of the undergraduate contestants provided teams with an ability to bring more than one discipline's perspective to bear on the problem. This typically resulted in an interesting array of hybrid modeling approaches. This year, however, there seemed to be a convergence to only a handful of approaches despite team demographics. Our speculation is that this effect is in direct response to the astronomical (no pun intended) increase in network connectivity via the Internet.

As many teams discovered during their weekend effort, using the Internet as a source of information in support of their analyses proved to be a two-edged sword. Sites such as those at Sandia Laboratories or the Jet Propulsion Laboratory provided interesting and in some cases accurate and relevant information dealing with asteroid impacts with Earth. Unfortunately, as evidenced

The UMAP Journal 20 (3) (1999) 269–271. ©Copyright 1999 by COMAP, Inc. All rights reserved. Permission to make digital or hard copies of part or all of this work for personal or classroom use is granted without fee provided that copies are not made or distributed for profit or commercial advantage and that copies bear this notice. Abstracting with credit is permitted, but copyrights for components of this work owned by others than COMAP must be honored. To copy otherwise, to publish, to post on servers, or to redistribute to lists requires prior permission from COMAP.



关注数学模型
获取更多资讯

in many papers, teams extracting information from these sites without first thinking about and discussing the problem soon found themselves under the spell of the siren, lulled into a mathematical approach that they were not able to bring to successful closure in the time allotted for the competition. Moreover, to judge from their lack of direct supporting documentation and reasoning, in the end they apparently found themselves unprepared to explain clearly and sufficiently the underlying assumptions and reasoning of the mathematics presented in the sites. As in most modeling efforts, this provided an all-too-fatal flaw to their paper.

A second general note also worth mentioning concerns team strategies for coping with the impending competition deadline. The vast majority of good papers represented a team strategy that, when faced with a decision either to present complicated mathematical analysis on only a portion of the problem or else to attempt a complete modeling effort, chose the latter. The exceptional papers contained a judicious amount of both elements woven together to answer the questions posed by the problem. Exactly how the balance was struck between the degree of inclusion of the two elements varied from paper to paper. However, it was clear that each team had chosen one or two appropriate mathematical techniques (e.g., partial differential equations, kinetic energy modeling, etc.) to develop within the context of a complete modeling effort.

By and large, the exceptional papers provided conclusive evidence that their teams had dedicated a substantial amount of time thinking about the problem prior to starting their quest for supporting information. This choice seemingly enabled them to weigh the cost and benefit of identifying exact modeling parameters versus making reasonable assumptions and working with approximate, in-range values. The many facts directly associated with the problem—such as the geological composition of both the asteroid and Antarctica, the typical source of Earth-bound asteroids, the angle of incidence upon impact, the human population distribution, and atmospheric currents and circulation—mandated adopting such a strategy. Those papers failing to provide evidence of having considered important problem characteristics, whether implicit or explicit, were eliminated from further consideration. As a minimum, it would have been better to identify and explain the impact of a particular feature (e.g., upper atmospheric wind currents) and then to choose explicitly not to include this factor for reasons of mathematical tractability.

Modeling assumptions fall into two broad categories: physical assumptions requiring justification with discussion, and numerical parameter assumptions that may result from citations noted. The plausibility and applicability of either type directly depended on how well teams linked a particular assumption to the problem as stated in the MCM, rather than to some problem stated in the reference source document. Regardless of a paper's calculations, a 10-meter instantaneous rise in all of the Earth's oceans is a bit too far-fetched of a result for the problem presented, even for the most devout of science fiction followers to accept.

As in past competitions, the need for precise supporting documentation



in the body of the report cannot be stressed enough. The exceptional papers all conveyed a clear link to verifiably credible information sources within the body of their paper. Lesser-quality papers showed a reliance on Internet sites for supporting information that failed to include necessary explanations of why certain parameter values were valid and what assumptions their methods were based on. Although the temptation to “cut-and-paste” directly from Internet sources is recognizably strong, doing so most often resulted in a paper that was predominantly statements of unsupported “facts” rather than one showing that the team had a clear understanding of the model. Additionally, dedicating an inordinate amount of time to display the derivation of known relationships (e.g., Kepler’s law of gravitational attraction) added little value to a paper.

Lastly, the finer papers presented complete summaries, contained few or no grammatical errors, and presented well-designed tables and graphics that illuminated their team’s underlying analytical reasoning.

About the Author

Pat Driscoll is an Academy Professor in the Department of Mathematical Sciences at USMA. He received his M.S. in both Operations Research and Engineering Economic Systems from Stanford University, and a Ph.D. in Industrial and Systems Engineering from Virginia Tech. He is currently the program director for math electives at USMA. His research focuses on reformulation-linearization techniques in the context of linear and nonlinear optimization. Pat was the Head Judge for the Asteroid Impact Problem.



关注数学模型
获取更多资讯



Determining the People Capacity of a Structure

Samuel W. Malone
 W. Garrett Mitchener
 John Alexander Thacker
 Duke University
 Durham, NC

Advisor: David P. Kraines

Summary

Many public facilities are assigned a “maximum legal occupancy” for how many people may be in the facility at one time. For typical facilities, we consider personal space, evacuation time, and ventilation to determine this number. We present several models of evacuation and flow of people to determine how quickly a given number of people can leave a room or complex of rooms in case of an emergency. We estimate the time for a room to become dangerous when toxins are leaking into the atmosphere, including the carbon dioxide produced by human respiration and by fire. In addition to an emergency situation, we investigate how the ventilation through a room might limit its maximum occupancy.

We expect each person to need 0.5 to 1 m² of personal space. For an elevator or a concert, in which close contact is not considered uncomfortable, smaller values may be used. For a swimming pool, where people need more room to maneuver, we recommend more.

We use three models of flow of people out of a room with a door. One assumes that the flow rate is constant, the second bounds it by a linear function of people-density (people per unit area) in the room, and the third bounds it by a concave-down quadratic function of people-density. In each case, the rate at which people exit is roughly proportional to the combined flow rates of all the doors. A room with a lot of small furniture is similar to an empty room, since people are not heavily restricted in direction of travel; but a room with large furniture that restricts motion is better considered as a complex of connected rooms. The space taken up by furniture must be subtracted from the whole when calculating capacity.

The UMAP Journal 20 (3) (1999) 273–286. ©Copyright 1999 by COMAP, Inc. All rights reserved. Permission to make digital or hard copies of part or all of this work for personal or classroom use is granted without fee provided that copies are not made or distributed for profit or commercial advantage and that copies bear this notice. Abstracting with credit is permitted, but copyrights for components of this work owned by others than COMAP must be honored. To copy otherwise, to republish, to post on servers, or to redistribute to lists requires prior permission from COMAP.



关注数学模型
获取更多资讯

A series of rooms can be represented as a graph with nodes for rooms and edges (marked with a flow rate) for doors. For constant flow rate, the Ford-Fulkerson algorithm gives the maximum flow through the room and hence an estimate of the time for any given number of people to evacuate.

For the constant and quadratic bound models, a computer simulation gives consistent results for a complicated cafeteria on campus. Unless there is a bottleneck somewhere inside, the limiting factor on the evacuation rate seems to be the flow rates of the doors.

Once we know how long it takes to evacuate N people is known, we can back-solve to determine the maximum number of people who can evacuate in time T . The problem is determining how much time to allow for evacuation. Based on the combustion of wood, we estimate that the sample cafeteria would take 2.5 min to evacuate but 2.5 h to fill with carbon dioxide.

Our evacuation models are flexible, in good agreement with each other for the sample buildings we used, and give reasonable times for evacuation. The ventilation model is likewise reasonable and flexible. Although we had to guess many of the parameter values used in the models, we designed experiments to determine some of these parameters. In particular, the estimate of time until fatality for a fire was extremely rough and should be refined.

We recommend that personal space be used as a first estimate of capacity. The evacuation models should then be applied to be sure that there are no bottlenecks. The ventilation system should be examined to ensure that enough fresh air comes in and that the room dissipates heat quickly enough.

Introduction

Two important factors affect capacity:

- **The Emergency Problem:** What should be the maximum capacity in terms of minimizing the time for every occupant to exit without sustaining injury?
- **The Comfort Problem:** How many people can fit in a room, for a given interval, before the room becomes overheated or the carbon dioxide level rises significantly above normal?

We present two models for the emergency problem, both of which give a method for determining the minimum time for a specified number people to exit a specified structure. Conversely, we use these methods to determine the maximum number of people who can exit a structure in a given period of time.

For the comfort problem, we estimate the maximum number N of people who can comfortably occupy a given space for a period of time T .

To avoid ambiguity, we use the following definitions:

- A *structure* is an assortment of interconnected spaces, each of which leads to at least one other space or an exit.



关注数学模型
获取更多资讯

- An *emergency* is a situation that poses sufficient potential or actual harm to the well-being of the group within a structure to require its complete evacuation.
- The assumption of *orderly movement* states that no personal injuries or other accidents occur that affect the minimum time to evacuate the structure.
- A *panic* is a situation in which orderly movement does not hold.
- A room is *comfortable* if the quality of its air is acceptable and its temperature falls within a specified range.

Further Considerations

One difficulty in developing a model for the emergency problem is deciding how different types of emergencies affect the rate at which people can exit a given structure. A bomb threat and a fire are both pressing reasons to evacuate a building. Imminent danger of smoke inhalation is more serious than the knowledge that five hours later a bomb may or may not explode; but a bomb threat called in five minutes before detonation could cause a panic that might leave many people injured in the rush to exit, whether or not the threat is real. The dynamics of the exiting processes for each of these situations present distinctly different modeling situations.

In addressing the emergency problem, we first consider orderly movement and then extend our analysis to what might happen in a panic.

Assumptions and Hypotheses

- The people in our models are adults weighing between 100 and 300 lbs.
- There are no “security guards” or individuals responsible for regulating evacuation. That is, every individual desires to exit the structure as quickly as possible and employs the same process for deciding on the best route.
- The ceilings are of normal height, and the uppermost floor is not extremely distant from ground level (i.e., the rooms are not crawl spaces nor are they penthouses of skyscrapers).
- The time for a person to move from one room to another is negligible compared to the time to evacuate all people from a room.
- The room is in a modern building in a town or city. We do not expect our results to apply to submarines, space stations, or other unusual structures.



关注数学模型
获取更多资讯

Personal Space Constraints

The simplest constraint on the capacity of any room is space. Each person requires about 1 m^2 (9 ft^2) to stand and move around comfortably. So if a room is designed for standing or sitting in an upright chair, an upper bound on the room's capacity is given by its area (less any area occupied by furniture) in square meters.

In special cases, such as a rock concert or an elevator, in which people are willing to stand closer together, the maximum capacity may allow for only 0.75 or 0.5 m^2 per person.

Evacuation Models

- How long would it take all the people in a full room to exit?
- What is the risk that someone would be injured during the evacuation? (by being trampled, left in the building, etc.)
- In an emergency, how long do people have to get out of the room?

To answer these questions, we develop several models of evacuation based on assumptions about kinds of emergencies and how people move through doors.

The Constant Rate Model

The constant rate model is based on the following assumptions:

- A door lets people through at a constant flow rate.
- The time for a person to get in line at a door is negligible compared to the time to evacuate the room.
- Doors do not become blocked during the evacuation.
- People are crowded around each door. Until the room is almost empty, there are enough people standing close to the door to use it to full capacity. When someone exits, the crowd pushes forward to fill the gap.
- People tend to go either to a nearest door or to a door that will allow them to exit the fastest.

First we analyze a room containing only people; later we add furniture. Similarly, we initially ignore the possibility of a panic.

Single Room with One Door

For a single room with one door, we assume that there are always enough people to use the door to capacity. If the door allows people through at rate r and there are n people in the room, it takes $t = n/r$ time for the room to empty.



关注数学模型
获取更多资讯

Single Room with Multiple Doors

If the room has multiple doors, each person initially goes toward the nearest door. If it becomes clear that one crowd is moving faster than the others, people at the end of slow lines move to the end of the fast line. In this way, all doors are crowded until the room is empty. Suppose that there are k doors with flow rates r_1, \dots, r_k and that n_1, \dots, n_k people exit through the doors, respectively. All lines finish at the same time, yielding

$$t = \frac{n_1}{r_1} = \frac{n_2}{r_2} = \dots = \frac{n_k}{r_k}.$$

If we let n be the sum of the n_i , we have

$$n = tr_1 + tr_2 + \dots + tr_k.$$

Defining r to be the total number of people divided by the total time of evacuation and substituting yields

$$r = \frac{n}{t} = r_1 + r_2 + \dots + r_k. \quad (1)$$

That is, a room with many doors is equivalent to a room with a single larger door whose flow rate is the sum of the rates of all the smaller doors.

Subroom and Corridor Decomposition

Now we consider furniture and other obstacles. First, imagine a dining room with a large number of tables and chairs (see **Figure 1**).

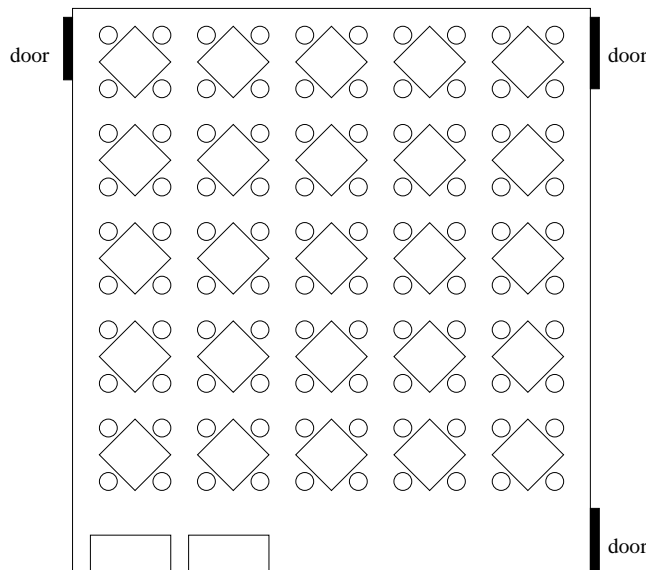


Figure 1. A dining room, view from above.



The furniture restricts people to certain paths, but the assumptions of the open-room model still hold. People can generally move in whatever direction they want, there is always a crowd at each door, and each door flows at maximum capacity. It is the combined flow rate of all the doors that determines the evacuation time, as in (1).

Alternatively, obstacles can divide a room into smaller rooms and corridors, a situation that requires a significantly different model. For example, consider a small lecture hall with rows of seats, a table, and several doors (see **Figure 2**). People would likely walk between the chairs rather than leap over them. So, the single room is broken up by the furniture into smaller "subrooms" and "corridors," as shown in **Figure 3**. This situation is different from the dining hall because the furniture of a lecture hall more severely restricts the directions people can move in. A person in the hall must first exit a row of seats, then go down one of the outside aisles. If one end of an aisle is blocked, it takes longer for the last person on that aisle to exit the room. In the dining hall, a blocked passageway is less critical because there are so many other passages.

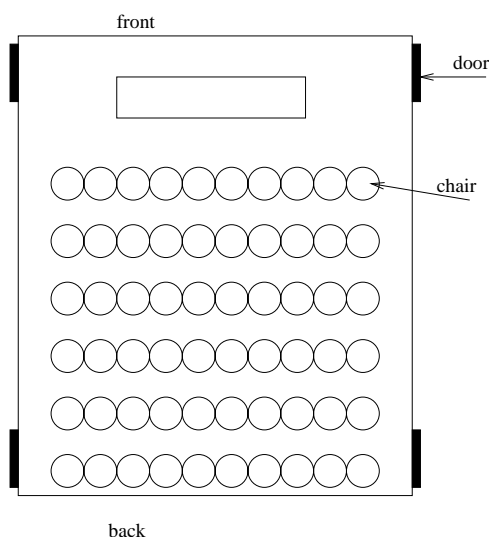


Figure 2. View of a lecture hall from above.

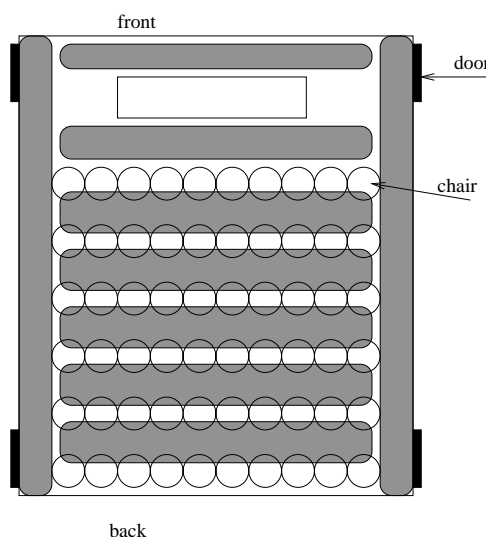


Figure 3. Corridors of movement (in gray) in the lecture hall.

Once a room has been broken up into subrooms and corridors, it is useful to think of them each as being separate rooms with doors connecting them, and the evacuation problem becomes one of evacuating a whole complex of rooms (see **Figure 4**). The diagram can be simplified somewhat by combining doors that lead to the same place as in (1). In this case, the exit doors can operate at maximum capacity the whole time, so the time for evacuation is determined entirely by their combined flow rate.

For a more complex example, consider the cafeteria floor plan shown in **Figure 5** (this is based on an actual building on campus). Most rooms are connected by open arches that function as doors with large flow rates. The



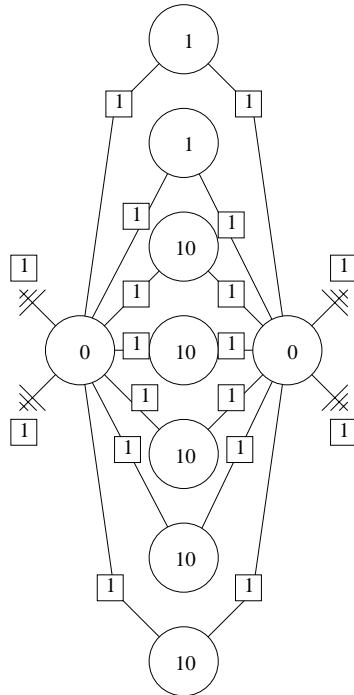


Figure 4. Schematic diagram of subrooms of the lecture hall. Circles represent subrooms, lines represent passage from one subroom to the next, and ground symbols represent doors leading to the outside. Each subroom is marked with how many people are in it and each connection is marked with how many people per second can flow through it.

cafeteria reduces to the schematic diagram shown in **Figure 6**. Here it is not so clear that the flow rate of the four exit doors determines the evacuation time, although our simulations and a method that we will describe show that this is in fact the case. If we had a large room connected to a lobby by a single small door, and a large door connecting the lobby to the outside, the evacuation time would be more dependent on the flow of people into the lobby. In other words, sometimes a small interior door is a bottleneck, but sometimes it is not. For a complicated network like the cafeteria, whether or not there is an interior bottleneck is not immediately apparent.

Maximum Flow Model

Curiously, the evacuation problem for a complex of rooms can be solved by ignoring the numbers of people in the rooms. Suppose that people constantly flow out of the complex and other people emerge inside at the same rate (think of people falling out of the ceiling as fast as other people exit). The rooms will have constant numbers of people, since people are replaced as fast as they leave. The problem is to find the flow rate of people through a complex.

The Ford-Fulkerson algorithm finds the maximum flow through a graph. Suppose that in a directed graph each connection has a known maximum capacity (e.g., people per second who can pass through a crowded door). One of the



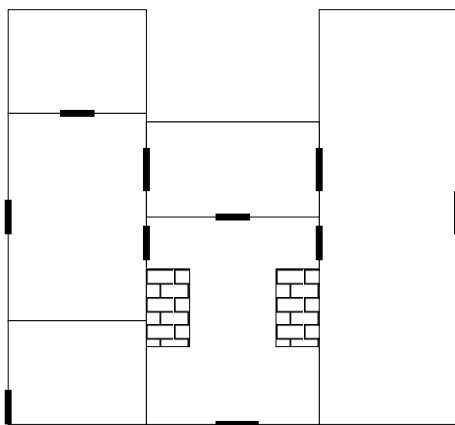


Figure 5. A large cafeteria viewed from above.

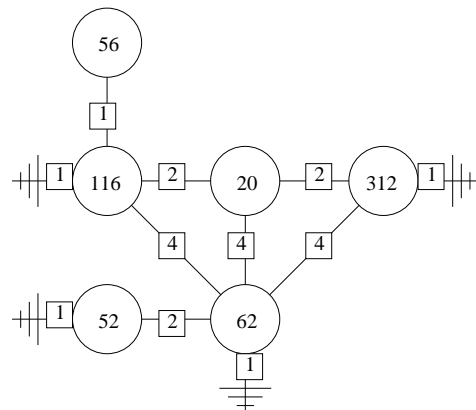


Figure 6. Schematic diagram of the cafeteria.

nodes is designated the “source” (people falling from the ceiling) and another is designated the “sink” (the outside). We assign to each connection the actual flow through it. Such an assignment can be improved if there is a path from source to sink in which the flow through every connection can be increased. An assignment is maximal if there is no such path. The Ford-Fulkerson algorithm looks at all possible paths until no improvements can be made.

The time for n people to leave the building can be estimated by dividing n by the maximum flow. To use the Ford-Fulkerson algorithm on a room graph, we must add two nodes: a source is connected to all rooms with lines of infinite capacity; and a sink node representing the outside is connected to all exits from the complex, with connection capacities equal to those of the exit doors.

For a continuation of the cafeteria example, see **Figure 7**. This graph is marked with a maximum flow. The flow cannot be improved because all the connections leading to the sink are at their maximum. The figure confirms that the rate of evacuation is determined by the flow rate of the exit doors; in other words, there are no internal bottlenecks. The same technique can be applied to any room graph.

Quadratic Rate Model

Motivation for the Negative Quadratic Model

A linear rate model proposes that the rate at which people can exit a room, $f(t)$, is bounded by a linear function of the number of people in the room. The evacuation problem can be stated as:

$$\text{maximize} \quad \int_0^T f(s)ds,$$



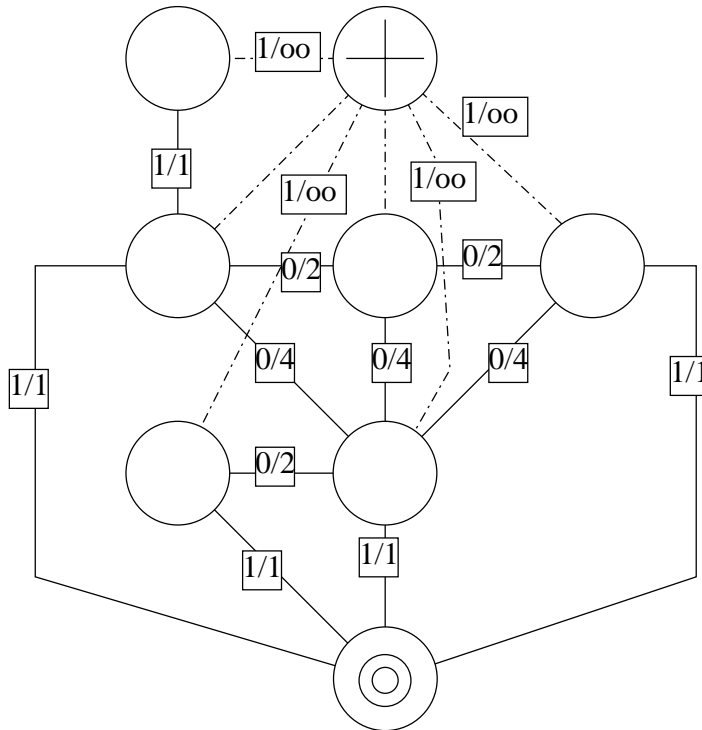


Figure 7. The graph for the Ford-Fulkerson algorithm for the dining hall. The + node represents the source and the bull's eye represents the sink.

that is, maximize the number of people who can evacuate in time T ,

$$\text{subject to } 0 < f(t) < a \int_t^T f(s) ds + b, \text{ for } 0 < t < T.$$

The integral gives the total number of people evacuated after time T minus the number of people who evacuated up to time t ; in other words, it is the number of people in the room at time t .

The linear model represents the situation where the number of people in the room has a “forcing” effect on the flow rate through the exits; the greater the constant a , the greater the forcing effect. The constant b represents the normal rate of flow when the forcing effect is negligible. Assuming that people exit the room in an efficient and orderly manner, the linear model hypothesizes that the maximum flow rate out of the room increases linearly with the number of people in the room.

However, this model does not take into account that for sufficiently large flows, the capacity function representing the upper bound of the flow rate should decrease to zero. The evacuation dynamics of an emergency require an upper bound model that takes large flow values into consideration: When, other than an emergency or a panic, would such large flow values occur and evacuation time be more crucial?



Developing the Negative Quadratic Model

We pose a model that assumes that the upper bound of the flow rate is a negative quadratic function of the number of people in the room at time t . The evacuation problem becomes:

$$\begin{aligned} & \text{maximize} \quad \int_0^T f(s)ds \\ & \text{subject to} \quad 0 < f(t) < q - r \left(\int_t^T f(s)ds - p \right)^2, \text{ for } 0 < t < T. \end{aligned} \quad (2)$$

The maximum flow rate q occurs when the room is occupied by an optimal capacity p of people. The motivation for the negative quadratic rests on two assumptions:

- The upper bound decreases when the number of people in the room is substantially less than p , because the time for people to walk to and through the exit becomes nonnegligible compared to the total time required to evacuate all people from the room.
- Conversely, when the number of people in the room noticeably exceeds p , the jostling, discomfort, and limitation of movement that occurs reduces the flow rate through the exits.

The value of p for a room depends on its floor space A and a critical density d (the number of people per area beyond which impediment to motion increases and flow efficiency decreases), with $p = Ad$. We assume that $d = 0.75$ people/ ft^2 .

To solve the evacuation problem using the quadratic model, we assume that maximum flow occurs. The constraint (2) becomes

$$f(t) = q - r \left(\int_0^T f(s)ds - \int_0^t f(s)ds - p \right)^2, \quad 0 < t < T.$$

Differentiating both sides twice with respect to t leads to

$$f''(t)f(t) - f'(t)^2 + 2rf(t)^3 = 0.$$

Using the initial values $f(T) = q - rp^2$ and $f'(T) = 0$ and the package Maple, we get the following solution for the flow rate out of the room at time t :

$$f(t) = \left(\frac{q - rp^2}{\cos((t - T)\sqrt{-qr + r^2p^2})} \right).$$

From this result, we compute the maximum number of people N who can exit the room in a time interval T :

$$N(T) = \int_0^T f(t)dt = \left(\frac{-\tan(T\sqrt{r(-q + rp^2)}) (-q + rp^2)}{\sqrt{r(-q + rp^2)}} \right).$$



Solving for T , we have

$$T(N) = \frac{\left(\frac{\arctan(-N\sqrt{r(-q+rp^2)})}{-q+rp^2} \right)}{\sqrt{r(-q+rp^2)}}.$$

The Relevance of the Negative Quadratic Model

In a panic, some people may sustain injury, fall down, or disrupt the flow of the crowd. Our justification for the quadratic model assumes something similar: People packed together at a density greater than the critical density slow each other down in their attempt to evacuate a room. The difference between the impediments to flow caused by crowding and the impediments caused by panic is one of degree.

To illustrate the predictions of the negative quadratic model, consider a room of size $A = 1,000$ square feet and suppose that the optimum flow rate is $q = 90$ people/min, that optimum flow occurs with $p = Ad = (1000)(0.75) = 750$ people, and that we have $T = 6$ min to evacuate. We take the value for r to be $a/p^2 = .01/(750^2) = 1.8 \times 10^{-8}$. Doing so yields $N(6) = 540$ for the quadratic model and $N(6) = 557$ for the linear model. It makes sense that these numbers are not too far apart, since we are not dealing with an extreme case where the number of people evacuated greatly exceeds or undercuts the critical value p . When p does not deviate significantly from Ad , this will usually be the case. However, if we set p , for example, to 10,000 and calculate as above with all else held constant, we get $N(6) = 501$ for the quadratic model; if we set $p = 100,000$, we get $N(6) = 195$. The negative quadratic model suggests that efforts of a packed crowded to evacuate may actually decrease the number of people evacuated, by causing injuries and inefficient flow.

Limitations of the Negative Quadratic Model

The negative quadratic model is designed to model the evacuation of a space, not of an entire structure. Applying it to a cafeteria on our campus gave results that agree with the constant rate model. An extension of our project would be to simulate a variety of panic situations using the negative quadratic model, the linear model, and the constant rate model and compare the results.

Our simulation works by computing the probability that a person leaves a room at a given time step. The quadratic model breaks down by giving zero or negative probability when the number of people inside is small, so the program switches to a linear model when there are 10 or fewer people in a room.

We estimated p and d . Since the results from the model depend heavily on the values of these parameters, it is important to estimate them accurately.



关注数学模型
获取更多资讯

Ventilation Models

Comfort level is another consideration for maximum capacity:

- The temperature should be between 65° and 90° F. In particular, the ventilation system should be able to dissipate the heat produced by the bodies of the people inside.
- Toxins in the air should be kept to harmless levels. The only one likely to apply to all situations is carbon dioxide (CO_2), produced naturally by human respiration. Jones [1973] recommends that the CO_2 level should be below 0.1%; at 8%, it can be fatal.
- If smoking is allowed, additional circulation must be allowed for.

Human bodies produce heat at a rate from 60 W (asleep) to 600 W (strenuous activity), with 100 W for moderate activity [Jones 1973]. Heat dissipation from a room depends upon its insulation, windows, and any air conditioning. Rooms that are used for several hours at a time should be able to dissipate 100 W/person so that the temperature remains roughly constant.

Jones [1973] recommends at least 0.21/s per person of fresh air, to dilute the CO_2 concentration and unpleasant odors, and 25 l/s if smoking is allowed.

The fraction of oxygen in the air can decrease to 13% before it becomes dangerous, so the presence of toxins is the limiting factor [Jones 1973]. In a tightly enclosed space, the CO_2 produced naturally by human respiration becomes important. A normal human breath is about 500 cc, 4.1% of which is CO_2 , and the breath takes 4 s [Hughes 1963]. Thus, humans produce CO_2 at a rate of 5×10^{-3} mol/s.

Given a room of volume V , the amount N of air molecules is given by the gas law $PV = NRT$, where P is pressure, T is the room temperature in Kelvins, and R is the gas constant. Denote by r the constant rate (in moles per second) of creation of a toxin, by q the fraction of the air that is toxic, and by t elapsed. Then we have

$$qN = rt \quad \text{or} \quad t = \left(\frac{qV}{r} \right) \left(\frac{P}{RT} \right). \quad (3)$$

At room temperature and pressure of 1 atmosphere, $P/RT = 41.4 \text{ mol/m}^3$. Substituting for q the lethal concentration of the toxin yields as t the time for the toxin to reach it.

Consider, for example, an elevator 3 m by 3 m by 3 m carrying 12 people that becomes stuck and is somehow completely air-tight. The people take up about half its volume. Using (3), we find that in 2.5 h the CO_2 level reaches 8%. Hence, we might limit the capacity of the elevator by the time that it takes to get a rescue crew in to open it up. However, elevators are usually well vented, so CO_2 buildup will normally not be a significant constraint.



关注数学模型
获取更多资讯

Swimming Pools

For an outdoor swimming pool, evacuation is not much of a consideration. For an indoor swimming pool, evacuation is basically the same as for an open room. People can exit the pool itself on all sides, except for weaker swimmers who may have to use a ladder, and then flow through the exit doors.

Personal space is the important safety issue. In the water, people must move their arms and legs over a greater range of motion to maneuver than in walking on land. Many swimming strokes limit a swimmer's vision and make collisions more likely. Some swimmers wear floats, which take up additional space.

We recommend 3 m^2 , giving each swimmer 1 m in all directions to move. A large space should be left open around diving boards and slides, perhaps a circle of 4 m.

Capacities for Elevators

Elevators usually have very wide doors and hold only a few people. Thus, evacuation time is negligible in case of an emergency. (The real time constraint will be getting the people down the stairs and out of the building, a problem that is similar to the room problem.)

We already considered the limitations imposed by possible lack of fresh air. More important factors would seem to be weight and space. Elevators have a weight limit supplied by the manufacturer, and a simple elbow-room constraint of 0.5 m^2 per person should provide sufficient personal space.

Strengths and Weaknesses

Our models are fairly robust, with the negative quadratic model being a more realistic tool than the linear model, since the former more accurately simulates panic. However, the negative quadratic model yields questionable results for large values of room occupancy.

Recommendations

For the negative quadratic model, we could extend an analysis of how to determine the value of p to a more comprehensive understanding of how the "forcing effect" operates to slow the evacuation of a panicked crowd. Also, we could develop techniques for measuring the value of the critical density d , such as observing how many people can evacuate a building in different time intervals T , and using those data to estimate the critical value at which maximum flow occurs.



关注数学模型
获取更多资讯

For improving our analysis of the comfort problem, we could develop ways to estimate better how long it takes a room takes to become overheated or stuffy.

Appendix: Computer Simulation

To test the evacuation times of complexes of rooms, we wrote a simulation engine in Python. Object-oriented programming techniques allow us to use different kinds of doors (always open, sometimes blocked, variable flow rate, etc.) and different strategies of selecting a path out of the building with the same structural models. Each door has a queue of people waiting to get through. At each time step, all the doors “warp” some number of people into the next room. Then everyone in line is given the opportunity to move to a different queue, based on their perception of the room. A special room object is designated the “outside” and throws an exception to halt the simulation when a specified number of people have arrived outside. A class diagram for the simulation is given in **Figure A1**.

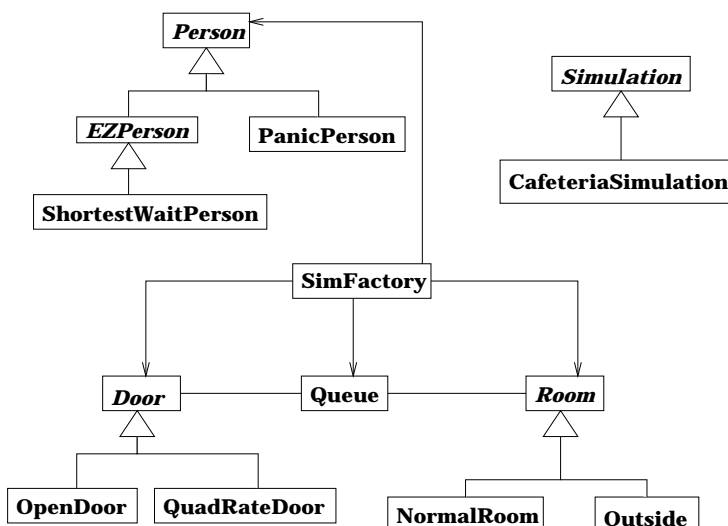


Figure A1. Class diagram of the simulation in abbreviated UML. Triangles indicate inheritance, hairline arrows indicate “creates.”

References

- Francis, R.L. 1984. A negative exponential solution to an evacuation problem. Research Report No. 84-36. Gaithersburg, MD: U.S. Dept. of Commerce National Bureau of Standards Center for Fire Research.
- Hughes, G. M. 1963. *Comparative Physiology of Vertebrate Respiration*. Cambridge, MA: Harvard University Press.
- Jones, W.P. 1973. *Air Conditioning Engineering*. London: Edward Arnold.



Hexagonal Unpacking

David Rudel
 Joshua Greene
 Cameron McLeman
 Harvey Mudd College
 Claremont, CA 91711

Advisor: Ran Libeskind-Hadas

Abstract

We present a model for movement within crowded structures, tessellating a room with hexagons and using a waiting-time function based on the harmonic mean of closest neighbors. We determine the maximum time required for all persons to exit, comparing this time to a target time based on the size of the structure. Our model is very general and its parameters can be modified for several types of buildings. We consider various specific cases, giving the maximum occupancy for each.

Assumptions

- When several people jockey for a vacated position, the probability that one of them occupies it is independent of how long each has spent in his current location. A person who has been waiting longer would seem to have an easier time, but this effect is compensated by the tendency, even in groups of people gathered around an exit, to move in lines. The forward momentum of moving into a new position gives an extra advantage, as the person may well be drafting behind someone else, forming a miniature line weaving through the crowd. Whichever advantage prevails, we posit that it is small enough to ignore.
- People exiting a building generally move so as to decrease their overall expected exit time. Years of selecting optimum shopping lines and struggling to get out of crowded theaters, along with a human's natural ability to see where holes are forming in the crowd, constitute a natural tendency to select paths that minimize the time to exit. Even if humans can't see instantly what course

The UMAP Journal 20 (3) (1999) 287–296. ©Copyright 1999 by COMAP, Inc. All rights reserved. Permission to make digital or hard copies of part or all of this work for personal or classroom use is granted without fee provided that copies are not made or distributed for profit or commercial advantage and that copies bear this notice. Abstracting with credit is permitted, but copyrights for components of this work owned by others than COMAP must be honored. To copy otherwise, to republish, to post on servers, or to redistribute to lists requires prior permission from COMAP.



关注数学模型
 获取更多资讯

will have the least resistance, they certainly can ascertain whether any given step will ultimately shorten their expected wait.

- *The average person can quickly accelerate to a speed of least 6 ft/s.* Normal walking speed is 4 ft/s, so a quick acceleration to 6 ft/s is feasible. The value of this parameter can be changed for kindergarten auditoriums, retirement homes, and other structures housing those likely to have less robust locomotion.
- *When people clump together in attempting to leave a structure, they are packed loosely enough to assign each a cell 1.4 ft in diameter.* While one could theoretically line people up in columns and pack them, standing still, into cells a bit smaller, greater space must be allowed for moving chaotic masses. The mechanics of the model depend very little on the size of the cells.
- *Movable furniture does not block an exit, though it may be in the immediate vicinity of the exit and thus affect the rate of egress.* We allow in the model for tables and other objects to be very close to doors. The safety code provides that doors cannot be blocked by such items, as time for their removal is so prohibitively high as to seriously depreciate the maximum occupancy. We do treat the possibility that one exit (in a multi-exit facility) can become blocked.

Practical Considerations

It is unclear what the target exit time should be. The bulk of our modeling determines exit times based on the parameters of a structure. We then give the maximum occupancy for various exit times.

Points That Must Be Considered

- The number of people exiting a facility during a crowding action is not necessarily the same as the maximum number of people who can leave through doors in orderly lines. To arrive at the total time for evacuation, one cannot simply divide the number of people in a room by how many can go through a door in a given time.
- The movements of individuals leaving a building are made individually, based on the position of the person and openings available.

Definitions

We tessellate the room with regular hexagons, each 1.5 ft along the diagonal (making them 1.299 ft from side to side, with side length 0.75 ft). These represent cells that people occupy while they are in a mass attempting to leave a building.



关注数学模型
获取更多资讯

Our model has a single exit but is easily extendable to more exits. For simplicity, we assume a rectangular room with the door on the north wall (the top wall in all figures).

The orientation of the tessellation makes very little difference in the time calculation, as it is only an abstraction allowing for algorithmic-based movement toward positions of greater desirability.

We define several terms:

- The *neighbors* of a hexagon are those six hexes (or fewer in the case of border hexes) with which it shares sides.
- An *allowed movement* is a movement from a hex to any of its neighbors.
- The *radius* of a hex is the minimal number of allowed movements to take a person at the hex to the door.
- A *level curve* for a radius R is the collection of all hexagons with radius R .
- Two hexes are *isoradial* if they have the same radius.
- A *good neighbor* for a given hex is a neighbor with a smaller radius.
- The *good-neighbor number* of a hex is its number of good neighbors.
- A *desirable neighbor* for a hex is either a neighbor with a smaller radius (a good neighbor) or a neighbor on the same level curve with more good neighbors. The inherent geometry makes some hexes on the same level curve worse than others in terms of waiting time. If we design our model so that people want to go only to hexes of smaller radius, then they will not move toward these better hexes of the same radius. Giving each hex a radius and good-neighbor number accommodates this kind of move.
- The *inherent waiting time* of a hex is how long it takes to traverse it. This is independent of the vacancy or occupancy of neighboring cells. This parameter can be varied to model situations where the terrain makes moving difficult or has a tendency to cause accidents.
- The *actual waiting time* of a hex is the expected amount of time one spends in the hex given the inherent waiting time and the waiting times and competition for neighboring hexes.
- The *equivalent waiting time* of one hex with respect to another is the actual waiting time multiplied by the number of people competing for the hex.
- The *expected exit time* of a hex is the sum of the waiting times of the hexes that form the minimal path to the exit.
- A *click* is the basic unit of time for people fleeing a room. It is based on the type of door being used. The click is the time it takes for a single person to leave a single hex next to a door. Thus, if a door were 3 hexes wide and could let out 6 people/s, a click would equal 0.5 s.



关注数学模型
获取更多资讯

Constructing the Model

We assign each hex an inherent waiting time based on the expected time to traverse it. When a position becomes available, the time to fill the opening is certainly nonnegligible. The base inherent waiting time of a hex that is otherwise free of obstacles and of danger of accident is set to 0.25 s, the time it takes to move 1.5 ft (the width of the hex) at the standard pace of 6 ft/s. Tables and other obstacles can be modeled as hexagons with higher waiting times. (One can jump over a row of seats in a theater, but it takes longer, there is increased chance of tripping, and so on)

To illustrate this step in the model, see **Figure 1**, our representation of a theater. The chairs are represented as hexes with a waiting time of 1 s. **Figure 2** illustrates level curves and good-neighbor numbers for a set of hexes.

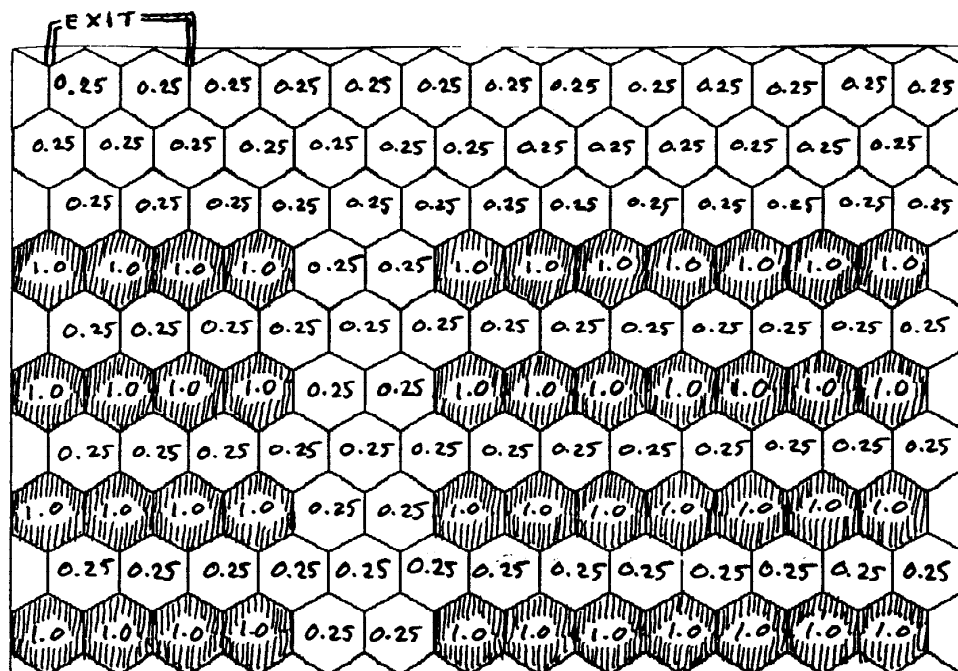


Figure 1. Intrinsic waiting times (in seconds) for cells in a hypothetical theater environment. Cells with value 0.25 represent free space; those with value 1.0 (shaded) correspond to the (fixed) seating.

After inherent waiting times are assigned, we determine how much time to assign to one click. A standard 7 ft \times 2.5 ft door takes up two hexes and can exit 3 people/s, so its click time would be 0.67 s. In general,

$$\text{click time} = \frac{\text{width of door}}{\text{total outflux}},$$

where the width is in hexes and the outflux in people/s. This click time is the maximum speed of egress.

Hexes adjacent to the doors (those with radius 1) are assigned an actual waiting time of 1 click; this represents the expected actual waiting time of someone right next to the door. Some hexes with radius 2 have only one hex



关注数学模型
获取更多资讯

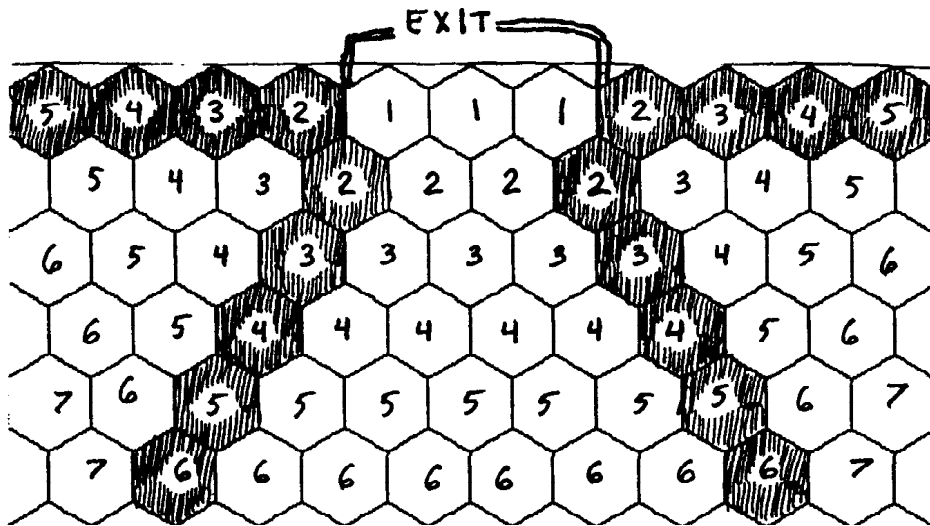


Figure 2. Cells numbered by their level. Cells with one good neighbor are shaded; all other cells are either adjacent to the exit or have two good neighbors.

next to them with a smaller radius, while others have two; the hexes with smaller radii are exit hexes. Hexes with only one neighbor of smaller radius have a good-neighbor number of 1 and are less preferred than those with two neighbors of smaller radius (they have a good-neighbor number of 2). The general rules of movement can be summarized as follows:

- Of two hexes with different radii, the hex of smaller radius is preferred.
- Among isoradial hexes, those with more good neighbors are preferred.

We consider all the hexes of greatest preference and determine the actual waiting time of these. Then we compute the actual waiting time of the next most preferred set of hexes. We thus work our way out from the door (since radius takes precedence over good-neighbor number).

Since the actual waiting time of a hex is based only on the actual waiting time of its desirable neighbors, the competition for these hexes, and its own inherent waiting time, we never need to know the actual waiting time of a hex less desirable than the one that we are working on.

Computing the Actual Waiting Time

Significant Factors

For each desirable neighbor, we compute an equivalent waiting time by multiplying the actual waiting time of the neighbor by the number of hexes vying for the desirable neighbor. If three people are all attempting to get a certain hex, then the equivalent waiting time for all three is three times the actual waiting time of the hex, since each of the vying hexes has a one-third



关注数学模型
获取更多资讯

chance of gaining the desirable hex each time it empties. Thus, competition for hexes tends to slow down a person's progress. However, many hexes have more than one desirable neighbor, just as there are typically more than one near position that someone in a crowd would occupy if given the opportunity. We model the effect of multiple desirable neighbors via the *reduced harmonic mean* (i.e., the harmonic mean divided by the number of desirable neighbors):

$$\text{RHM}(A, B) = \frac{AB}{A+B} = \frac{1}{\frac{1}{A} + \frac{1}{B}};$$

$$\text{RHM}(A, B, C) = \frac{ABC}{AB+BC+AC} = \frac{1}{\frac{1}{A} + \frac{1}{B} + \frac{1}{C}}.$$

Justifying Use of the Harmonic Mean

- We can model the actual waiting times of the desirable neighbors as resistors. The higher the actual waiting time, the longer it takes to shove the same current through a wire. When we have two (or more) desirable neighbors to use as conduit, they combine as resistors in parallel. This is precisely the same function as the reduced harmonic mean.
- All that concerns us is the amount of time that we expect to stay in the given hex. If one hex is open to us once every A clicks, and another is open once every B clicks, then every AB clicks there are B openings from the first and A from the second, so the average number of openings per click is $AB/(A+B)$, which is just the reduced harmonic mean.

The Final Factor

After the reduced harmonic mean of the equivalent waiting time of the various desirable neighbors is computed, the inherent waiting time assigned to the hex is added. This final value is the actual waiting time for the hex. Figures 3 and 4 illustrate this computation applied to a simple model.

The Time Factor

For our model to determine maximum occupancy, it must have a target time. We decided to trust the actual posted occupancy maximums on simple structures with very few obstacles. A curve that fits these numbers well is the power curve $T = 0.4A^{3/4}$, where T is the target time and A is the area of the building in square feet.



关注数学模型
获取更多资讯

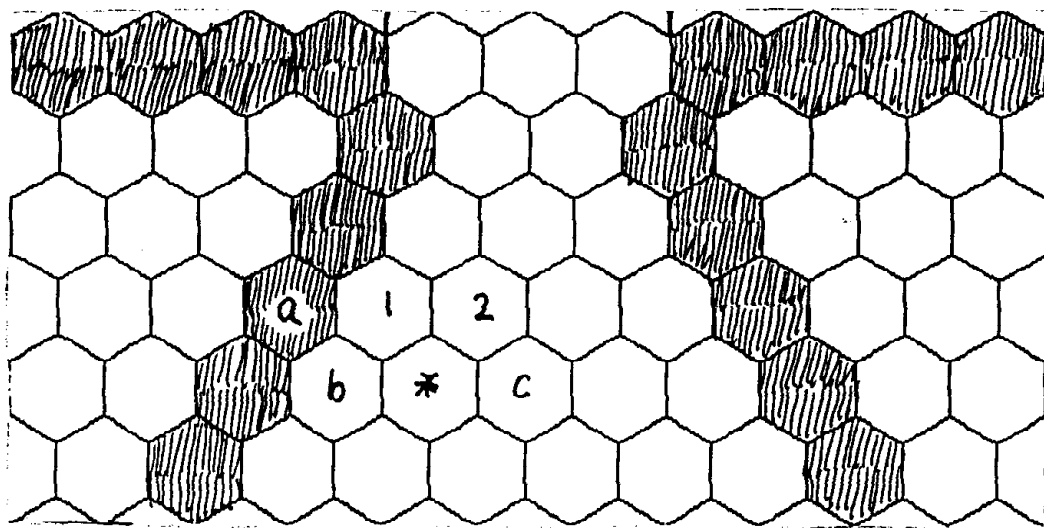


Figure 3. Illustration of the algorithm to compute waiting time of cell (*) in a rectangular room with a single exit at the top three cells wide. We first identify its good neighbors (cells (1) and (2)) and any neighbors on its level curve with a greater number of good neighbors (none in this case). For each of the cells for which (*) vies, we determine the total number of cells vying for that same spot. In the case of (1), this number is 3 (due to (a), (b), and (*)); for (2), it is 2 ((*) and (b)). The waiting time of (1) is then multiplied by the number of cells vying for it, and similarly for (2). The harmonic mean of these equivalent waiting times is divided by the total number of spots for which (*) vies; this reduced harmonic mean, plus the inherent waiting time of (*), gives the actual waiting time for (*).

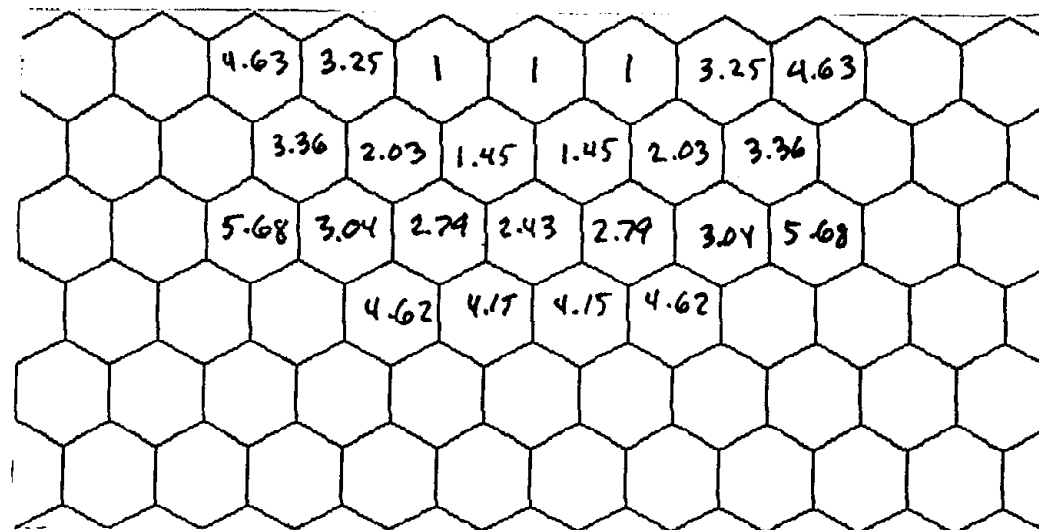


Figure 4. Waiting times for the room of **Figure 3**.



关注数学模型
获取更多资讯

Testing the Model

Consider a bare room, say a gymnasium, with only one exit. If our model is accurate, the time prescribed by the model should be a bit higher than the ratio of number of occupants to greatest number able to leave in a given time—higher because of time lost due to people competing for positions, etc.

A standard gymnasium is built as a full-size basketball court (94 ft long) with one full-size volleyball court turned sideways per half (60 ft wide). With buffer space, the size is 80 ft \times 110 ft, corresponding to a tiling of 84 \times 53 hexagons. At the center of a longer side we place the exit: two sets of double doors, 110 in total width, or approximately 6 hexes. At the standard rate of 2 people/s per door hex, we get a maximum egress rate of 12 people/s.

Assume that there are 875 people in the building (fewer than the maximum capacity of about 1350 listed on such gymnasiums). The formation of a clump of people takes a while. We use a very elementary dynamical-systems approach to finding how long it takes. Consider a person as far as possible away from the door, $\sqrt{55^2 + 80^2} = 97.1$ ft away. Let T be the time for the aggregate to form when there are initially P people in the gymnasium; this is how long it takes the farthest person to walk freely to the back of the accumulated people. The number of hexes within radius R of the door is a quadratic expression in R with leading coefficient 1.5; the radius of the farthest one out is approximately $\sqrt{P/\pi} \approx P/3$. Prior to aggregation, people leave at the maximum rate of 12 people/s, so $P(t) = 875 - 12t$. Thus, noting that each hex has a diameter of 1.4 ft (the average of its diagonal and its side-to-side lengths), we have

$$T = \frac{97.1 - 1.4\sqrt{P(T)/3}}{6}.$$

Substituting and solving gives $T = 10.9$ s. Thus, after 10.9 s, 131 people have left, leaving 744 clumped around the exit.

We tessellate the gymnasium and compute the actual waiting times for the various tiles. We then compute for each hex the shortest expected exit time by finding the shortest path (where shortest here is the path that minimizes the sum of the actual waiting times). We sort these times and find the 744th. This is the time that it should take 744 people to leave the gymnasium. Our model gives approximately 221 s. This added to the approximately 11 s gives a total time of 232 s for leaving the building. This total time is three times as long as the 73 s predicted by simply dividing the number of people in the room (875) by the number of people able to go through the doors per second (12). We feel that the longer estimate from our model is much more realistic.

Results of the Model

Table 1 gives the intrinsic waiting times that we assigned to various entities in rooms, and **Table 2** gives our results.



We ran the model on several structures, giving an occupancy for various times. Each building was created by modifying the appropriate intrinsic wait times. We give a value for the maximum capacity and an estimated time for the evacuation of the building. Some special cases that we feel could not be accurately modeled included structures that do not have discrete doors: swimming pools, open fields, and so on. A similar algorithm described later can deal with most of these. Since there are reasons other than emergencies for wanting to monitor the number of people in a room, for each situation we have provided two other times and their expected total number of exitable people.

One added use of this model for leaving time is to estimate how long it takes a group of people to get out of a maze or a hall of mirrors at a funhouse. This can be simulated by setting the intrinsic waiting time of the hexes to higher levels. As can be seen in the chart, this greatly reduces the number of people who can exit in a given time.

This model also gives a nice way to compare various furniture orientations. We give models of a theater with its door in the center of the back, along with a model of a theater with its door in the back corner. Similarly, large and small classrooms are modeled with two different desk configurations. One model used long tables while the other used individual desks. As one would expect, the long tables produce a longer expected exit time for given number of people; consequently, the maximum allowed occupancy is less.

Table 1.
Inherent waiting times for various objects.

Object	Time (sec)
Free air	0.25
Theater chair	1
Maze in hall of mirrors	3
Table	0.7
Desk	1.2
Stall	20
Sink	20

Strengths and Weaknesses

The strength of this model lies in its general utility to model a broad range of structures by simply varying a few parameters. It demonstrates well how seemingly minor changes such as door position or furniture configuration can change the overall expected exit time.

Another strength of the model is that it gives more than simply the maximum safe occupancy level: It gives a specific time for any occupancy level, so that a user can estimate how long an exiting should take.



Table 2.
Results from the model.

Room Description	Area (sq ft)	Time (sec)	Max. cap.	Time	No.	Time	No.
Theater, 15 rows, door at corner	900	63	98	30	54	120	153
Theater, 15 rows, door at back center	900	63	98	30	54	120	174
Dance room	375	34	83	10	27	60	125
Elevator	60	6	21	3	10	10	26
Large classroom, 4 long tables across	750	57	99	30	57	120	187
Large classroom, 7 rows of 7 desks	750	57	96	30	55	120	186
Small classroom, 3 long tables across	300	25	51	15	27	45	75
Small classroom, 5 rows of 4 desks	300	25	44	15	27	45	67
Bathroom, 5 stalls and 4 sinks	200	21	25	10	15	30	33
Hall of mirrors	1200	82	32				

Implementation requires only a modest microcomputer, and run-time of our program is polynomial in the area of the tessellated region. The code we used took less than one minute of run-time on our computer for each building.

Limitations of the model include restriction to rooms with only one door, but we address this limitation below. Our implementation is confined to rectangular structures, but this is not a limitation of the model itself. The model does not account for individuals who wish to keep up with certain others in a crowd (family members, etc.). The model also does not use in any way the height of the ceiling; for certain emergencies, the volume of a room may well be more important than the area.

Possibly the greatest limitation of the model is basing the target exit-time function on existing codes for certain structures. If the simplest buildings cannot be trusted to have an accurate maximum capacity figure, then the target time function must be changed.

An Improved Implementation

A better implementation of the model, though more computationally complex, allows any number of doors (thus allowing for structures such as swimming pools, where the entirety of the border is a door). A hex has several different radii, one for each door, and the smallest radius determines which door to assign it to. The assignment of actual waiting times to hexes starts at the various doors and flows outward from each equally.

This implementation can be used to model such situations as doors becoming blocked. To model a door becoming blocked at time t_0 , we count how many hexes have total exit times less than t_0 , subtract this number from the total number, and then remodel the room without the door, using the new (reduced) number.



关注数学模型
获取更多资讯

Don't Panic!

Timothy Jones
 Jeremy Katz
 Allison Master
 North Carolina School
 of Science and Mathematics
 Durham, NC 27705

Advisor: Dot Doyle

Assumptions and Hypotheses

- People evacuating in a fire always move towards the nearest exit, regardless of which path to an exit is least crowded and what obstacles are in their way. Thus, a room with multiple exits can be treated as several smaller rooms, each feeding one exit.
- People only become crowded at a finite number of “bottlenecks”—points at which a line develops and evacuating people must wait. In all other areas, people can move freely. However, the line at these points occupies a minimal amount of space.
- Individuals all move through open areas (where there are no bottlenecks) at the same constant rate. This rate depends on the type of occupants in the room and the presence or absence of inanimate obstacles.
- We disregard building construction, panic hardware (such as pushbar doors), and alarm systems.
- The time for an individual to move through the line at a bottleneck follows an exponential probability density function. However, the variation among people is relatively small.

Analysis and Model Development

All of the different reasons to limit the capacity of a building space are more or less independent of one other. For example, during a fire, the sanitation of

The UMAP Journal 20 (3) (1999) 297–309. ©Copyright 1999 by COMAP, Inc. All rights reserved. Permission to make digital or hard copies of part or all of this work for personal or classroom use is granted without fee provided that copies are not made or distributed for profit or commercial advantage and that copies bear this notice. Abstracting with credit is permitted, but copyrights for components of this work owned by others than COMAP must be honored. To copy otherwise, to republish, to post on servers, or to redistribute to lists requires prior permission from COMAP.



关注数学模型
获取更多资讯

a room and the amount of weight that a structure can carry are not immediately important; likewise, when the day-to-day health of a room's occupants is considered, the fact that there might one day be a fire is irrelevant. Thus, we calculate maximum occupancies considering each concern independently and then choose the lowest value.

Simple Rooms in a Fire

In the event of a fire, two elements contribute to the speed with which a room can be evacuated:

- the maximum speed at which the occupants can safely move, and
- the extent of crowding in the room.

We assume that people are free to move except in certain critical areas ("bottlenecks"). At these places, a line builds up, and any individual who reaches the line must wait before moving on to the exit. Thus, in the simplest case—a room with no inanimate obstacles and one exit—the problem can be broken up into two steps: describing how occupants move to the queue at the door, and describing the dynamics of the queue itself. To find how much time is required to evacuate the room, we find the time for the length of the exit queue to drop below 1.

We define a probability density function $P(x, y)$ for the likelihood that an individual is located within a certain region of the room. The coordinate system has the center of the door at the origin and the wall containing the door along the y -axis (**Figure 1**).

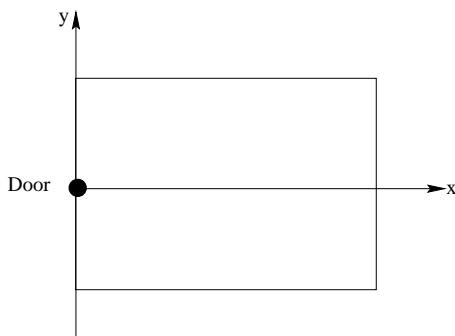


Figure 1. Coordinate system for a room.

We would like to find a second pdf, $q(t)$, to describe the probability that any given individual reaches the door within a certain period of time. Then the probability that an individual reaches the door queue within an interval of time Δt is

$$\int_t^{t+\Delta t} q(t)dt,$$



关注数学模型
获取更多资讯

where t is the time since the alarm first sounded and people began to move to the exits. For simplicity, we call this integral $Q|_t^{t+\Delta t}$. If there are initially n people in the room, the number of people entering the exit queue over the interval $(t, t + \Delta t)$ is $n \cdot Q|_t^{t+\Delta t}$ and the rate at which people are entering the queue is

$$\frac{n \cdot Q|_t^{t+\Delta t}}{\Delta t}. \quad (1)$$

Next, we assume that the time that each individual takes to move through the door queue is described by an exponential probability density function of the form $p(t) = \lambda e^{-\lambda t}$. The expected value of the time required for one person to move through the line is $1/\lambda$ and the average rate at which people leave the queue is λ . Because we assume that most people take the same amount of time to move through the doorway, the rate of a steady stream of people moving through the doorway is never much more or less than λ . However, the queue at the door may have so few people that it can empty completely in time Δt , so that the rate that it empties may be less than λ . In other words, if there are fewer than $\lambda \Delta t$ people in the queue at time t , then by time $t + \Delta t$ they will all have left; if there are more than $\lambda \Delta t$ people, only some can leave. We therefore express the rate at which people leave a queue as

$$\rho = \begin{cases} \frac{L_{n-1}}{\Delta t}, & \text{for } L_{n-1} < \lambda \Delta t; \\ \lambda, & \text{otherwise,} \end{cases} \quad (2)$$

where L_{n-1} is the number of people waiting in the queue at time t and ρ is the rate at which people are leaving the bottleneck.

Combining (1) and (2) gives the rate at which the length of the exit queue is changing in the situation of a room with one exit:

$$\frac{n \cdot Q|_t^{t+\Delta t}}{\Delta t} - \rho.$$

From this, we can write a system of recursive equations (Euler's method) to approximate the length of the line (L_n) versus time:

$$\begin{aligned} t_n &= t_{n-1} + \Delta t, \\ L_n &= L_{n-1} + \left(\frac{n \cdot Q|_t^{t+\Delta t}}{\Delta t} - \rho \right) \cdot \Delta t, \end{aligned} \quad (3)$$

where $L_0 = 0$ is the case for a room in which the people are initially distributed throughout the room.

If these equations are iterated until the length of the exit queue is less than 1, we will learn the time required to evacuate the room in an emergency. However, we still must find a general form for $Q|_t^{t+\Delta t}$ in terms of $P(x, y)$. To accomplish this, we divide the room into a set of concentric circles centered at the door, such



关注数学模型
获取更多资讯

that any person located within a ring-shaped region of the room defined by two of these circles requires between t and $t + \Delta t$ seconds to reach the door. We then divide each of these regions into k smaller segments (**Figure 2**), each of which can be defined in polar coordinates (with the door at the origin) (**Figure 3**). Since each ring corresponds to a certain interval of time, finding the probability that an individual is located within each ring gives the probability that they arrive at the door within that period of time. To approximate this probability, $P(x, y)$ is evaluated at the center of each small wedge-shaped segment and multiplied by the area (ΔA) of the segment; all of these probabilities are then summed to give an approximate value of $Q|_t^{t+\Delta t}$ for each particular t :¹

$$Q|_t^{t+\Delta t} \approx \sum_{i=1}^k P(x_i, y_i) \cdot \Delta A. \quad (4)$$

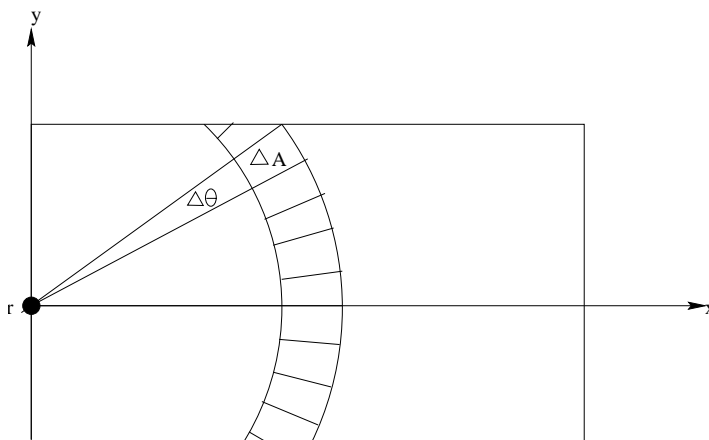


Figure 2. Ring-shaped region divided into k segments.

To compute the sum, we need to express x and y in terms of r (which is constant over the summation) and θ (which varies). From **Figure 3**, we see that

$$x = \frac{r_1 + r_2}{2} \cos\left(\frac{\theta_1 + \theta_2}{2}\right), \quad y = \frac{r_1 + r_2}{2} \sin\left(\frac{\theta_1 + \theta_2}{2}\right).$$

Since the speed s at which a person can move is known, we can express r_1 and r_2 in terms of t :

$$r_1 = st, \quad r_2 = s(t + \Delta t).$$

Rewriting ΔA in terms of r_1 , r_2 , and $\Delta\theta$ gives:

$$\Delta A = \frac{\pi(r_2)^2 \Delta\theta}{2\pi} - \frac{\pi(r_1)^2 \Delta\theta}{2\pi} = \frac{(r_2)^2 \Delta\theta}{2} - \frac{(r_1)^2 \Delta\theta}{2}.$$

¹At the edges of the room (where $P(x, y)$ goes to zero), the small wedge-shaped sections do not accurately follow the wall. As a result, some of the sections “spill over” across the edge; however, since Δt and $\Delta\theta$ are both very small, the effect of this error is minimal.



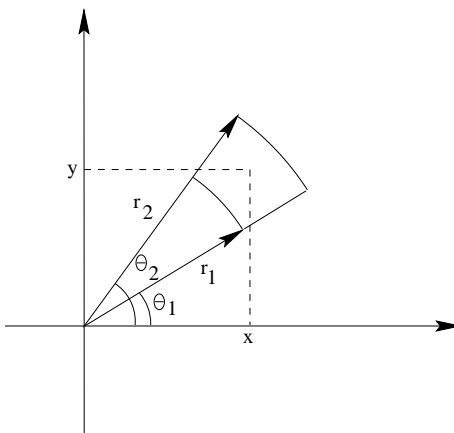


Figure 3. Coordinates of center point.

Thus, (3) can be expressed in terms of t , Δt , $\Delta\theta$, and s . (Note that since the wall containing the door is always along the y -axis, θ_i need only be incremented from $-\pi/2$ to $\pi/2$.) Given these parameters, along with $P(x, y)$, we find the value of $Q|_{t}^{t+\Delta t}$ for each value of t . With these values in hand, we can use (2) to find the length of the exit queue versus time. Once the length of the queue has dropped below one, the room has been successfully evacuated.

More Complex Evacuation Patterns

Because most situations involve multiple bottlenecks, we need to expand the above model for it to be practical. During normal use, occupants of a room are often distributed throughout one or more “reservoirs”—for instance, aisles in an auditorium, regions served by ladders in a swimming pool, sections of seating at a stadium, or tiers of bleachers in a gymnasium—that are separated from the rest of the room by bottlenecks. As soon as the alarm sounds, people begin to move into the first set of bottlenecks and queue at each one (a “feeder queue” of the main exit). As the first set of feeder queues clears, people move to the second bottleneck and enter the queue there. For instance, in an auditorium people must first leave their own aisles (the first level of feeder queues), proceed to the main exit, and wait in line there.

Since a given group of people head only for one exit, each bottleneck has its own independent reservoir of people; the output rates from all the feeder queues can therefore be added to give the input rate of the final exit queue. The rate at which each feeder queue releases people is given by (1), but since it depends on the value of L_{n-1} the entire set of iterations (3) and (2) used to calculate L_n above must be evaluated for each feeder queue in the more complicated situation. Furthermore, the time for a person to move from the output point of a feeder queue to the main exit queue creates a delay; thus, the final Euler’s method equation (which approximates E_n , the length of the exit queue at time t_n) will not depend on the value of L for each feeder queue



关注数学模型
获取更多资讯

at time t_n . Rather, we use $L_{n-\beta}$ (the rate at time $t_{n-\beta}$) for each feeder queue, where β represents the number of Euler's method iterations that pass between the time a person leaves a feeder queue and the time she reaches the final exit queue. The value of β for feeder queue j is therefore given by

$$\beta_j = \left\lceil \frac{\sqrt{x_j^2 + y_j^2}}{s\Delta t} \right\rceil,$$

where (x_j, y_j) is the location of the output point of feeder queue j , $\sqrt{x_j^2 + y_j^2}$ is the distance between the output point and the door, $s\Delta t$ is the distance that can be traveled in one iteration, and we take the ceiling (nearest integer at least as large) of the resulting value.

Since people leave the exit queue in the same way as they leave any bottleneck, we can define ρ_E , the rate at which people leave the final exit queue:

$$\rho_E = \begin{cases} \frac{E_{n-1}}{\Delta t}, & \text{for } E_{n-1} < \lambda\Delta t; \\ \lambda, & \text{otherwise.} \end{cases}$$

Thus, the Euler's method approximation for E_n , the length of the final exit queue at time t_n with m feeder queues, becomes

$$E_n = E_{n-1} + \left[\left(\sum_{j=1}^m \rho_{j-\beta} \right) - \rho_E \right] \cdot \Delta t. \quad (5)$$

As in the previous example, all of the iterative equations (2) to (4) must be evaluated in parallel to calculate values of E_n vs. time, and the room is considered to be successfully evacuated after the line length drops below 1.

Using a hypothetical square room ($10 \text{ m} \times 10 \text{ m}$) with $P(x, y) = 0.01$ everywhere within the room and $P(x, y) = 0$ everywhere else, $n = 100$, $s = 2$, and $\lambda = 2.8$, we generated a graph of length of exit queue vs. time (Figure 4). We measured s and λ empirically for an average person and an average single-width door. Although we have no experimental or theoretical basis for assigning a maximum allowable exit time, we arbitrarily choose 30 s. Since the line has almost disappeared after 30 s, 100 people is just over the maximum capacity for this hypothetical room.

Applications of the Model

Case 1: A Lecture Hall

Our model describes each row of seating in a lecture hall as a bottleneck, the aisle as an open space, and the exit as the final bottleneck. Since the queue at each row forms immediately after the fire alarm sounds and no people enter



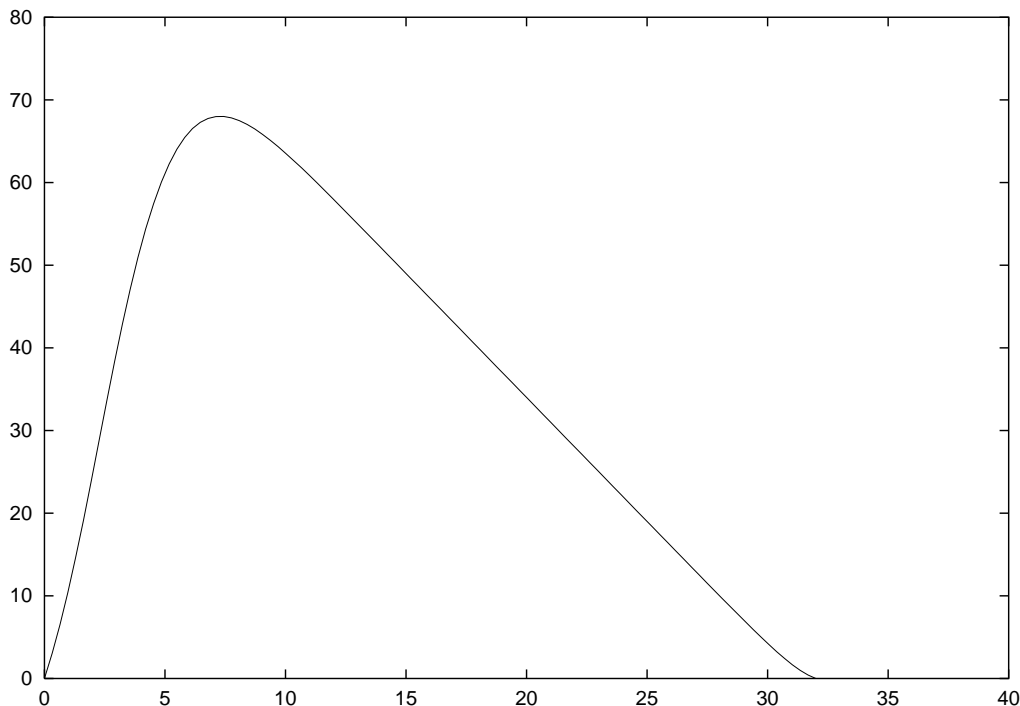


Figure 4. Typical graph of line length vs. time.

the queue thereafter, the value of $Q|_{t_0}^{t+\Delta t}$ is zero for every feeder queue, and the number of people in the room is given by the summation of L_0 for each feeder queue (in addition to any people on the stage). Lecture halls also typically have a plane of symmetry bisecting the seating and the stage, with each half served by its own exit; thus, only half of the room needs to be considered.

Case 2: A Cafeteria

With the presence of many small obstacles (chairs, tables, etc.), occupants cannot move as fast through the “free” spaces. In other words, the value of s is smaller in a room with movable furniture than in a room without such obstacles. A more thorough discussion of the effects of s on the evacuation time is given in **Sensitivity Analysis**.

Case 3: A Swimming Pool

For a swimming pool, we can assume that the only way out of the pool itself is up the ladders. In this case, the pool represents one feeder queue for each ladder, with each ladder serving a specific region of the pool. To account for people distributed outside of the pool in the event of an alarm, we simply add a $Q|_{t_0}^{t+\Delta t}$ term to the final exit Euler’s method equation (4) to represent the rate



at which these people enter the exit queue. Thus,

$$E_n = E_{n-1} + \left(\sum_{j=1}^m (\rho_j - \beta) + \frac{n_{\text{outside}} \cdot Q|_t^{t+\Delta t}}{\Delta t} - \rho_E \right) \cdot \Delta t,$$

where n_{outside} is the number of people outside the pool when the alarm sounds. Another complication is that people move much more slowly in the water; thus, a smaller s -value must be used inside the pool (computing the value of ρ_j) than outside (computing β -values and $Q|_t^{t+\Delta t}$ for the people outside). To incorporate people exiting the pool at areas besides the ladder, we could add another term into the rate portion of (4).

Case 4: An Indoor Arena

Since sports arenas usually exhibit some approximate radial symmetry, only one segment of the building (served by one final exit gate) must be considered. Within each segment, there are usually several sets of seating sections, each served by one stairwell and one smaller gate leading to an aisle. These are the first set of bottlenecks. Within each section of seating, the aisle serves a number of different rows—these represent the second set of bottlenecks. Thus, a stadium presents a three-stage evacuation system: rows of seating lead to aisles, aisles pass through a small gate to an open stairwell, and several stairwells feed a main exit gate. A similar method could be used to evaluate the fire risks of any large building; however, the number of computations required rapidly becomes cumbersome.

Testing the Model: A Lecture Hall

Although the lack of a definite maximum allowable exit time prevents us from properly testing our model, we applied it to a lecture hall at our school for which the established occupancy limit is 117. Only half of the lecture hall has to be considered, as each half of the room has an exit. From the blueprints, we measured the distance from the output point of each of the aisle lines to the exit (from which the program calculates each β). Then, using $\lambda = 1.4$ for the queue at each row (arbitrarily chosen to be half the value for a standard door), $\lambda = 2.8$ for the exit, $s = 2$, and $\Delta t = 1$ s, we found that 117 people could be evacuated in about 30 s, confirming our arbitrary choice of 30 s for the maximum allowable time.

Sensitivity Analysis

The major factors that needed to be accounted for are the rate λ at which people can move through a queue, the speed s at which they can walk, the



size of the room, and the pdf $P(x, y)$ used to describe the occupants' initial locations.

First, we looked at the effect of changes in λ on the time required for various numbers of people to exit the particular room ($4.5\text{ m} \times 6.5\text{ m}$). We iterated the functions until the length of the queue returned to zero, varying both the number of people and the value of λ . (We found $\lambda \approx 2.8$ in our own trials.) Our results show that λ has a greater effect when the number of people in the room is large (see **Table 1**). Therefore, we recommend installing double, or very wide, doors in facilities intended to be used by large numbers of people.

Table 1.
Evacuation time as a function of queue distribution λ and number of people.

$n \setminus \lambda$	1.00	1.25	2.00	2.80	4.00
10	3	3	3	3	3
20	4	4	3	3	3
30	7	4	4	4	4
40	9	6	5	4	4
50	11	7	6	5	4
60	14	8	8	6	5
70	16	9	9	6	5
80	18	10	10	7	6
90	21	11	11	8	6
100	23	13	12	9	7

Second, we looked at the effects of changing the speed of people's movement within the room. For point of reference, in our experiments s ranged from 1 m/s (with obstacles) to 2 m/s (a fast walk in a room with no obstacles). Increased speed does lead to a decreased evacuation time (see **Table 2**)². Even so, our model does not incorporate the negative effects of haste, such as tripping over obstacles or being trampled on by others. Therefore, we feel that a swift but moderate pace should be kept.

We also investigated the effects of increasing area on the evacuation time of a room. Not surprisingly, an increased area (and thus a longer distance to the exit) increases the evacuation time (see **Table 3**).

Finally, we considered the effects of different distributions of people throughout the room. Although we used a uniform distribution for all of our simulations so far, we decided that a normal distribution would make more sense in some cases. Redefining $P(x, y)$ as a three-variable normal pdf, with the hump of the curve in the center of the room, and truncating and renormalizing it over the domain of a $10\text{ m} \times 10\text{ m}$ room, we generated graphs of the length of the exit queue versus time for each distribution (**Figure 5**).

Using a distribution in which the majority of people are closer to the door (like the normal pdf used in **Figure 5**) decreases the time to evacuate.

²The gaps in the table result because no line ever develops at the exit queue, and the program does not know when to end the simulation. This represents a fundamental weakness of our method of determining evacuation time but does not compromise the overall model.



关注数学模型
获取更多资讯

Table 2.

Evacuation time as a function of speed (m/s) and number of people.

$n \setminus s$	0.50	1.00	2.00	3.50
10			3	2
20		5	3	2
30		7	4	3
40	10	7	4	3
50	12	7	5	4
60	14	7	6	4
70	14	8	6	5
80	14	8	7	5
90	14	9	8	6
100	14	10	9	7

Table 3.Evacuation time as a function of (square) room size (m^2) and number of people.

$n \setminus A$	25	100	400	2,500	10,000
10	4	6	11		
20	8	7	12	25	
30	11	10	13	27	
40	14	13	15	29	51
50	17	16	18	30	53
60	20	19	20	31	54
70	24	22	24	31	55
80	27	25	26	32	57
90	30	29	29	34	59
100	33	32	32	36	59

A noteworthy feature of all the graphs is that once the line grows to its maximum length, it decreases linearly thereafter. This implies that the rate at which the room can be evacuated depends primarily on the rate at which people can leave the room, since for the entire linear section (from $t = 5$ to $t = 30$ in **Figure 5**) the rate at which people are entering the queue at the door is close to zero and the rate at which they are leaving is close to λ . This confirms our recommendation that rooms intended to hold large numbers of people should use doors as wide as possible.

Strengths and Weaknesses

The greatest strength of our model lies in its flexibility. Without any fundamental changes, our model can be used on any of a number of different kinds of spaces in which maximum occupancy may be an issue, including auditoriums, pools, lecture halls, board rooms, classrooms, cafeterias, and gymnasiums. In addition, the model can be extended to circumstances in which the exits from the room lead only to an intermediary location, such as a hallway, which then



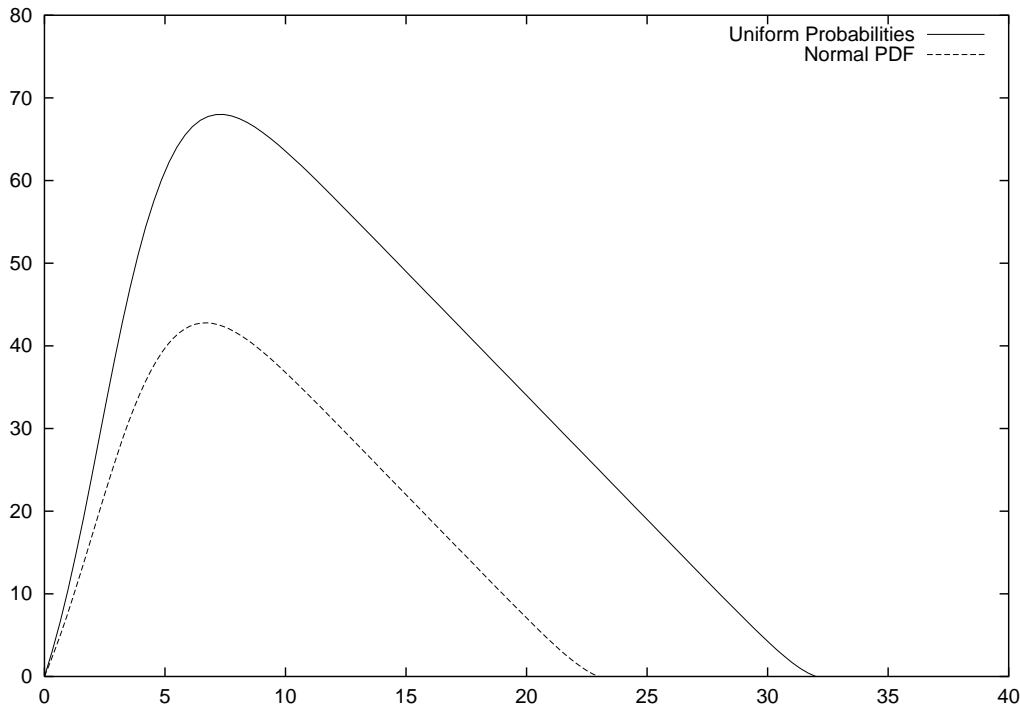


Figure 5. Effect of different pdfs on line length vs. time.

leads into another exit out of the building. This flexibility also leads to one of the larger weaknesses of our model, that it can get overly complex. But, for the majority of situations, our model remains reasonably simple. Furthermore, because the value of $Q|_t^{t+\Delta t}$ can be computed numerically for any given $P(x, y)$, a room of any size or shape and with any distribution of occupants can be considered.

Another strength of our model is that the initial parameters and constants are flexible. Though we used values for λ and s that we determined experimentally, repeated experiments could be done with different audiences to determine more accurate values for these parameters. In addition, λ and s can be modified to include many other variables, such as the type of occupant a room usually holds (for instance, small children and adults have different maximum speeds) and door construction (which dictates λ).

A final strength of our model is its consideration of other factors. By picking the minimum of several maxima, we could determine the maximum occupancy of a room considering other factors such as room size, amount of personal space required by the people in the room, sanitation concerns, and weight capacity.

Our model also has several weaknesses. A sensitivity analysis is difficult to perform. As we were unable to find much data on many of the constants which were needed, we had to determine just a few values experimentally, which may not be representative.

A major weakness concerns our assumptions. In many cases, these may be



large oversimplifications of the actual circumstances of evacuating a room or building (i.e., the assumption of a constant rate leaving a queue). Furthermore, we have no reasonable basis for determining the maximum permissible time to evacuate a room; without this information, we cannot firmly establish the maximum occupancy of a room or building.

Another weakness of our method is the way in which we determine when everyone has left a room. In general, we do this by seeing when the length of the exit queue returns to zero; unfortunately, some people may still be reaching the door and immediately leaving the room, maintaining the length of the queue at zero but still requiring extra time to evacuate. However, this does not invalidate the overall model, and more sophisticated ways of determining when the room is empty could easily be applied.

References

- Allen, Arnold O. 1978. *Probability, Statistics, and Queueing Theory*. Orlando, FL: Academic Press.
- Bartkovich, Kevin G., et al. 1996. *Contemporary Calculus Through Applications*. Dedham, MA: Janson Publications.
- Mendenhall, William, Richard L. Scheaffer, and Dennis D. Wackerly. 1986. *Mathematical Statistics with Applications*. Boston, MA: Duxbury Press.
- O'Brien-Atkins Architecture. 1995. Education Technology Complex Blueprints. March 24, 1995.
- Press, William H., Brian P. Flannery, Saul A. Teukolsky, and William T. Vetterline. 1988. *Numerical Recipes in C: The Art of Scientific Computing*. New York: Cambridge University Press.

Appendix A: Newspaper Article

A guy walks into a bar and the bartender says, "Hey, man, you can't come in here. We're at maximum capacity already." The man replies, "But there's plenty of room—what's the problem?"

This illustrates one of the most threatening evils plaguing our society today—apathy about maximum occupancy. People just don't realize the importance of being able to evacuate quickly from a facility in the event of an emergency. Sure, it may seem fun to see how many people can squeeze into a phone booth together, but what if the phone booth catches on fire? We won't even consider the possible catastrophes in a clown car.

Seriously, public safety is an important concern, especially when considering evacuation speed from a facility. During emergency situations, people



are likely to panic or not think clearly, so extensive planning for the event of an emergency could save lives. Since businesses like restaurants may be more concerned with making money than with safety, a standard method of determining maximum safe occupancy would be helpful in enforcing this issue.

Obviously, one of the most important considerations during an evacuation procedure is that people tend to get backed up at places like doors and other types of exits. We were able to mathematically incorporate this buildup of people into a model to determine the maximum occupancy for many different public facilities. Using queuing theory and Euler's method, we looked at how long various numbers of people took to vacate a certain room. Given a minimum evacuation time (say, thirty seconds or a minute), we can calculate the maximum safe number of people for that room.

However, additional factors must be considered in addition to evacuation speed. For instance, people need a certain amount of personal space. When people are crowded together for long periods of time, certain health hazards might result, especially in a restaurant or cafeteria. Also, many elevators have a maximum weight capacity, which has more to do with the strength of the cables than with evacuation. Looking at all these different factors enables us to find a reasonable and justifiable maximum capacity. Our model, in accurately representing reality, would be an invaluable tool in predicting the likely outcome of an emergency evacuation. Its ability to handle complex situations and extreme flexibility make it ideal for practical use.

So, the next time you see a sign stating maximum safe occupancy, take the time to consider it carefully. If the number of people in the room exceeds the limit, you may want to consider immediately hurrying towards an exit. Just don't panic.



关注数学模型
获取更多资讯



Standing Room Only

Frederick D. Franzwa
 Jonathan L. Matthews
 James I. Meyer
 Rose-Hulman Institute of Technology
 Terre Haute, IN 47803

Advisor: Aaron D. Klebanoff

Letter to the Editor

To the Editor:

Recently, the city has decided to review the current public safety ordinances pertaining to the capacity limits on buildings and public areas. Our team has been asked to reconsider the current ordinances and suggest modifications. Our recommendation will be discussed and voted upon at an upcoming city council meeting, which has stimulated public interest and discussion.

We began our review by defining the purpose of such regulations. We felt that the primary purpose is to preserve public safety. Limiting capacity for other reasons is unnecessary and is likely to promote disagreement and repeated requests for exceptions.

Threats to public safety take two forms: emergencies that require evacuation, and incidents within the venue that require access by police or rescue personnel.

Our analysis is based on statistical data taken of crowd motion in public areas. These data were then incorporated into a computer model that allowed us to investigate crowd behavior in the context of many different situations, including general purpose assemblies of various sizes, classrooms, lecture halls, cafes, and banquet halls, as well as outdoor events from small rallies and demonstrations to parades. This investigation was broad enough to encompass nearly every type of public event.

Only two simple regulations are needed to ensure public safety. First, *there must be no more than 40 people for each exit in the facility*. This rule assures that any room in a facility can be evacuated in one minute or less.

The UMAP Journal 20 (3) (1999) 311–320. ©Copyright 1999 by COMAP, Inc. All rights reserved. Permission to make digital or hard copies of part or all of this work for personal or classroom use is granted without fee provided that copies are not made or distributed for profit or commercial advantage and that copies bear this notice. Abstracting with credit is permitted, but copyrights for components of this work owned by others than COMAP must be honored. To copy otherwise, to republish, to post on servers, or to redistribute to lists requires prior permission from COMAP.



关注数学模型
获取更多资讯

The second regulation is that *each person must have at least 5 sq ft of floor space*. This limitation ensures that small groups of individuals can move throughout a crowd in a reasonable time. Even if there are unlimited exits, a high density of people can be very dangerous; in the event of a personal emergency (heart attack or possibly severe allergic reaction), rescue workers must have sufficient access to the area. These problems are compounded in the event of a riot or mob situation. We found that if the amount of space per person is much less than 5 sq ft the difficulty of moving through the crowd increases drastically.

Overall, we feel this change to regulation will be beneficial to everyone. It will maintain a high standard for public safety and is not unduly complicated or cumbersome. We urge anyone with questions or concerns to contact us. We would be happy to share any additional information or details of our analysis.

Sincerely,

The Room Capacity Assessment Team

Reasons for Legal Capacity Limit

Capacity limits must be considered from the standpoint of convenience and comfort. For example, an overcrowded concert hall can diminish the elegance of the facility, and likewise it is very frustrating to be stuck in line to leave a stadium with fewer exits than optimal. However, we feel that the only justification for a capacity limit is public safety, which falls into two basic categories:

- **Emergency evacuation time:** In the event of a fire or other emergency, the room must be able to be completely emptied quickly.
- **Mobility of small groups of individuals:** Any time a large number of people are packed closely together, there is potential for a mob or riot situation. There is also the possibility of medical emergencies occurring in the crowd. Police, security personnel, and rescue workers must be able to reach any location in a timely manner.

We discuss special cases with unique considerations in the **Appendix**.

Qualities of a Good Capacity Limit

A good capacity limit preserves public safety and is fair and defensible. The model must be easy to understand and implement, to reduce confusion and promote fairness. It is very likely that at times an organization will petition for special permission to hold an event, which may require that the regulation be defended in a courtroom, so the model must be well supported.



关注数学模型
获取更多资讯

Overview of the Approach

We created a model of motion of individuals in a crowd and implemented it on a computer. This model was then used to observe the behavior of the crowd and test various capacity-limiting criteria. Test rooms of various sizes and layout were constructed, and for each room several trials were run, each time increasing the density of individuals in the room.

We made two measurements on each room/crowd-density trial. The first measured the time to empty the room completely, while the second counted the number of individuals whom a security guard is likely to encounter when moving from one side of the room to the other.

Assumptions

- We are concerned only with safety factors. Any other factors need to be addressed by the owner but should not be taken into account in deciding if the capacity is “unlawful.” Customers of the facility will hold the venue owner responsible for comfort issues.
- The people have perfect knowledge of the state of the room at all times. This is reasonable because people do have a good sense of the state of the room.
- People try to get out of the room in the shortest possible time.
- People act in their own best interests, not necessarily in the best interests of the group.

Crowd Escape Model

Description

We simulated people leaving a room. We created rooms in an Excel spreadsheet and then imported the data into a program written in Visual C++. We represented the room as a grid of 1-ft squares, where every spot on the grid was an open space, an immovable object, or an exit. A specified number of people were placed into the room in random locations, with each person occupying a single 1-ft square.

In the simulation, people exit the room according to the Personal Movement Algorithm described below. The algorithm is executed for each person in the room then repeated. Each iteration allows a person to move 1 ft. We measured average walking speed to be approximately 3 ft/s, so each iteration represents 1/3 s.



关注数学模型
获取更多资讯

Personal Movement Algorithm

- Find the best exit and move toward it, taking into account the size of the crowd waiting to use that exit and the distance to the exit.
- If your path is blocked, move in the next best direction. If no moves get you closer to the door, stay in place.

This algorithm is an appropriate model of people exiting a room. People in the model initially head for an exit close to them; but if that exit becomes too congested and another exit clears up, they may head for the less busy exit (much like switching checkout lines at the grocery store). The second rule is reasonable because this is the best way for a person to minimize the time in line. There are two additional restrictions on moves:

- No person can move onto a square that was occupied by another person in the previous time step.
- Flow through each exit is limited to one person every 1.33 seconds.

To gain a qualitative sense of crowd behavior, we collected data by observing people leaving a movie at a local theater. We recorded how many people traveled through a double door per second and the density of the crowd passing through the door, as well as the speed and density in an open area. This information motivated the additional restrictions.

Without the first restriction, the model is unrealistic because people get much too close to one another. Our observations indicate that the density is much less than 1 person/ ft^2 when people are moving; otherwise people would be walking on the heels of the person in front of them.

At the theater, we also noticed that people tend to move more slowly going through a doorway than in an open area. This necessitated the introduction of the second restriction to ensure a realistic flow rate through each exit.

Description of Test Rooms

After defining how people leave the room, we constructed a set of test rooms. The characteristics of the room that could influence the exit time can be grouped into four basic categories (**Table 1**) or a special case.

For each category, we constructed rooms of various sizes, composed of immovable objects (walls, desks, etc.), open space, and exits (**Table 2**).

Exits

One exit represents an opening large enough for one person to walk through at a time. Single doors are represented by one exit. Though three people can walk abreast through a set of double doors, our research at the movie theater shows that a crowd will move through such a doorway two at a time; so we model double doors as two adjacent single doors.



Table 1.
Room classification.

Category	Example
Limited exits	Parties, conventions, concerts, many indoor assemblies
Rows and aisles	Auditoriums, lecture halls, movie theaters, stadiums, inside sporting events
Unlimited exits	Outside sporting events, rallies, demonstrations, parades, air shows, some outdoor concerts
Movable objects	Banquets, cafeterias, restaurants

Table 2.
Test Rooms—Escape Model.

Category	Name	Size (ft ²)	Description
Limited Exits	Small room	144	1 exit
	Medium room	800	3 exits
	Large room	3,000	9 exits
	End exit	800	3 exits all at one end
Rows and aisles	G220 (classroom)	380	2 exits with rows of tables
	E104 (lecture hall)	1182	4 exits with rows of seats
Unlimited exits	Soapbox speech	229	Small outside assembly
	Parade	931	Large outside assembly
Movable objects	Small cafe	411	1 exit with tables and chairs
	Banquet hall	1498	3 exits with tables and chairs
Special cases	Airplane (normal deboarding)	286	1 exit with rows and aisle
	Airplane (crash)	286	6 exits with rows and aisle

Movable Objects

An object small enough to be stepped over should not be considered in the model. Other objects that can impede flow can be treated as immovable. For example, if a chair is in your way in a very crowded room, there is no place to move the chair because of the high density of people. On the other hand, if the density of people is low enough to allow the chair to be moved, you could instead simply use that space to move around the chair. Either way, you are delayed, either by changing your path to move around the chair or by pushing it out of the way. Therefore, our model assumes that people move around movable objects.

Test Room Results

Each test room was simulated with 10 trials, each trial increasing the number of individuals in the room, from 20 ft² / person to 2 ft² / person:

- **Limited Exits:** As expected, increasing the number of people in the room also increased the escape time. There was not a noticeable change when the exits were all placed on one end.



- **Rows and Aisles:** Rows and aisles did not seem to have a significant impact on the escape time. Like the open-room tests, people simply crowded up around the exits.
- **Unlimited Exits:** Escape time seemed to be limited by how far the individuals had to move.
- **Movable Objects:** Movable objects did not seem to have a significant impact.
- **Special Cases:** When exiting an aircraft, the use of emergency exit doors greatly expedites the evacuation process.

Overall, we found that

The ratio of persons to exits determines escape time.

Variations in the data can be explained by several factors. First, the size of the room does play a role. In large rooms, the exit time is slightly longer than for a small room, mainly because even if there are few people in the room, it is large enough that the exits are underutilized while people initially start moving towards them. This effect is best shown in the large room at low densities.

Also, the presence of additional objects does seem to slow progress slightly, as in the airplane example, where the number of available paths is very limited.

Weaknesses

- **Parameter values are debatable:** We based our packing and flow rate constants on a restricted data set. Our observations from the movie theater give us a handle on the situation, but more information is desirable.
- **People don't slow for obstacles:** When a person has to change path to avoid a chair, person, or other obstruction, the person does not slow down. This would only become a major concern when the limiting factor for room escape is the time to reach the exit, as in a large sparsely populated area.
- **People move too much:** In real life, people realize that moving left and right will not get them any closer to the exit. In the model, people always try to get closer to the exit by making extraneous movements. These extra movements help to keep people spread out so that the crowd density doesn't get too high, but do not seem to affect exit utilization.
- **Abnormal rooms:** There are certain room setups where the Personal Movement Algorithm will not lead all persons to exits. For example, people will never move away from an exit to navigate around large obstacles. This can result in people becoming stuck within the room. This problem can be avoided by creating submodels. If a room contains an area in which people can become stuck, then that portion can be modeled separately from the rest of the room. In this way, we can handle any possible room configuration.



关注数学模型
获取更多资讯

Strengths

- **Movement models observed data:** Our model is grounded with data from a situation very similar to the ones we are modeling. This gives a higher confidence in the conclusions and promotes better applicability to actual situations.
- **Movement looks realistic:** The path of a single individual in the simulation follows the path that we would expect of a real person.
- **Adaptable and robust:** Our algorithm works on a large number of rooms and venues. Nearly any given room can be modeled.
- **Expandable:** It would be easy to incorporate more data into the model.

Group Mobility Model

Description

The group mobility model is used to determine the critical factors that predict the ability of a person (e.g., security guard) to get to a specific location in a crowd. This model is a modified version of the crowd escape model. Five guards start on one side of a room filled with people who are moving in random directions, and the guards move across the room to the other side.

Instead of measuring the time required to cross the room, we count the number of people whom the guards encounter along the trip. An encounter is when any person occupies a grid location directly adjacent to the guard's path. "Encounters per foot traveled" measures how much the crowd impedes travel through the room.

Description of Mobility Test Rooms

With these modifications to the computer simulation, we tried to correlate mobility with the size, shape, number of people, number of obstacles and the density of people in the room. This gave rise to the test rooms of **Table 3**.

Table 3.
Test rooms—Group Mobility Model.

Room name	Description
Small room	144 ft ²
Medium room	800 ft ²
Large room	3,000 ft ²
Cafe	800 ft ² with tables and chairs



关注数学模型
获取更多资讯

Results of Mobility Test Rooms

For each room, we ran the simulation 50 times, 5 times each for 10 different densities. We counted the total number of encounters that the 5 guards made while crossing the room. The distance that the guards traveled (as the crow flies) was divided by the total number of encounters.

The data suggest that

The number of encounters per foot is inversely proportional to density.

None of the other four factors is a significant contributor. The number of people and size of room cannot be factors, since the four rooms (when they have the same density) all show the same flow impedance even though they are different sizes and have different numbers of people in them. The four rooms are not the same shape yet exhibit the same behavior under similar densities. Finally, the café has many small obstacles but follows the same trend. (Note: The density in the café was calculated as the number of people divided by the amount of open space.)

Weaknesses

This model exhibits many of the same strengths and weaknesses as the previous model, with some additional characteristics.

- **People move for guards:** Usually, when people see a security guard coming, they tend to move out of the way. Our simulation assumes that people never move out of the way—a worst-case scenario. However, the simulation does represent how easy it is for an ordinary person to get out of the room in case of an allergic reaction or other pressing issue.
- **Densities vary throughout crowds:** Chances are that people will not be evenly spread out. They could be clumped around the place the guard needs to go, creating further difficulty. Our model does not attempt to simulate this sort of behavior.

Strengths

The strengths of this model that pertain solely to the changes we made to the basic model are:

- **Multiple runs:** We ran each simulation 5 times with randomized starting positions for the people and came up with data that were highly correlated. This implies that our model is not sensitive to small changes.
- **Stability:** Our model is not sensitive to relatively large changes in any aspect except the density of people in the room.



Proposal and Conclusion

We feel two limitations should be placed on the number of people in a particular room:

- **Persons per exit:** The overwhelming limitation to the escape time is the number of people per exit. If the maximum escape time is to be 1 min, then there should be no more than 40 people per exit. This requirement will ensure that the room can be evacuated in a reasonable of time.
- **Area per person:** To maintain good accessibility by security personnel, each person should have at least 5 ft^2 of floor space; tables, chairs, and other obstructions must be subtracted from the gross floor space of the room.

Based on our conclusions, we present this formal proposal:

The Maximum Occupancy for said room shall hereby be determined as the lesser of the two following quantities: the number of existing exits multiplied by a factor of 40, and the entire square footage of the room that is deemed usable for walking divided by a factor of 5.

This requirement possesses all the qualities of a good model as specified in the introduction. It ensures public safety by being based on both a maximum time to clear the room and a maximum resistance that people will have trying to traverse through the crowd. It also is simple, requiring only two easy calculations, and defensible, since we have shown above that any other consideration for deciding maximum capacity is negligible.

The specific values for persons per exit and area per person might need to be adjusted depending on the particular situation. For example, if a room is deep within a building, it may need to be evacuated in 30 sec to ensure that the occupants get outside quickly enough. Also, if there is a known hazard in the room, the occupants may need to be able to evacuate the room even faster. The safe density of people could be different for a room depending on whether it is used for rock concerts or for basketball games.

An additional desirable restriction would be that every spot in a room should be within a certain number of feet of an exit. This restriction is especially relevant in large rooms where the capacity is low, since neither of the limitations we recommend takes this situation into account.

Appendix: Special Cases

Elevators

There would be few evacuation problems with a well-functioning elevator due to the small size of an elevator and the close proximity of all spaces in the elevator to the door. The primary safety consideration with an elevator



关注数学模型
获取更多资讯

due to capacity would be exceeding the weight limit of the elevator. Access of emergency personnel wouldn't present a problem, either, because the entire elevator could be quickly evacuated to make room for the personnel.

Because of the safety measures in modern elevators, a broken elevator is rather stable. When an elevator is stuck between floors, the primary time concern for evacuating the elevator would be accessing the elevator compartment rather than removing individuals from the elevator once the elevator has been accessed. There would probably be very little difference in removing one person from a stopped elevator than there would be for removing many.

Pools

The two models can be made to apply to pools by applying them first to the pool itself with different speed information than for walking individuals. The standard model would then be applied to the outer rim area with the actual pool area treated as an immovable object.

A pool has other considerations that should be regulated. The maximum occupancy of a pool with lifeguards on duty should be limited with proportion to the number of lifeguards on duty.

Acknowledgment

Special thanks to the General Manager of the local Keresotes Theaters for permitting access to theaters to collect data on the motion of patrons.



Room Capacity Analysis Using a Pair of Evacuation Models

Gregg A. Christopher
 Orion Lawler
 Jason Tedor
 University of Alaska Fairbanks
 Fairbanks, AK 99775-6660

Advisor: Chris Hartman

Introduction

We present two models for determining the amount of time for a given number of people to evacuate a given room. A room's maximum capacity can be derived from this by imposing a maximum evacuation time, which must take into account factors such as the fire resistance of the room.

We develop a graph-based network flow simulation. People are modeled as a compressible fluid that flows toward and out the exit. This model assumes people's interaction properties, based on industry research.

We also develop a discrete particle simulation. People are modeled as disks that attempt to reach the exits. In this model, people's interaction properties emerge from local, per-person assumptions.

We compare and evaluate the models' outputs and analyze the capacity of several local rooms.

Graph Flow Model

Overview

The graph flow model is a pool-flux model that operates on a graph representing areas of open space within a room. The graph consists of a set of nodes N and a set of directed edges E . Each node is valued as the number of people in a square patch of floor. Each edge represents the direction of traffic flow from one node to another node.

The UMAP Journal 20(3)(1999) 321–329. ©Copyright 1999 by COMAP, Inc. All rights reserved. Permission to make digital or hard copies of part or all of this work for personal or classroom use is granted without fee provided that copies are not made or distributed for profit or commercial advantage and that copies bear this notice. Abstracting with credit is permitted, but copyrights for components of this work owned by others than COMAP must be honored. To copy otherwise, to republish, to post on servers, or to redistribute to lists requires prior permission from COMAP.



关注数学模型
获取更多资讯

The ability of occupants to exit a node is constrained by the congestion in the node and the bandwidth of the edge leading to another node. Bandwidth represents the rate that people can move between nodes. A higher bandwidth is used when there are no obstacles or doors between nodes, and a lower bandwidth is used when an exit constricts flow.

The number of occupants who enter a node is constrained by the number of people leaving the node and the tendency of a node to pack tighter. This tendency is referred to as *fill rate*.

Because there are interdependent relations, each time step of the model is calculated in a cascading pattern from the exits. After the flow rate out of a node is calculated, it becomes possible to calculate flow into the node. By this method the flow rate calculations can be determined for the entire graph.

Assumptions

1. All people are aware of the emergency and attempt to exit.
2. People move only toward a single exit.
3. People are safe, and removed from the simulation, when they reach an exit node.
4. People in crowds move at a speed determined by the density of the crowd.
5. People's movement is restricted by the width of the area that they are trying to move over.
6. People will move to the exit as quickly as possible, without regard to the effect on crowd density.
7. The increase in crowd density over time is limited.
8. People are treated as continuous populations, allowing for fractions.

Weaknesses of the Assumptions

Assumption 1 is not completely supported by the literature—not everyone is aware of or willing to leave during a real emergency.

Assumption 2 implies that people pick a single exit and head for it. In reality, people might observe that an exit is less congested and choose that exit as their new target. This assumption precludes the existence of barriers directing traffic flow or preset fire escape routes within a room.

Assumption 3 ignores the exit discharge capacity. In reality, the number of people leaving by an exit will affect the total evacuation time for a building. With this assumption, the model is limited to a single room.

Assumptions 4 and 5 are based on literature describing pedestrian movement in a transportation terminal [Benz 1986]. Movement in a transportation



关注数学模型
获取更多资讯

terminal is not an escape or evacuation situation, so it could involve different dynamics.

Assumption 6 does not take into account human intelligence or the possible presence of authorities regulating traffic flow.

Assumption 7 was included to reduce the tendency of nodes to fill from empty to maximum capacity in a very short period of time.

Assumption 8 can create situations that are contrary to reality. A person cannot split into fractional parts and flow in two different directions. This assumption is loosely justified by the fact that people can be partially across the boundary of two nodes. This assumption is required by the model mechanics when using small time steps.

Mathematical Structure of the Graph Flow Model

Graph Structure:

N_i = graph node i , representing a patch of floor space

E_i = exits: the set of all nodes N_i may exit to

I_i = inputs: the set of all nodes that exit to N_i

Spatial Values:

P_i = number of people at N_i [persons]

A_i = area of N_i [ft^2]

Constants:

W_{ij} = bandwidth: flow rate from N_i to N_j [persons/ ft] (parameterized)

$W_{ij} = 0.541$ between two nodes [persons/ ft]

$W_{ij} = 0.325$ to an exit node [persons/ ft]

s^α = base movement constant for S_i [58.678, dimensionless]

s^β = movement multiplier constant for S_i [58.669, dimensionless]

s_{\min} = minimum movement at maximum compression [2.5 ft/s]

T = maximum (terminal) compression of an area [3 people/ ft^2]

r^α = fill rate constant [4.333 ft/s] (parametrized)

t = the time step of the model [1 s] (parametrized)

Parameter values are derived from industry research. We omit the derivations for brevity.

Derived Constants:

$A_i T$ = maximum occupancy of node [persons]



Flux Capacity Equations

Let S_i denote the walking speed inside a node due to congestion [ft/sec]:

$$S_i = S(P_i, A_i) = \max \left[s^\alpha + s^\beta \ln \left(\frac{A_i}{P_i} \right), S_{\min} \right].$$

Let FR_i denote the fill rate: the maximum number of people who can be added to N_i over time t [persons]

$$\text{FR}_i = \text{FR}(N_i, t) = r^\alpha t \frac{A_i T - P_i}{A_i T}.$$

Let OF_{ij} be the desired (maximal) outflow: the number of people capable of moving out of N_i into N_j [persons]

$$\text{OF}_{ij} = \text{OF}(N_i, N_j, t) = t S_i W_{ij}.$$

Let IF_i be the maximum inflow: the number of people who can enter a node from any direction in t [persons]. Note that IF_i cannot be calculated until FFA_{iE_j} is calculated for all N_j in E_i .

$$\text{IF}_i = \text{IF}(N_i, t) = \sum_{E_i} \text{FFA}_{iE_i} + \text{FR}_i.$$

Let FF_{ij} be the final flow: the number of people capable of moving from N_i to N_j that N_j is capable of accepting [persons]. Note that FF_{ij} cannot be calculated until IF_j is known.

$$\text{FF}_{ij} = \text{FF}(N_i, N_j, t) = \begin{cases} \text{OF}_{ij}, & \text{if } N_j \text{ is an exit;} \\ \text{OF}_{ij} \frac{\text{OF}_{ij}}{\sum_{N_k \in I_j} \text{OF}_{kj}}, & \text{if } \text{IF}_{ij} < \sum_{N_k \in I_j} \text{OF}_{kj}; \\ \text{OF}_{ij}, & \text{if } \text{IF}_{ij} \geq \sum_{N_k \in I_j} \text{OF}_{kj}. \end{cases}$$

Let FFA_{ij} denote the actual number of people who move from N_i to N_j . Note that FFA_{ij} cannot be calculated until FF_{iE_j} is calculated for all N_j in E_i .

$$\text{FFA}_{ij} = \text{FFA}(N_i, N_j, t) = \begin{cases} \text{FF}_{ij}, & \text{if } P_i \geq \sum_{k \in E_i} \text{FF}_{ik}; \\ P_i \frac{\text{FF}_{ij}}{\sum_{k \in E_i} \text{FF}_{ik}}, & \text{otherwise.} \end{cases}$$

This is a pool-flux model. The P_i are pools, and FFA_{ij} is the only flux that is ever applied to a pool.

Development of the Flow Functions

For constant t and W_{ij} , OF_{ij} is linearly proportional to walking speed due to congestion (S_i). For constant t and S_i , OF_{ij} is linearly proportional to bandwidth (W_{ij}).



Because IF_i is a function of the actual final flows out of a node, IF cannot be calculated until these actual final flows have been calculated first. These final flows are a function of the IF for the nodes that N_i flows into. Because of this dependency, the node graph must be acyclic. If the graph contains a cycle, then no IF_i for any node that is a member of the cycle can be calculated because it is dependent on IF for another node that is a member the cycle. Then IF equals to the total number of people that flow out of a node plus the fill rate for that node.

The final flow FF_{ij} (the number of people capable of moving from N_i to N_j that N_j is capable of accepting [persons]) is a function of IF_j , unless N_j is an exit.

The relationship between final flow and actual final flow is straightforward. Final flow calculates the number of people that can flow out of a node. However, if final flow is more than the population of the node, then this population is divided evenly among the available final flows. Otherwise, actual final flow is equal to final flow.

Particle Simulation Model

Overview

The particle simulation models humans one at a time as discrete, independent entities, instead of treating a flow of people as an undifferentiated group.

The simulation begins with a single, 2-D room at the start of an emergency. People in the room each choose a visible nearby exit and walk toward it. People navigate obstacles such as furniture, and, if crowded together, interact with one another. The simulation continues until everyone has reached an exit.

Individual humans (especially during an emergency) are concerned primarily with getting to an exit, greedily maximizing their own chance of survival. This model thus operates on a local level, allowing the overall global properties (such as total exit time and walking speed vs. congestion) to emerge.

Assumptions

Although human behavior is in general very complex, the modeling task is substantially simplified in a crowd during an emergency. Still, the primary weaknesses of this model lie in its restrictive and somewhat arbitrary assumptions.

1. All humans are aware of the emergency, and all attempt to exit.
2. People pick exits based on congestion (number of people near that exit), distance, and visibility—people cannot see through walls. Occasionally, people check for a better exit.



3. People are safe, and removed from the simulation, when they reach an exit.
4. People walk at 4 ft/s.
5. People may change direction and speed instantly.
6. If a person's intended path would pass through another person, that person stops and tries to go in some other direction.
7. People cannot walk through walls or furniture. For these purposes, people are treated as disks.
8. People plan a path around furniture to reach an exit.

Weaknesses of the Assumptions

Assumption 1 is not completely supported by the literature—not everyone is aware of or willing to leave during a real emergency.

Assumption 2 is more restrictive than reality—humans remember the location of out-of-view exits, and often “follow the crowd” to an exit that they can’t see.

Assumption 3 neglects the finite person-handling capacity of many exits (e.g., narrow stairwells).

Assumption 4 neglects the very young, old, or handicapped, who may move more slowly, as well as the panic-stricken, who move more quickly.

Assumption 5 is contrary to basic physical principles, but significantly simplifies interactions.

Assumption 6 neglects people’s sophisticated path planning, which allows us (usually!) to avoid walking into each other without stopping.

Assumption 7 treats people as hard, inelastic 2-D disks.

Assumption 8 neglects the panic-stricken, who may in fact run directly into furniture.

Example

Despite their disadvantages, these assumptions produce behavior that is remarkably crowd-like and consistent with research data.

We simulated 400 people leaving a 110 ft × 120 ft gymnasium, with the people initially distributed uniformly across the room. Moving independently, people quickly form groups near the exit. As people near the exit flow out, the groups shuffle around to bring more people to the exit. The model produces loose clumping around the exits, a natural result of people’s desire to go towards the exit but with aversion to running into one another.



关注数学模型
获取更多资讯

Human Interaction in Crowds

The overall result emerges only from our single assumption about how people interact: If your intended path will intersect another person, stop and try another (random) direction. We analyzed other potential ways for people to interact, but they produced decidedly non-human behavior.

We would have preferred to pick a deterministic interaction, because we would rather not have the results of our model change with each execution of the model. For each deterministic interaction we considered (e.g. if your path will intersect someone, go around them to your right), we could always find cases that created a circular-wait condition. This situation, in which object A waits for object B, who in turn waits on object A, is known to computer scientists as *deadlock*.

We can make the model give us the same results each time by using a pseudorandom (deterministic, but uniformly distributed and statistically uncorrelated) number generator to pick directions. Thus our randomized interaction scheme runs the same way each time, yet produces behavior that is reasonably similar to that of actual people—for example, they don't deadlock.

Test Scenarios and Model Validation

We used both the particle model and the graph flow model to evaluate exit time from test rooms. Each test room has one exit. One test room is 15 ft × 15 ft and has a 3-ft-wide exit in the center of the left wall. Each model was run repeatedly, using a different occupancy for each run.

The graph flow model was applied to a space that was equal in size to the particle flow model space.

After both models were executed repeatedly for different room occupancies, we obtained the results of **Figure 1**.

The results of both models (for this room and for others not shown here) appear to be very nearly linear for the rooms tested. However, the slope of the nearest linear approximation of each model differs. Since both models are driven by arbitrary parameters, specifically bandwidth for the graph-flow model and person radius for the particle model, it is not surprising that this difference exists.

We consider it significant that both models display similar trends. Each model was derived from an independent set of driving assumptions and data, but the behavior trends of the models are strongly correlated. This reflects positively on both models.



关注数学模型
获取更多资讯

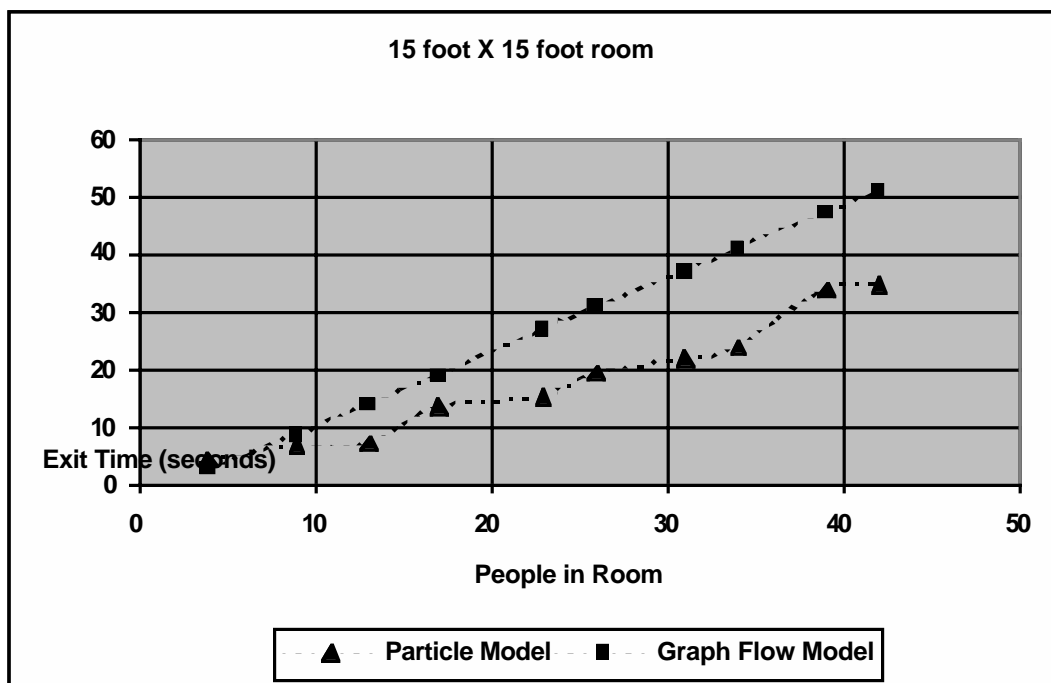


Figure 1. Results of simulations of the two models, for a 15 ft × 15 ft room.

Strengths/Weaknesses

The graph-flow model has several weaknesses. It treats people not as indivisible entities but as a fluid. Its results depend on an arbitrary choice of bandwidth, as well as on the source graph, and we did not address the problem of building this graph.

Human behavior in the graph-flow model is deterministic, but much of the mathematical structure of the graph-flow model is driven by actual research.

The particle simulator model has several weaknesses. Its results are a function of an arbitrary choice of radius. Its decisions are nondeterministic, so they can vary significantly for tiny input changes. The model is also occasionally subject to pathological, non-human behavior—for example, people occasionally lose sight of a nearby exit and travel a long distance to a visible exit.

The particle simulator model, however, also has several advantages. It models people as individual, indivisible entities. People can move independently of their neighbors. No assumptions need be made about the global flow in the room.



关注数学模型
获取更多资讯

Conclusion

We have presented two models for determining how long it takes to evacuate a room. Despite their very different approaches and assumptions, both models substantially agree on our test cases.

Based on our test cases and the analysis of several local rooms, we find that a time-to-exit vs. initial population graph is nearly linear. The actual slope of the line depends on the layout of the room and the size and number of exits.

We expected the exit rate to decrease as more people tried to pack into the exits, but the actual exit rate (for both models) remains constant. We attribute this to the fact that exits become congested very quickly, even if only a few dozen people are attempting to exit. This is in agreement with our experience—it doesn't take many people (under a dozen) to block an exit.

The posted maximum occupancies of the local buildings that we simulated were adequate. At maximum occupancy, everyone evacuated in under 3 min, an acceptable time [Life Safety Code 1997, Section A-21-1.3].

To determine the maximum occupancy of a room, we suggest first consulting a fire marshal to determine the maximum acceptable time for evacuation. Then use the simulator to find the largest number of people who can escape in less than the maximum time. This is easy because the function relating the number of occupants to evacuation time is nearly linear.

References

- Benz, Gregory P. 1986. Application of the time-space concept to a transportation terminal waiting and circulation area. In *Transit Terminals: Planning and Design Elements*, Transportation Research Record 1054. Washington, DC: Transportation Research Board, National Research Council.
- Egan, M. David. 1978 *Concepts in Building Fire Safety*. New York: John Wiley and Sons.
- Life Safety Code*. 1997. National Fire Protection Agency. Quincy, MA: National Fire Protection Association.
- The Uniform Fire Code*. 1991. International Conference of Building Officials, Western Fire Chiefs Association. International Fire Code Institute.



关注数学模型
获取更多资讯



Judge's Commentary: The Outstanding Lawful Capacity Papers

Jerrold R. Griggs

Department of Mathematics
University of South Carolina
Columbia, SC 29208
griggs@math.sc.edu
homepage: <http://www.math.sc.edu/~griggs/>

Introduction

Judging the Lawful Capacity Problem in this year's contest was an enjoyable experience because of the diverse approaches taken, and the Outstanding papers published here display a truly wide range of modeling approaches. We leave it to the reader to decide which is best!

One nice approach is to use a graphical/network flow model. One paper employs a series of queues to handle the bottlenecks. Another model tiles the room with one-person-sized hexagons and calculates the expected waiting times for each. There is a sophisticated motion simulation model that represents people by disks that naturally flow around obstacles towards exits.

We judges had a tough job selecting the Outstanding papers—one of my favorites didn't get selected! Here are some of the things that we looked for.

Many teams took an overly simplified approach to determine appropriate room capacity restrictions. This basic approach works as follows:

Determine

- an exit flow rate of r people per second per exit,
- the number of exits n in the room, and
- the number of seconds s to clear the room safely,

then obtain a room capacity of rns people.

The UMAP Journal 20 (3) (1999) 331–333. ©Copyright 1999 by COMAP, Inc. All rights reserved. Permission to make digital or hard copies of part or all of this work for personal or classroom use is granted without fee provided that copies are not made or distributed for profit or commercial advantage and that copies bear this notice. Abstracting with credit is permitted, but copyrights for components of this work owned by others than COMAP must be honored. To copy otherwise, to republish, to post on servers, or to redistribute to lists requires prior permission from COMAP.



关注数学模型
获取更多资讯

However, the best papers, including the Outstanding ones published here, allow for a range of significant factors to be included in the model. Among these, they consider the flow of people through the room—not just at the exit—as well as crowd congestion due to bottlenecks created by the room shape and furniture placement. A strong model allows a variable initial distribution of people in the room. Judges were impressed by models that permit people to react to crowding at a nearby exit by switching towards a less crowded, though more distant, exit.

Many entries omit several of the elements requested in the problem; while very few papers manage to cover all of these points, the best ones all come close. These include:

- considering different room arrangements and environments,
- comparing models to posted requirements or codes,
- discussing criteria other than safety, and
- writing an explanatory article suitable for the newspaper.

Researching the problem impressed the judges, such as by consulting existing codes or by gathering data directly from crowd observations. One paper even considers capacity reductions mandated by the Americans with Disabilities Act!

Some papers present easily understood graphs of exit time as a function of the number of people in the room; such displays make it easy for the decision maker.

It was nice to see analysis of model run-time complexity, which is important in dealing with very large or complicated arrangements, along with improvements made by simplifying calculations.

Papers stood out that consider factors that could be included in a more elaborate model, such as crowd panic, accessibility of emergency personnel, ventilation, and crowd flow out of the entire building.

Advice

We conclude by giving advice to future entrants by listing some general tips that the judges feel are applicable to any contest problem.

- *Teams should attempt to address all major issues in the problem.* Projects missing several elements are eliminated quickly.
- *A thorough, informative summary is essential.* Papers that are strong otherwise are often eliminated in early judging rounds due to weak summaries. Don't merely restate the problem in the summary, but indicate how it is being modeled and what was learned from the model. The summary should not be overly technical.



- *Develop a model that people can use!* The model should be easy to follow. While an occasional “snow job” makes it through the judges, we generally abhor a morass of variables and equations that can’t be fathomed. Well-chosen examples enhance the readability of a paper. It is best to work the reader through any algorithm that is presented; too often papers include only computer code or pseudocode for an algorithm without sufficient explanation of why and how it works.
- *Supporting information is important.* Figures, tables, and illustrations are very helpful in selling your model. A complete list of references is essential—document where your ideas come from.

About the Author

Jerry Griggs a graduate of Pomona College and MIT, where he earned his Ph.D. in 1977. Since 1981, he has been at the University of South Carolina, where he is Professor of Mathematics and a member of the Industrial Mathematics Institute. He received the 1999 award at the University for research in science and engineering.

His research area is combinatorics and graph theory, both fundamental theory and applications to database security, communications, and biology. He has published more than 60 papers and supervised 11 doctoral and 9 master’s students. He serves on the Board of the Mathematics Foundation of America, which oversees the Canada/USA Mathcamp. He has been an MCM judge since 1988.



关注数学模型
获取更多资讯



关注数学模型
获取更多资讯

Practitioner's Commentary: The Outstanding Lawful Capacity Papers: The Answer Is Not the Solution

Richard Hewitt, Ph.D.

U S WEST Communications Performance Systems
1801 California St., Suite 4595
Denver CO 80202
rhwitt@uswest.com

Introduction

I would first like to thank *The UMAP Journal* for inviting me to write the practitioners article for this years Mathematical Contest in Modeling. The topic is of interest to me in that I have some direct experience solving problems and implementing solutions in the public safety arena. My hands-on training in this area includes spending time in burning buildings, cutting people out of wrecked cars, and, unfortunately, putting a few people in body bags.

As a result of these experiences, I developed sufficient knowledge and credibility to develop a method that the Denver Fire Department uses for selecting sites for new fire stations. The station-siting problem that I addressed is similar to your contest problem in that my mathematical training enabled me to find the correct answer, but focusing exclusively on a mathematical solution moved me further away from a solution which could be implemented. As the practitioner commentator for this years Contest in Modeling, let me suggest that in pursuing a mathematical solution to the maximum occupancy problem you may have moved away from a solution which could be implemented.

Let me outline what I plan to discuss:

- I want to congratulate not only the five winning teams whose papers are published in this issue but also the 202 other teams whose papers were not selected for publication.

The UMAP Journal 20 (3) (1999) 335–341. ©Copyright 1999 by COMAP, Inc. All rights reserved. Permission to make digital or hard copies of part or all of this work for personal or classroom use is granted without fee provided that copies are not made or distributed for profit or commercial advantage and that copies bear this notice. Abstracting with credit is permitted, but copyrights for components of this work owned by others than COMAP must be honored. To copy otherwise, to republish, to post on servers, or to redistribute to lists requires prior permission from COMAP.



关注数学模型
获取更多资讯

- I would like to discuss some of the common assumptions made in solving the maximum occupancy problem.
- I would like to challenge the contest participants and readers to elevate their problem-solving skills by focusing on what's required to get a solution implemented. Hence my title, "The Answer Is Not the Solution."
- Finally, I would like to offer some suggestions regarding how to effectively communicate technical information to the public.

Background (Mine)

To accomplish these objectives, let me provide a bit of personal background which should help the reader interpret my comments. I hold three graduate degrees in quantitative / analytical fields: a Ph.D. in operations research, a master's degree in mathematics, and a master's degree in economics. I mention these academic credentials not to impress you but to impress upon you that my academic training only helped me begin to solve "real-world problems"—and in the initial stages of my career, it actually got in the way.

I might have successfully convinced you that the training required to complete three graduate degrees would enable me to solve virtually any quantitative or analytic problem. I used to believe that myself, until I left the safety of academia. What I quickly found out is that in the real world, all bets are off. There are no pure analytic problems. There are no standalone quantitative problems. There are quantitative problems embedded in political problems. There are analytic problems embedded in economic problems. There are technical problems encrusted in hidden agendas with stakeholders whom you don't even know exist, much less their agendas, interrelationships, or side agreements. I'm not saying these things to discourage you, but rather to let you know up front that they do exist—and to let you know that these problems are much more fun to solve than the textbook problems that you encounter in school. I also want to let you know that if you can solve these types of problems (and based on what I've seen, you can), you can solve just about any problem.

Congratulations

I want to congratulate all those who participated in this year's contest. To dedicate an entire weekend focused on a single problem, particularly one foreign to your prior problem solving experience, is commendable. Further, to outline and detail the quality of solutions evidenced by the published articles is extraordinary. You truly exhibit the problem-solving skills needed in the world today.

I was particularly impressed by your abilities to outline a solution approach (including your assumptions) and decision criteria. The communication of



关注数学模型
获取更多资讯

these components will be critical to your future success. Frequently when one presents a solution to senior management, the assumptions and methodology are more important than the answer. That may sound strange at this point in your academic training; but trust me, after you graduate and present a few solutions, you will understand what I'm saying. It is your assumptions and modeling approach that determine, to a great degree, the answer that you get. It is in developing the approach and building the model that you gain a rich understanding of the problem. Your ability to truly understand a problem not only enables you to solve the problem, but more important, empowers you to implement the solution—and implementation is where you provide value to an employer and prove value to yourself.

I was impressed as I read the five solution approaches published in this journal. The level of understanding and variety of mathematical tools employed to solve the problem were far beyond anything I encountered at the undergraduate level. Of course, back then we scratched our solutions on cave walls and held up torches so that our professors could read them. Well, I'm exaggerating a bit; but your understanding and sophistication are well beyond anything I possessed or encountered at the undergraduate level. I was also impressed with your written communication skills, your ability to put thoughts on paper and communicate them clearly and succinctly. Frequently, the people who master problem-solving are among the weakest at communicating the results. I encourage you to continue to refine your communication skills. They will serve you well and are perhaps even more important than your quantitative problem solving skills.

Assumptions

Enough congratulations, I was truly impressed. Let's discuss some assumptions. The common assumption that I saw in the models was the one I will paraphrase as, "when exiting a room or building, during an emergency, people will exit via the nearest exit." Unfortunately, this not the case. According to Denver Fire Chief Richard Gonzales, "studies have shown that in the case of fire, people exit via the door they entered, regardless of the nearest exit. During a fire people do not always act rationally. They generally remember the way they came in and retrace that path even if another exit is much closer." This finding, based on actual experience, further complicates the maximum occupancy problem and creates a need to understand how people enter a room or building to determine how they will exit. This adds a level of complexity to determining how quickly people will exit and therefore the maximum number to let in.

Let's examine another common assumption. I will paraphrase this one as, "the average person can exit at a rate of x feet per second." Having entered and exited burning buildings on more than a few occasions, I can challenge this assumption based on first-hand experience. I have been in several burning



关注数学模型
获取更多资讯

buildings where the smoke was so thick that I couldn't see my hand in front of my face. It's also not unusual for the power to go out because of the fire or water used to fight it. Unless the room has emergency lighting (or it's daytime and the room has exterior windows), you're moving around in darkness. In smaller fires, or in the early stages of a fire, it can be difficult to see across a well-lit room; and many public places, such as restaurants, bars, dance halls, and theaters, are not well lit. The point is that visibility is a critical variable that impacts the speed at which people can exit or even find the exit they remember entering.

In addition, most people have never exited a room or building during a fire, and this lack of experience impacts the way they react. Our common evacuation experiences occur during fire drills, and fire drills do not accurately represent emergency conditions. (As an aside, when was the last time you participated in a fire drill at a restaurant, bar, dance hall, or theatre?) The reason why people practice fire drills is so that they know where the exits are and which one to use in the event of a fire. But knowing what to do and doing it are two different things. If they were the same, we would ace every exam, never get in a car wreck, and always say the right thing.

The next assumption that I would like to address was actually implied in each of the published articles. I will paraphrase the assumption as "people behave rationally in an emergency." In a private conversation, Chief Gonzales cited several examples of just how irrationally some people behave. The Chief's examples are best summarized by the comments of a restaurant patron who refused to leave a burning building, even as the room was filling with smoke. The man argued with fire department personnel, "I paid for this steak and I'm going to eat it." This may be an extreme example; but extreme or not, it highlights a point: You have to account for human behavior, whether it's logical or not, because that behavior represents reality. Failure to do so leaves your model, and therefore your solution, open to attack.

The message that I hope you're hearing is this: Your model or solution approach must account for critical real-world conditions. Failure to do so will impact your credibility and therefore acceptance of your solution.

Will They Use Your Solution?

Let's move on to implementation requirements. To maximize the probability of a successful implementation, your solution, model, or method must address the issues of each stakeholder. This implies that you must first figure out who the stakeholders are. In the case of the maximum occupancy problem, Chubb and Williamson [1998] provide a fairly complete list of construction project stakeholders, each of which has a stake in the maximum occupancy decision:

Construction projects require an owner or developer who defines a specific need. The owner must usually obtain or arrange for the acquisition



关注数学模型
获取更多资讯

or transfer and expenditure of capital to finance the project. This capital will be used to procure skilled designers, builders, and the materials they need to execute the project. To protect this investment, insurers will be retained to underwrite the performance of the contracted designers and builders, and insurers will ultimately assume a portion of the risk exposure once the project is completed. Regulators will insist on reviewing the project throughout design and construction as well as throughout the period of occupancy to ensure compliance with regulatory mandates. Besides preserving public confidence in building safety and safeguarding the public from involuntary exposure to fire risk, their activities also help ensure a secure tax base. Finally, the occupants or tenants themselves will often participate to see that their individual needs are met. ... The complexity of fire safety decisions is amplified by the individual agendas these actors bring with them.

After the relevant stakeholders have been identified, you have to identify the needs and concerns of each stakeholder group. This is best done by talking to them, in person, on their turf and in their terms. During the discussion, ask lots of "why" questions ("Why is that important?" and "Why do you feel that way?"). The answers to these questions enable you to understand what each stakeholder values. You can then define a solution space that incorporates what the stakeholders told you was important. You then begin to weigh priorities and make tradeoffs based on politics, economic impact, risk, importance to the decision makers, and/or the ability of a stakeholder group to block the implementation of your solution. And yes, you can now incorporate your mathematical findings.

For what it's worth, I have never (outside of academia) seen a mathematical solution dominate the other decision criteria. In really good solutions, the mathematical findings complement the solution, but they never dictate it. Regarding the use of mathematical models to solve real-world problems, my point is best captured in the words of Chief Gonzales, "These models work in an ideal world, but that world doesn't exist."

Telling the Story

Let me address the newspaper articles written for local newspapers, defending your analysis. It has been my experience that when communicating to the general public, one's message is best received when it is presented in simple, clear, and succinct terms that address the audience's hopes, fears, and dreams as they pertain to the topic at hand. To that end, let me suggest that an article defending your method should focus on its ease of use, grounding in common sense, and the amount by which the results you generate exceed what they already have. A quote from a highly visible and respected official never hurts either.



关注数学模型
获取更多资讯

As an example of what not to do, I submit the following.

Dear Mr. And Mrs. Public,

Concerning our award-winning method to determine the maximum occupancy level of your child's elementary school classroom, we used a polyhedral approach to approximate a statistically unbiased estimator that incorporated Euler's formula to model crowd movement based in small rooms. This model incorporated Chebyshev's inequality as it applies to elementary-school traffic patterns.

We then fed our results into a simulation model utilizing software that we built ourselves based on tools that we downloaded from the Internet.

While this method is probably way over your head, we have full confidence in its ability to forecast the probability of an emergency during school hours.

This information enables us to set the maximum occupancy of your child's classroom at 183 plus or minus 7%.

Yours truly,
Contest Winners

The correct approach would be to convince the public that your method yields a solution that increases their safety and improves the likelihood of the survival of their loved ones. As an old farmer once told me, "No one wants to know how we make sausage, they just want to know how good it tastes."

Summary

Let me close by summarizing my key points:

- I commend you on your ability to frame the problem and communicate your assumptions and solution approach.
- Always test your assumptions to make sure they are grounded in reality.
- Identify the relevant stakeholders, elicit their concerns, and address those. You don't have to give everyone what they want, but you do have to demonstrate that you listened and considered each request.
- When communicating to the public (written or oral), use simple, clear, and succinct language that address the audience's hopes, fears, and dreams as they pertain to the topic at hand. Focus on the benefits that they will receive and how your solution represents an improvement over what they now have.



关注数学模型
获取更多资讯

If you do these four things, your successes will outnumber your failures and people will respect your work.

Good luck and keep up the good work.

Reference

- Chubb, M.D., and R.B. Williamson. 1998. Value-based fire safety: A new regulatory model for mitigating human error. In *Human Behaviour In Fire—Proceeding of the First International Symposium*, August 30—September 2, 1998, edited by T.J. Shields, 105–114. Belfast, Northern Ireland: University of Ulster.

About the Author

Richard Hewitt has solved problems and implemented solutions in a variety of industries, including oil and gas exploration, public safety, and telecommunications. His work includes two trips to Antarctica on behalf of the National Science Foundation to realign support operations for the NSF Antarctic Research Program. Dr. Hewitt's work has directly resulted in the generation of over \$500 million in new revenue and annual cost savings in excess of \$65 million. Dr. Hewitt is currently developing a performance feedback system for U S WEST, a Fortune 100 corporation in the telecommunications industry.



关注数学模型
获取更多资讯



关注数学模型
获取更多资讯

Pollution Detection: Modeling an Underground Spill through Hydro-Chemical Analysis

James R. Garlick
 Savannah N. Crites
 Earlham College
 Richmond, IN 47374

Advisors: Mic Jackson and Tekla Lewin

Summary

Data from ten monitoring wells in a region of suspected underground pollution are used to assess the source, time, and amount of pollutant released into the ground. The chemicals are sorted based on changes recorded in their concentrations over time to determine which were active pollutants during the data collection period and to account for discrepancy caused by an incomplete data set. Those chemicals found to be active during this time period change concentration simultaneously, indicating that each chemical is a component of a single leaking liquid involved in two major spills. The concentrations of selected active chemicals are combined to form a composite indicator whose concentration value is found at each well on each date. The composite indicator reveals that two spills occurred, the first between July 1991 and March 1993, and the second between January 1995 and April 1997, possibly continuing until the end of the data collection period. The primary chemical constituents of the leaking liquid are identified.

A Delaunay triangulation is used to interpolate a gradient of concentration for the composite indicator at each date between the monitoring wells. Given that the general flow of groundwater in this region is directed toward well 9, the time and location of the pollution source can be approximated based on changes in the concentration gradient over time. This spill is estimated to have originated in the region surrounding the point (8000, 4500). Following the initial triangulation, Voronoi polygons are used to construct a convex hull

The UMAP Journal 20 (3) (1999) 343–354. ©Copyright 1999 by COMAP, Inc. All rights reserved. Permission to make digital or hard copies of part or all of this work for personal or classroom use is granted without fee provided that copies are not made or distributed for profit or commercial advantage and that copies bear this notice. Abstracting with credit is permitted, but copyrights for components of this work owned by others than COMAP must be honored. To copy otherwise, to republish, to post on servers, or to redistribute to lists requires prior permission from COMAP.



关注数学模型
 获取更多资讯

representing the total volume and position of the spill (the volume of the contaminated area). This polygon is comprised of smaller segments, each of a specific uniform concentration. The program Geomview is used to generate graphics of these polygons and convex hulls. A volume can be calculated at each concentration, and ultimately the total volume of polluting liquid can be found, if the concentration of the composite indicator in the original polluting liquid is known.

Finally, various testing and interpretation methods are explored and incorporated into a procedure for evaluating underground pollution. Each method is discussed in terms of its application to the scenario in Problem Two and uses information given in the data set to test the validity of the method.

Introduction

Given the location and elevation of eight groundwater monitoring wells (two more wells exist at unknown locations), a complete chemical analysis taken periodically at each well between 1990 and 1997, and the general direction of groundwater flow, it is possible to accurately estimate the location, source, time of origin, and total volume of pollutants seeping underground. In the case of a suspected leak in a chemical storage facility built over homogeneous soil, cost and safety prohibited collection of analytical data directly below the suspected sight of the spill. Data from monitoring wells surrounding the periphery of but not necessarily directly in the suspected polluted region are used in a mathematical model to determine whether a leak has occurred, the time and location when the leak occurred, and the amount of liquid that has leaked during the data collection period.

Assumptions

- All monitoring wells are located below ground and are contained within an aquifer (a geological unit capable of storing and transmitting substantial volumes of water). This aquifer has an unobstructed constant flow rate which is inversely proportional to the porosity of the soil medium. The monitoring wells are permanent, allow free flow through their measuring devices, have no effect on the chemical or geological composition of the region, and provide an accurate reflection of the surrounding area. This ensures that the wells themselves do not contaminate or pollute the region to be assessed [Soliman et al. 1997, 32].
- The volume of fluid is constant in each well, and all wells have the same volume. Assuming a consistent volume between wells allows direct ratios to be assessed comparing concentrations of solutes in each well.



关注数学模型
获取更多资讯

- Different chemicals may travel through the aquifer at different rates. Chemical substances have a constant and specific ability to move in aqueous solutions depending on polarity of the molecules, hydrophobicity, and the initial concentration of each compound.
- Some chemicals found present in the data set occur naturally in the groundwater and are not products of pollution. Any chemical that exhibits no significant change in concentration at any monitoring well over the course of the data collection period can be removed from consideration in the data. In addition, certain naturally appearing chemical components of groundwater can be expected to fluctuate between standard levels.
- Concentrations of pollutants are highest near their source, and concentrations decrease as time and distance from their source increases.
- The given data set is incomplete. Some trends may be misrepresented or missed entirely due to lack of available data. Also, the values that are given must be appropriately evaluated so as not to treat the N/A values as zero.
- Discrepancies in the data can be attributed to variations in the equipment used or in sampling and analyzing techniques over the course of the study and should not always be interpreted as changes in the environment, especially those occurring on the same data in every sample tested.
- *Pollution* is defined as a contaminant that is harmful to an organism, while *contamination* refers to a greater concentration of a substance than would occur naturally without necessarily causing harm [Blatt 1997, 76]. In this problem, we assume that both terms refer to the artificial contamination of an underground region, regardless of the effect that the contaminants may have on organisms.

Dealing with the Data

To use or interpret such a large and varied data set effectively, specific criteria must be employed to organize and sort the known information. We converted the data from its original spreadsheet form into a database so that we could set up queries and selectively access any portion of the information.

Several components of the data were not chemical concentrations but other factors necessary for a thorough chemical analysis, such as specific conductivity and total dissolved solids. These were separated and stored in another spreadsheet. Although some methods of modeling pollution use these measurements, our models do not, because we could not detect a significant pattern in these values to indicate the presence or absence of pollution.

Using line graphs mapping the concentration of a given chemical at all dates and at each well, we identified chemicals that exhibited a negligible change in concentration. These were removed and stored in a separate spreadsheet. This left 23 chemicals from an original set of 106 measurement categories.



关注数学模型
获取更多资讯

Determining the Presence of Pollution

From the rapid increases shown in the line graphs of chemical concentrations over time, it was apparent that new pollution had occurred in this region over the testing period. Those chemicals detected as new pollutants include: acetone, ammonia, arsenic, barium, bicarbonate, calcium, chloride, iron, lead, magnesium, manganese, nickel, nitrate/nitrite, potassium, sodium, TDS, sulfate, vanadium, and zinc.

The concentration of the majority of the chemicals in the active data set rise and fall together, indicating that each is a constituent of a single liquid involved in the spill. Although the concentrations of all active chemicals in the data set follow obvious trends, the changes in concentration are much more amplified for some than for others. We chose these amplified chemicals as indicator chemicals to track the movement of the spill. To further simplify spill detection, we added the concentrations of these indicator chemicals (chloride, sulfate, and nitrate/nitrite) together to form a composite indicator chemical, the concentration of which indicates the presence of pollution at each test site on a given date. We chose these chemicals also because they are common components of pollutants and are often used to monitor pollution [B.C. Ministry of Environment, Land, and Parks 1999].

In choosing chemicals to serve as indicators for a spill, it is essential to find chemicals that were measured consistently on the same dates and at all wells throughout the data collection period. Three chemicals in this data set that fit this criterion are chloride, sulfide, and nitrate/nitrite, and we used those in the composite indicator. Because the data set is not complete and the measurements were not taken consistently for all chemicals at all points or on all dates, it is important to ensure that the concentration of this composite indicator does not misrepresent trends in the movement of the spill due to a lack or abundance of data for a given well or on a given date. We went through the data set and eliminated dates that were recorded twice (taking an average of the concentrations listed at each well) and corrected other abnormalities in the data until each of the three chemicals had exactly one value at each test location on all dates needed. Exceptions to this include those wells for which values are not available at the beginning of the testing period; these are added as data from these wells became available.

The Time of the Spill

A series of line graphs showing the concentration of the composite indicator at a given well over time can be used to estimate the time of the spill. When plotted together so that each line represents a monitoring well, these graphs of concentration over time show when concentrations first start to increase and at which well(s) this increase is first recorded. This record of which wells show the first rise in concentration provides a rough estimation of the location of the



source as well. [EDITOR'S NOTE: We cannot effectively reproduce the authors' graphs here in black and white.]

Two spills probably occurred, the first between July 1991 and March 1993. During these times, the concentrations in wells believed to be closest to the spill increased dramatically, then receded back toward normal levels. The second probably began in January 1995 and continued at least until January 1997. At this time, concentrations were starting to descend, but this could result from a decrease in the rate of the spill and may not indicate that the leak stopped.

Locating the Source

The line graphs generated by queries from the database are extremely useful in determining the presence of a spill, the time at which it occurred, and the chemicals involved. However, finding the source of the spill is more effectively accomplished with a visual interpolation showing the concentration of the composite indicator at each well over time. This way, we can determine where the concentrations rose first and the general direction the spill moved in. Knowing the general direction of the spill, we can develop bounds within which the source of the spill must lie. This can be done in three dimensions by creating a Voronoi polygon. This method of interpolation organizes data points into a triangles with their natural neighbors and partitions areas around each known point into polygons such that an arbitrary point placed in the polygon is closer to that data point than any other. The triangulation of a map is unique and effectively weights the value of any point in the region as a function of its distance from three natural neighbors.

While the line graphs show approximate dates when a spill might have occurred and at which wells the changes in concentration were detected, the Voronoi polygon method interpolates between the known data points to show more precisely the location of the spill source. From a series of diagrams of the concentration of the composite indicator chemical at each well over a selection of dates, the progress of the spill is very apparent, and the location of the source can be found by following the flow patterns in the underground system backward from the point where the spill first occurred. [EDITOR'S NOTE: We do not reproduce the authors' maps.]

A Procedure for Evaluating Underground Contamination

The problem of detecting the presence of underground liquids is an old one, and due to its applications in locating water sources, petroleum reserves, and mineral deposits, an abundance of information about techniques and methods is available. Drilling sampling or monitoring wells is clearly necessary at some



point to determine the exact properties of an underground region. However, such sampling and the analysis that follows is time consuming, dangerous, expensive, and has the potential to contaminate or destroy the flow of groundwater in the region. There are numerous surface or superficial measurements that help determine the most effective placement of such wells. In addition, data gained from existing wells can help determine the need for and placement of additional monitoring wells when properly applied. Several useful measurements can be gained from a surface geophysical survey before drilling a well, including gravitational, electrical, and magnetic conductance readings. These involve the passage of electrical current or magnetic fields through surface soil and measuring the drop in voltage or potential magnetism, as well as the density at a given location. By comparing the conductance of surface soils at various locations in the region, the presence of sand or gravel beds can often be detected below the surface [Walton 1970, 61]. This is useful because sand and gravel beds have a high porosity, or ability to contain free flowing fluids in the form of groundwater tables known as aquifers. These aquifers are the mechanism by which underground pollutants are contained and spread, so an understanding of the flow and direction of the aquifer is crucial to accurately predicting the location or the source of contaminants [Soliman et al. 1997, 32].

Drilling and Monitoring A Well

Once the location of an initial well has been decided (surface measurements should indicate the presence of an aquifer), several types of wells are available. Because drilling the initial bore hole for the well is the most dangerous and expensive part of the process, permanent monitoring wells such as those used in collecting the data set for this problem are the most economical in the long term. Such a well should be capable of detecting the direction and rate of flow of fluids in the aquifer, determining the level of the water table, and providing core samples to be chemically analyzed in a laboratory. These wells must be permeable to water in the region and cannot disrupt flow in the aquifer or introduce new contaminants due to the drilling process or corrosion of the well itself over time.

How Many Wells Are Needed?

The number of wells needed to determine the source, time, and volume of an underground chemical spill can vary widely based on the circumstances of the spill. For the models described here, a minimum of three wells is necessary. From the initial well, the direction and flow of the water system can be determined, along with the concentration values of chemicals dissolved in the groundwater. Additional wells should be drilled along the path of the water table, considering the general location of a chemical storage facility or other suspected source of contamination, if known. If contaminants are detected



关注数学模型
获取更多资讯

by the initial well, others should be drilled "downstream" to the spill, and if no contaminants are detected, wells should be drilled "up stream," or possibly along a different aquifer, depending on the geological constitution of the region.

When at least three wells are available to detect the flow and concentration of contaminants, the following models can be used to estimate the location of the source of any contaminants found to be present, as well as the time of a spill, and the total volume of liquid spilled. In each case, the more wells used for data collection, the more accurate predictions can be made about the spill.

Model 1: A Graphical Approach

This model requires the assessment of chemical concentrations at a minimum of three different locations on at least three dates per location. The more wells or locations of data collection, the more accurate the model.

The first step is to enter the concentration values into a database so that they can be accessed by date, collection location, chemical, or concentration. Using the database, line graphs showing concentrations of all chemicals by date can be generated for each well or collection location. From these graphs, the presence of pollution can be determined, as well as the date of significant changes in concentration of measured chemicals. Dramatic increases in concentration indicate the introduction of a pollutant in this model. In many cases, as in this problem, many of the chemicals detected in a chemical analysis will rise and fall simultaneously, indicating that they are components of a common pollutant. It is possible that the chemicals would fall into two apparent groups, indicating that two liquids are leaking. In this case, one chemical, or preferably a group of detected chemicals, is consolidated to form an indicator chemical. This simplifies future graphs by allowing only one concentration value to be monitored.

In creating a consolidated indicator, it is imperative that the data be consistent. The same type of data must be available at all sites and on all dates, or adjustments must be incorporated to prevent anomalies in the data set from drastically misrepresenting the concentration of chemicals detected in the groundwater.

Having developed a consolidated indicator by adding the concentration values of representative chemicals at each site on a given date, we can generate new graphs to determine the time and source of a spill. Overlaying graphs showing concentrations over time at each well can effectively be used to determine the time of a spill. It is useful to collect enough data to develop a baseline concentration for the chemicals being measured. Tables published by the EPA, the British Columbia Department of the Environment, Land, and Parks, and other regulatory agencies list normal ranges of concentrations of various chemicals in groundwater and are also useful in distinguishing those chemicals present naturally in a system from those caused by pollution.



关注数学模型
获取更多资讯

Interpreting these graphs is relatively simple. On a chart showing the location of each well or test location, identify those wells (if any) that never show a definite increase in concentration of the indicator. Then the well or wells reached first by high concentration values and the wells showing the highest concentration of chemical overall must be identified. Using this information, as well as the direction and rate of flow in the system (measured at each well or given in the problem statement), the contaminants can be traced back to an estimated source location.

The results of this process for each of the two spills indicated are included in **Figure 1**. Both spills reached wells 9 and 12 fastest, showing an increase at wells 3 and 11, and 7 later. This indicates that both spills began somewhere in the region surrounding the point (8000, 4500).

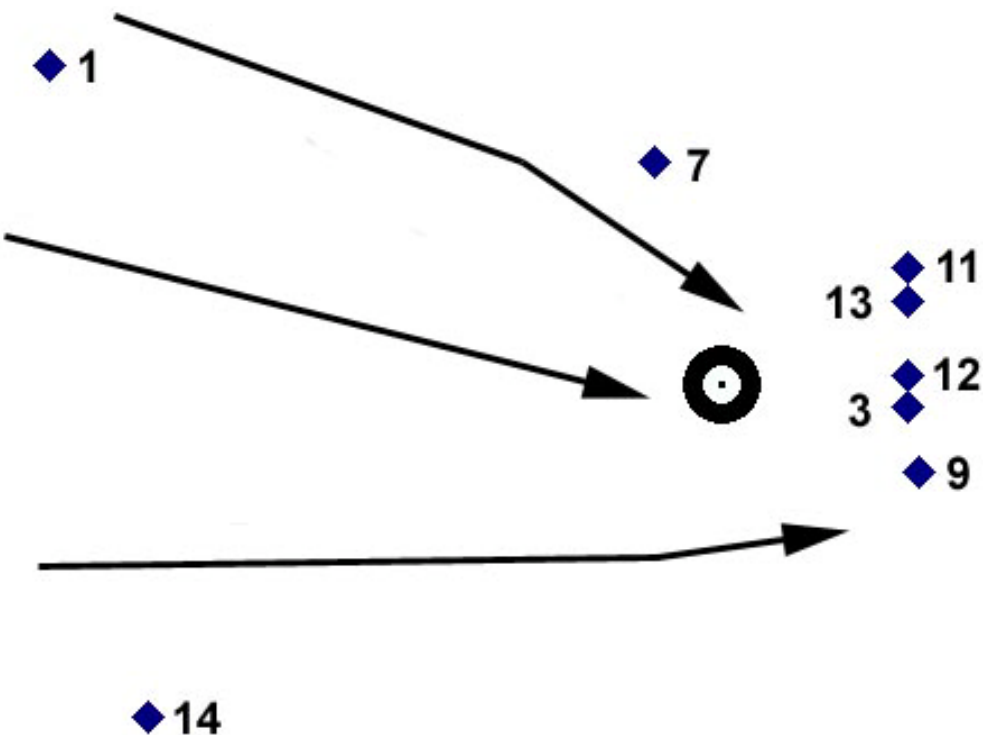


Figure 1. Location of the spills, indicated by a bull's eye, with directions of flow in the aquifer.

The delay of the spill reaching well 7 may be due to a pattern in the flow direction of the aquifer. It may at first seem strange that well 3 shows less concentration than well 7, which is clearly farther from the spill. This is probably due to the lower elevation of this well. The measurements taken at the top, bottom, and middle of the monitoring wells indicate that the spill is seeping in a downward direction, and that it never reaches the bottom of the wells. This also explains why well 13, directly in the path of the spill, never shows an increase in chemical concentration—its only samples were taken from the bottom of the well.



关注数学模型
获取更多资讯

Strengths and Weaknesses

The greatest strength of this method is its efficiency in interpreting a large and complex data set. Most computers are able to build and utilize such a database from a spreadsheet, and once the data are organized, the time needed to compute and interpret the results is minimal. Because it bases the placement of new wells on information gathered by existing ones and provides rough approximations with as few as three wells, the model is very efficient in terms of drilling and well maintenance. However, it provides only a very general approximation of the time and location of the source and has the potential to be greatly affected by irregularities in the positioning of the wells or uneven flow patterns in the groundwater system. In situations where samples are unavailable directly below a suspected pollution source, leaks cannot be detected until they have already penetrated into the groundwater supply, precluding attempts to stop the leak before it poses a problem to the surrounding community. This method provides no way to accurately determine the volume of polluting liquid spilled.

Model 2: Interpolation with Triangulation in Three Dimensions

Using the same methods described above, this model requires the creation of a database and line graphs to determine the presence of a pollutant and the chemicals involved. It also uses changes in the concentration of a composite indicator of chemicals to monitor the flow of the pollutant.

Computational geometry describes a method known as *natural-neighbor interpolation* by which sets of highly irregular data can be organized and represented visually. Using Delaunay triangulation, a unique set of triangles can be arranged in an arbitrary set of points. The value of an arbitrary point is defined entirely locally based on the values of the three nearest known points, the vertices of the triangle in which the point lies.

Delaunay triangulation and Voronoi polygons are extremely useful for interpolation in this type of system for two primary reasons:

- They provide a linear system by which the value of any arbitrary point can be determined, and the original data points are exactly recovered if solved for using this system.
- The interpolation of every point is influenced only by its natural neighbors such that irregularities in the data set are reflected in the model but do not distort the accuracy of the model at other points [Sambridge et al. 1995, 3].

The computer program Geomview takes concentrations stored in the database and the location coordinates of the monitoring wells and generates a convex hull that represents of the spill as a whole. The convex hull is the outermost surface of a Voronoi polygon, comprised of smaller tetrahedrons, each called a



关注数学模型
获取更多资讯

datum, representing the space between three “natural neighbors.” Each datum has a specific and constant concentration based on the known concentrations at the three points that define it [Watson 1992, 108].

The data entered into this program are divided such that only concentrations above an established baseline appear in the visual model representing the spill. The program weights each datum by volume at a specific concentration and, by adding each of these weighted concentrations, calculates the total volume of liquid in the spill. The convex hull can be used in this model to visually represent the location and volume of the entire contaminated area of the spill. We used Geomview to generate maps to show the spill defined by this data set at six dates during the data collection period and the volume of the contaminated area at that time. [EDITOR'S NOTE: We do not reproduce the authors' maps.]

This model is also useful in determining the source of the chemical spill. It produces a new diagram on every date requested based on the concentrations entered from the data set for that date. At the start of the data collection period, no pollution is visible. As time progresses, the diagram clearly indicates which wells experienced higher than normal concentrations of the indicator chemical. The approximate source of contamination, as well as the direction of flow in the groundwater table, are apparent when several successive convex hulls are viewed together.

Error Analysis

To test the error of this model and the linear model, a data set can be computed for which the source location of contaminant, the date on which the leak occurred, and the total volume of liquid spilled are known. The difference between predicted values and the actual location, time, and volume, divided by the actual values, determines the percentage error of the interpolation. The amount of error will depend on numerous factors specific to the individual test including how far the source is from the nearest monitoring well, the flow rates in the underground system, the size of the spill, the number of monitoring wells, and many more factors.

Strengths and Weaknesses

This model is inherently stronger than the graphical method because it allows a three-dimensional visualization of the data and because it uses a unique and algorithmic interpolation to evaluate the presence of contaminants between known points. Delaunay triangulations and the Voronoi polygons and convex hulls that can be derived from them are extremely accurate when used to interpolate in highly irregular data sets, because of the natural-neighbor principle. The presence of irregular data points or wide variations in distribution of points is reflected in the resulting projection but does not result in a misrepresentation of the data or inaccurately skew the values of known points.



关注数学模型
获取更多资讯

[Sambridge et al. 1995]. The more data points available, the more accurate this interpolation is, because—like any interpolation—the model is most accurate nearest the known points.

Because the data set given with this problem is highly irregular and contains very few sampling locations, the predictions of this method may not be entirely accurate, but they are highly superior to most interpolation methods.

As with the previous model, this method cannot detect a spill until it has already entered the water table.

Also, the only obvious method of error analysis is to test more points. The values given are still approximations, and the process of sorting such a large data set is still rather tedious. If such a method were employed from the start of a project and data were collected in a specific and consistent manner, analysis using this model would be relatively simple using the database and the processes described here.

This model can determine whether or not a leak has occurred, approximate the time of the spill, and give an estimated location of the source of the spill. Its greatest advantage is its ability to determine the volume of contaminated area and to model its location underground. When the initial concentrations of chemicals in the leaking liquid are known, this model can also determine the volume of liquid that has leaked.

This model is extremely cost-effective, generating approximate boundaries of a spill based on known information. Successive wells should be drilled at these boundaries to ensure that the spill is in fact accurately predicted by the current information. If new wells detect additional areas of the spill, new boundaries will be generated and the process can be repeated. In either case, unnecessary wells are never drilled once a contaminated area is identified.

Results and Recommendations

New pollution occurred in this region during the testing period between 1990 and 1997. Two separate spills of the same liquid occurred, the first beginning in July 1991 and ending approximately in March 1993, and the second beginning in January 1995 and tapering off about February 1997, although possibly continuing for the remainder of the collection period. These spills originated from the region marked in **Figure 1**.

The spill was composed of the following chemicals which were released into the ground as pollutants: acetone, ammonia, arsenic, barium, bicarbonate, calcium, chloride, iron, lead, magnesium, manganese, nickel, nitrate/nitrite, potassium, sodium, TDS, sulfate, vanadium, and zinc. The total volume of the polluted area by 1997 was approximately 32 million cubic feet. (When the initial concentration of the composite indicator in the liquid that spilled is available, it is possible to determine the total volume of liquid leaked by weighting each datum of a Voronoi polygon and finding the sum of the concentrations, multiplied by the total volume of contaminated area.)



关注数学模型
获取更多资讯

Recommendations for future testing include:

- Identify surface properties to most effectively place the initial monitoring well.
- Test the same chemicals on the same dates at all wells to ensure complete and accurate data.
- Use the information generated by previous wells to predict the borders of the spill and place additional wells along this boundary to minimize the number of test locations needed to accurately determine the size of the spill.
- Determine the rate and direction of flow of the aquifer in which monitoring wells are located to accurately predict the time and location of the pollution source.

References

- Blatt, Harvey. 1997. *Our Geologic Environment*. Upper Saddle River, NJ: Prentice Hall.
- British Columbia Ministry of Environment, Land, and Parks. 1999.
<http://www.env.gov.bc.ca/wat/gws/gwbc/>.
- Flanagan, David. *Java in a Nutshell*. 1996. Sebastopol, CA: O'Reilly and Associates.
- Levy, Stewart, Tamara Munzer, and Mark Phillips. 1996. GeomView—1996.
<http://www.geom.umn.edu/software/download/geomview.html>.
- Sambridge, Malcolm, Jean Braun, and Herbert McQueen. 1995. Geophysical parameterization and interpolation of irregular data using natural neighbours. *Geophysical Journal International* 122: 837–857.
<http://rses.anu.edu.au/geodynamics/nm/SBM95/SBM.html>.
- Sedgewick, Robert. 1988. *Algorithms*. 2nd ed. Reading, MA: Addison-Wesley.
- Soliman, Mostafa M., Philip E. LaMoreaux, Bashir A. Memon, Fakhry A. Assaad, and James W. LaMoreaux. 1997. *Environmental Hydrogeology*. New York: Lewis Publishers.
- Levy, Stewart, , Tamara Munzer, and Mark Phillips. 1996. GeomView—1996.
<http://www.geom.umn.edu/software/download/geomview.html>.
- Todd, David Keith. 1959. *Groundwater Hydrology*. 2nd ed. New York: John Wiley and Sons.
- Walton, William C. 1970. *Groundwater Resource Evaluation*. New York: McGraw Hill.
- Watson, David F. 1992. *Contouring: A Guide to the Analysis and Display of Spatial Data*. New York: Pergamon Press.



关注数学模型
获取更多资讯

Locate the Pollution Source

Shen Quan
 Yang Zhenyu
 He Xiaofei
 Zhejiang University
 Hangzhou, China

Advisor: Zhang Chong

Summary

We develop a model for a strategy to detect new pollution. Three processes govern the movements of pollutants in groundwater: advection, dispersion, and retardation. Information from the wells is used to

- determine the rate and direction of groundwater movement,
- determine the horizontal and vertical extent of the pollutants, and
- analyze the underground structure and characteristics.

Regarding the diversity and complexity of the given data, we employ a two-step data selection to determine the pollutants most likely to cause new pollution during this period of time. We refine the data to choose those chemicals that best represent the variation during this period of time. Then, by using a grid-search algorithm, we write a computer program to simulate the movement process and identify the location and start time of the pollution source. The program is written in C and runs on a PC. Four kinds of new pollution sources are located. The graph resulting from our model is in a good agreement with the given data. Finally, we test parameter sensitivity.

Assumptions

- All soil and aquifer properties are homogeneous and isotropic throughout both the saturated zone and the unsaturated zone.
- The aquifer consists of sand and gravel.

The UMAP Journal 20(3) (1999) 355–368. ©Copyright 1999 by COMAP, Inc. All rights reserved. Permission to make digital or hard copies of part or all of this work for personal or classroom use is granted without fee provided that copies are not made or distributed for profit or commercial advantage and that copies bear this notice. Abstracting with credit is permitted, but copyrights for components of this work owned by others than COMAP must be honored. To copy otherwise, to republish, to post on servers, or to redistribute to lists requires prior permission from COMAP.



关注数学模型
 获取更多资讯

- Steady, uniform water flow occurs only in the vertical direction throughout the unsaturated zone, and only in the horizontal (longitudinal) plane in the saturated zone in the direction of groundwater velocity.
- Physical processes play the greatest role, while the chemical processes are negligible.
- All the parameters describing the characteristic of both zones are constant throughout the monitoring period.
- All the sources of the pollutants are point sources.

Problem One

This problem is to estimate the location and start time of the source, so we consider the movement process of the pollution and the structure of the underground.

Data Analysis and Processing

We assume that there is no interaction between pollutants so that we can process each pollutant separately. With the given data of the coordinate and water level of each well, we plot the water level map by using linear interpolation on the elevations of the monitoring wells, as in **Figure 1**. For simplicity of computation, we assume that all the underground water flows in the same direction.

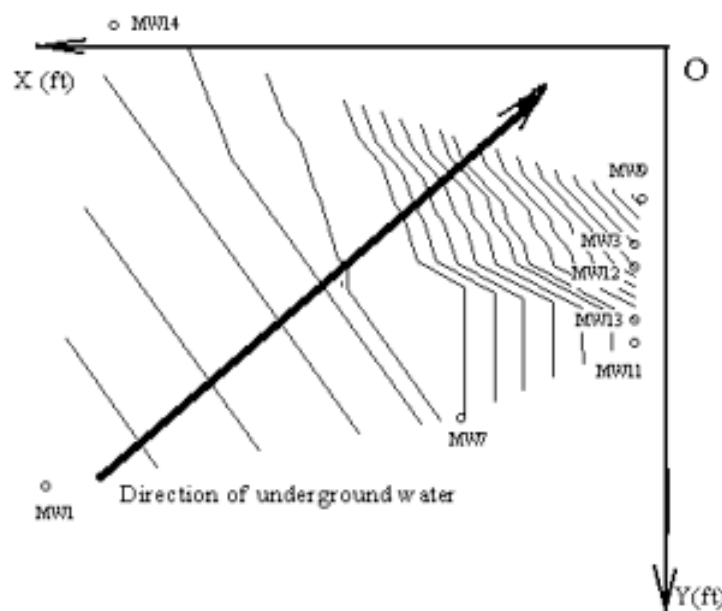


Figure 1. Water-level map.



关注数学模型
获取更多资讯

Data Selection

Because we have thousands of data points about concentration of various pollutants, we must select data carefully. We do this in the following steps:

- Because pollutants are strongly influenced by layers of different permeability, measurements of critical parameters and pollutant concentrations need to be done at intervals over the depth of the aquifer. We need a method for sampling at different depths in an aquifer. By analyzing the data set, we find that almost every pollutant affects only one part of a well (top, middle, or bottom). Thus, for each pollutant we need to consider only the effect on one layer of the well. Furthermore, the data from the bottom of each well (if any) remain constant or nearly so, hence we can neglect such data.
- We delete the data for some pollutants, such as tetrachloroethane, acrolein, benzene, bromomethane, chlorobenzene, cobalt, and so on, because there are hardly any changes in concentrations of these pollutants in each well.
- We think that the pulse fluctuation about the pollutant concentration during a relatively stable period, such as for manganese, is caused by random factors. Thus, we eliminate these pollutants from the data set.
- There is a particular constituent, the CarbonTotalOrganic, whose concentration value decreases significantly, from more than 1000 to less than 1.5. Thus, we eliminate it.
- Now only four pollutants remain: calcium, chloride, magnesium, and TDS.

Reselection

For each remaining pollutant, to accurately reflect the tendency for the concentration to change, we reselect its data as follows:

- For each well, we choose two concentration values for each year, one from the first half of the year and the other from the second half.
- Because we do not know the locations of MW-27 and MW-33 and, moreover, the concentration changes in these two wells are small, we do not consider their data.
- According to the groundwater flow direction, the average concentration value of MW-9 should not be higher than that of MW-3 and MW-12, which contradicts the given data for calcium, chloride, and so on. This is also true for barium. (In 1997, concentrations in MW3M and MW12M vary from 50 to 85, whereas they vary from 80 to 95 in MW9M.) Therefore, we think that MW-9 is a pumping well (**Figure 2**). Thus, we do not use the data from MW-9 in our analysis.

Finally, we list in **Table 1** the data for calcium that we use to calculate the source location.



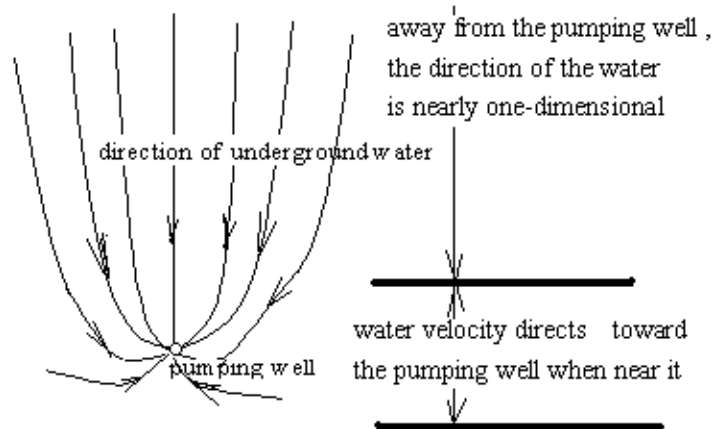


Figure 2. Groundwater movement near a pumping well.

Table 1.
Data for calcium used in the model.

Date	MW-3M	MW-7M	MW-11T	MW-12M
12/7/93	41	50	39	42
3/7/94	42	50	43	47
9/19/94	42	45	41	41
7/10/95	36.5	54.3	44.7	59.5
10/10/95	19.2	53	43.2	54.7
3/6/96	62.4	65.1	50.7	82.4
10/9/96	60.2	61.9	53.3	87.6
3/18/97	63.8	125	53.2	87.6
12/15/97	61.4	115	63.8	88.4

- According to the data, there is some pollutant detected in an early year such as 1990; we name it the *background concentration* (C_b). We think that the later pollutants' concentrations consist of background concentration plus new injected concentration. According to **Figure 1**, MW-1 must be at the headwater level. Moreover, the data from its bottom hardly change during this period according to the data set. Thus, we estimate C_b using data from MW-1B as follows:

$$C_b = \text{arithmetic mean of the concentration value from MW-1B during this period for a certain pollutant}$$

In **Table 2** we collect the symbols used in this paper and their definitions.



Table 2.
Symbols used.

α_L	horizontal dispersion coefficient (m)
α_T	vertical dispersion coefficient (m)
C	pollutant concentration (mg/liter)
C_b	background concentration (described above)
C_0	concentration in the pollutant source (mg/liter)
D	pervasion coefficient (m^2/s)
H	water level (ft)
I	hydraulic gradient
K	hydraulic conductivity (gal/day/ft ²)
L	horizontal distance in the direction of water flow (ft)
m	discharge rate of the pollutant (mg/day)
n	effective porosity
q	discharge rate of the pollutant (liter/day)
R_d	retardation factor
S	compound parameter
t_0	start time of the pollution (yr)
θ	angle between the direction of underground water and the x -axis
V_d	groundwater velocity (ft/day)
W	hantush function
(x_0, y_0)	pollution source coordinate

Model Design

Model Formulation

The movement of pollutants consists of advection, dispersion, and retardation. Furthermore, regarding the large scale of the area, the vertical movement is negligible. Thus, movement of pollutant in the soil (saturated and unsaturated) can be described by the following two-dimensional equation:

$$R_d \frac{\partial C}{\partial t} = V_d \alpha_L \frac{\partial^2 C}{\partial x^2} + V_d \alpha_t \frac{\partial^2 C}{\partial y^2} - V_d \frac{\partial C}{\partial x}. \quad (1)$$

Model Explanation

The model equation applies to steady uniform flow. An analytical solution to the equation can be developed for both continuous (step-function) and pulsed inputs of pollutants as boundary conditions. A step function implies the input of a constant concentration pollutant for an infinite amount of time, while a pulse load is a constant concentration input for a finite amount of time. The terms “infinite” and “finite” are relative to the time frame of the analysis.

We assume that the pollution source is applied as a step function (continuously) with the following boundary conditions:

$$\begin{aligned} C(x, y, 0) &= 0, & (x, y) &\neq (0, 0); \\ C(0, 0, t) &= C_0; \\ C(\pm\infty, y, t) &= C(x, \pm\infty, t) = 0, & t &\geq 0. \end{aligned}$$



Model Solution

The function is a second-order partial differential equation. Equations of this form apply to a wide variety of problems, including mass transport, fluid dynamics, and heat transfer.

For an instantaneous point source at time $t = 0$, there is an analytical solution of the form

$$C(x, y, t) = S \exp\left(\frac{x}{2\alpha_L}\right) [W(0, b) - W(t, b)], \quad (2)$$

where

$$m = C_0 q, \quad S = \frac{m}{4\pi V_d (\alpha_L \alpha_T)^{1/2}},$$

and $W(u, b)$ is the *hantush function*

$$W(u, b) = \int_u^\infty \frac{\exp\left[-y - \frac{b^2}{2y}\right]}{y} dy \quad \text{with} \quad b = \sqrt{\frac{x^2}{4\alpha_L^2} + \frac{y^2}{4\alpha_L \alpha_T}}.$$

Before computing, we classified the parameter used according to our assumptions above:

- During the data processing, the coordination and time of the pollution source are unknown, and so is the value of m . Thus, x_0 , y_0 , t_0 , and S are variable.
- The parameters α_L , α_T , θ , and V_d are constants.

The main task is to find the location and the start time of the pollutants. Hence, we develop a grid-search optimization routine to get an optimized solution:

- We estimate the location of the pollutant source and transform coordinates as follows:
 - Set the point of the pollutant source to be the new origin.
 - Set the new x -axis to be parallel to the direction of the underground water flow.
 - Set the new y -axis to be perpendicular to the new x -axis.
- We construct an equation to calculate the movement of the pollutant under the ground. We calculate the concentration changes in each well and compare with the changes according to the data set. We repeatedly adjust the location of the pollution source, the value S , and the value t_0 (detailed in the following) until there is a satisfactory agreement. The criterion for convergence is the sum of the squares of the residuals between the data and the model predictions. The objective function to be minimized is

$$\sum_i [(C_i - C_b) - C'_i]^2,$$

where C_i is the pollutant concentration data value for well i , C'_i is the model prediction, and C_b is the background pollution level.



Parameter Estimation

We estimate the parameters for the saturated zone as following:

- **Hydraulic Conductivity K :** We consider hydraulic conductivity, measured in gallons per day per square foot, only in the horizontal direction. According to the literature, $K = 265 \text{ gpd}/\text{ft}^2$ ($1 \text{ gpd}/\text{ft}^2 = 4.72 \times 10^{-5} \text{ cm/sec}$).
- **Hydraulic Gradient:** According to **Figure 1**, made by interpolation, we assume that the direction of the underground water is one-dimensional.
- **Ground-Water (Interstitial Pore Water) Velocity V_d :** According to Darcy's Law, V_d is defined as

$$V_d = -KI/n,$$

where I is the hydraulic gradient, K is hydraulic conductivity, and n is effective porosity. We assume that the soil type of the saturated zone is sand with porosity 20%, so we estimate $V_d = 1.5 \text{ ft/day}$.

- **Dispersion Coefficient α :** This coefficient incorporates two forms of dispersive process: dynamic dispersion and molecular diffusion. According to the literature, the horizontal dispersion coefficient and the vertical dispersion coefficient are approximately equal. Both have the estimated value 25 ft.
- **Retardation Factor:** Retardation is based on pollutant characteristics and aquifer composition. Since its effect is not very significant, we estimate $R_d = 1$.
- **Concentration in Pollution Source:** According to the literature, when the water table is usually sufficiently high so that the pollutant directly enters ground water, the C_0 value is the estimate of the source concentration.

Results

There are four new pollutants: calcium, chloride, magnesium, and TDS. The location and the start time for the pollution sources, as predicted by our model, are in **Table 3**.

Table 3.
Source and start time for pollutants.

Pollutant	x -coordinate (ft)	y -coordinate (ft)	Start time (m/d/y)
TDS	7077	6538	8/12/91
Magnesium	6423	7461	1/1/94
Chloride	6931	5823	5/18/91
Calcium	7750	6040	9/1/93

Finally, we mimic the movement process of the pollutant in reverse and compare with the given data set (**Figure 3**). From the graphs, we conclude:



关注数学模型
获取更多资讯

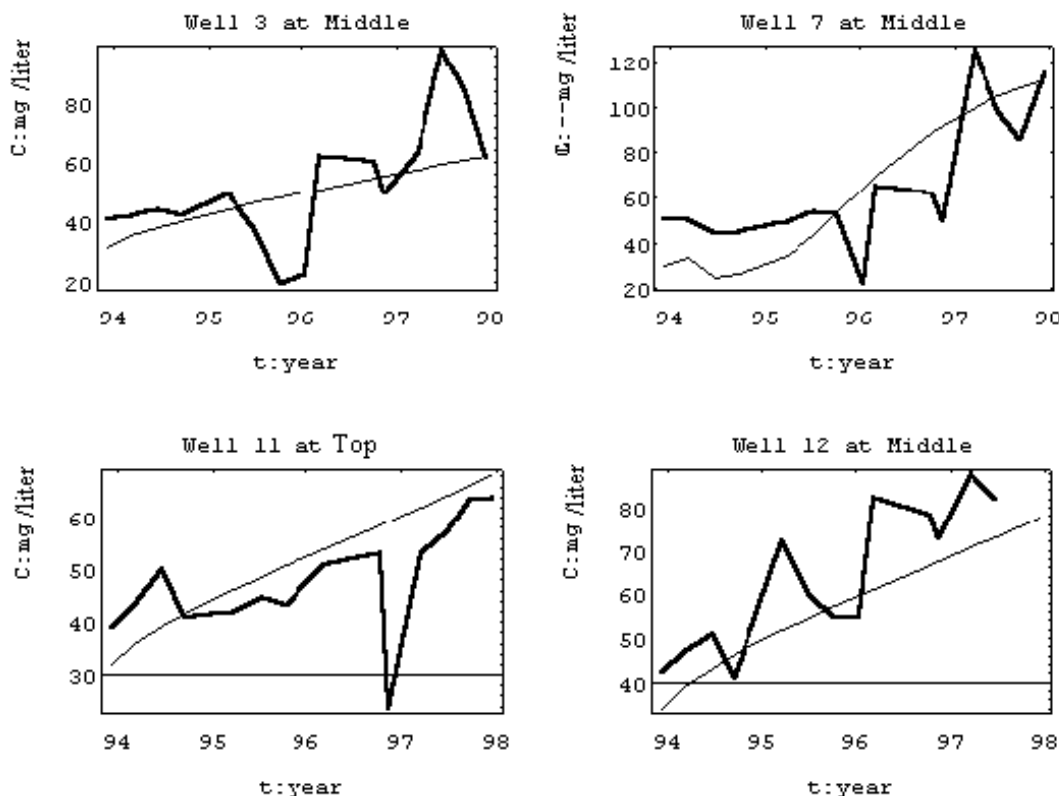


Figure 3. Calcium concentrations at four wells. The thick curves are data, the thin curves are model predictions.

- For near-ideal conditions, the model is suitable; for regular use, a more robust model is desired.
- Even though the two curves do not fit very well, they show a similar change tendency.

Sensitivity Analysis

We conduct a rudimentary sensitivity analysis to explain the stability of our model. We separately vary the values of the constants α_L , α_T , θ , and V_d by 10% and compute the corresponding changes in the values of the location and time of the pollution source (**Table 4**).

The model demonstrates good stability, but θ has a relatively significant influence on the result of the model. Thus, it is reasonable to consider the parameter θ as a variable and repeat our grid-searching algorithm in a five-dimensional space of θ , x_0 , y_0 , t_0 , and S . For calcium, we get the comparative results shown in **Table 5**.

In the expanded model, the value for θ is 7% larger. We think that there is some deflection of the direction of the groundwater flow, as shown in **Figure 4**.



Table 4.
Effects of perturbations of the parameter values.

Parameter	Change in location (ft)	Change in time (yr)
θ	70	0.2
α_L	<10	<0.1
α_T	10	<0.1
V_d	<10	<0.1

Table 5.
Comparison of 4- and 5-dimensional models.

Dimension	θ	x_0 (ft)	y_0 (ft)	t_0 (yr)	S $\times 10^6$
4	0.785	7750	6040	93.75	2.1
5	0.84	7750	6100	93.60	2.2

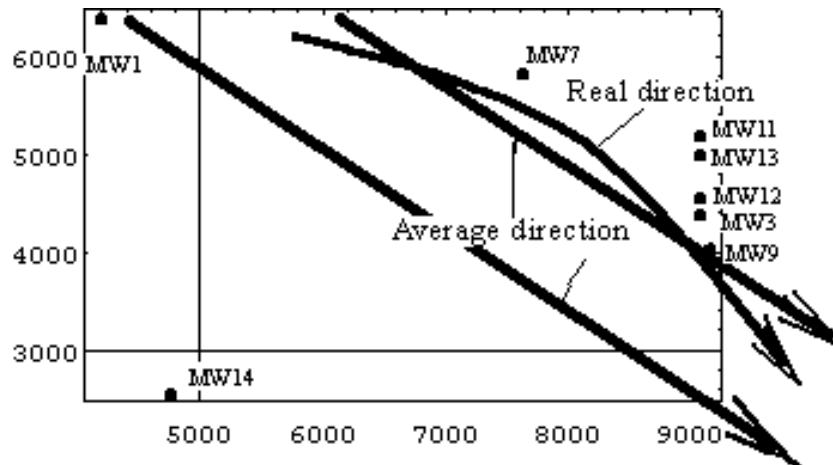


Figure 4. Suspected deflection of groundwater flow.

Problem Two

Local Assumptions

- The storage tanks are located underground in the saturated zone.
- The direction of the groundwater flow remains the same.
- The saturated zone is semi-infinite.
- The leak process is continuous, since the primary cause of leaks in steel underground storage systems is corrosion.



关注数学模型
获取更多资讯

Model Design

To detect the pollutant rapidly and accurately, we develop a three-step method.

- According to the shape and size of the storage and the direction of the groundwater flow, we determine the number and location of the first group of wells. Provided that the storage is a square S m on a side, the number of the first group of wells is $N = S/20$. That is, we drill a well every 20 m in a line perpendicular to the direction of the groundwater, as shown in **Figure 5**. We monitor the data from the wells.

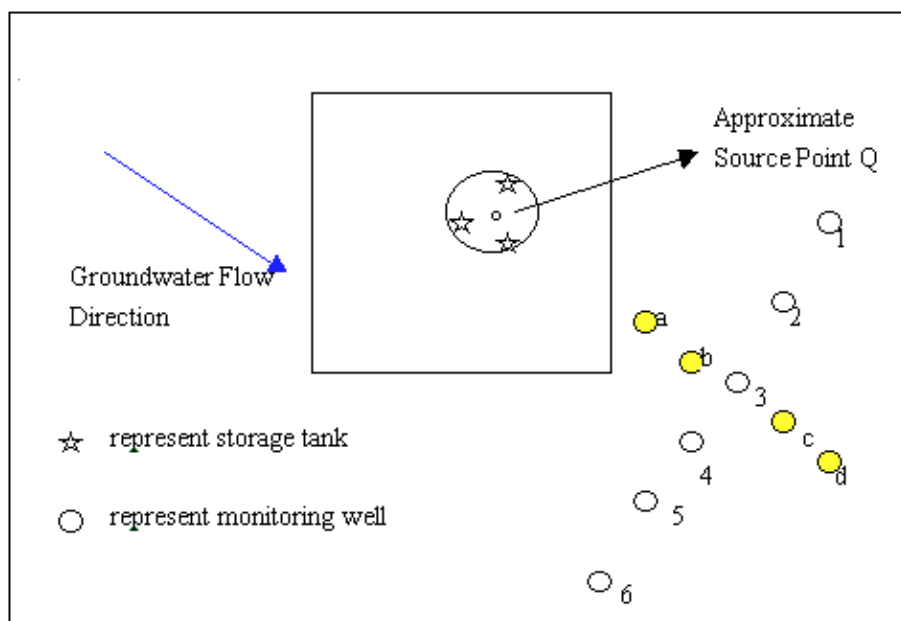


Figure 5. Locations of monitoring wells. Empty circles represent the initial monitoring wells; filled circles are the wells drilled after pollution is detected and found to affect well 3 most of all.

- Once there is some evidence of pollution, we determine which well is most affected by the pollutant. Near this well, we drill a series of wells (perhaps five or more) along the direction of the groundwater flow. Thus, we can construct a three-dimensional formulation to calculate the fluctuation of the pollutant concentration. Here the area occupied by the storage facility may not be very large (with side less than 1000 ft), so we cannot use (1). We employ the three-dimensional equation

$$R_d \frac{\partial C}{\partial t} + V_d \frac{\partial C}{\partial x} = D \left(\frac{\partial^2 C}{\partial x^2} + \frac{\partial^2 C}{\partial y^2} + \frac{\partial^2 C}{\partial z^2} \right) + \frac{m}{n}.$$

Because the leaking is a continuous process, we assume that the pollution



source is applied as a step function (continuously) with boundary conditions

$$\begin{aligned} C(x, y, z, 0) &= 0, \quad (x, y, z) \neq (0, 0, 0), \\ m(x, y, z, t) &= qC_0\delta(x, y, z), \\ C(\pm\infty, y, z, t) &= C(x, \pm\infty, z, t) = C(x, y, \pm\infty, t) = 0, \quad t \geq 0. \end{aligned}$$

For an instantaneous point source at time $t = 0$, this equation possesses an analytical solution of the form

$$\begin{aligned} C(x, y, z, t) &= \frac{R_d q C_0}{8\pi n D r} \exp\left(\frac{V_d}{2D}\right) \\ &\times \left\{ \exp\left(\frac{V_d x}{2D}\right) \operatorname{erfc}\left[\frac{r + V_d t}{2} \left(\frac{R_d}{D_t}\right)^{1/2}\right] \right. \\ &\quad \left. + \exp\left(\frac{-V_d}{2D}\right) \operatorname{erfc}\left[\frac{r - V_d t}{2} \left(\frac{R_d}{D_t}\right)^{1/2}\right] \right\}, \end{aligned}$$

where $r = (x^2 + y^2 + z^2)^{1/2}$.

When $t \rightarrow \infty$, a steady-state equation results:

$$C(x, y, z, t) = \frac{R_d q C_0}{4\pi n D r} \exp\left(\frac{V_d(r - x)}{2D}\right). \quad (3)$$

For convenience, we employ the symbol $C_m(x, y, z, t)$ to represent the right side of the (3).

For constant V_d , R_d , n , q , and D , we can draw an equal-concentration plane with the concentration value $0.01C_0$, as in **Figure 6**.



Figure 6. Large dose.

Let Height be the maximum height of the equal-concentration plane. We transform the Cartesian coordinates in the same way as Problem One.

For a monitoring well at (x, y) and aquifer thickness b , we consider the concentration in the well for three situations:

- If $b \ll \text{Height}$ or $b \ll \text{Size of the storage facility}$, we can transform (3) into a two-dimensional equation like (1).
- If $b \geq \text{Height}/2$, it is reasonable to consider $b = \infty$. Thus, the problem can be simplified. We assume that the substance in the aquifer cannot enter the unsaturated zone except at the source point. Thus, $\partial C / \partial z|_{z=0} = 0$.



Moreover, for every point (x, y, z) under the water table, the concentration is double that depicted by (3) in the case of semi-infinite space:

$$C(x, y, z, t) = 2C_m(x, y, z, t).$$

- Otherwise, for (x, y, z) on the upper or lower surface of the aquifer (see **Figure 7**), we have

$$\frac{\partial C}{\partial z} \Big|_{z=0} = \frac{\partial C}{\partial z} \Big|_{z=-b} = 0.$$

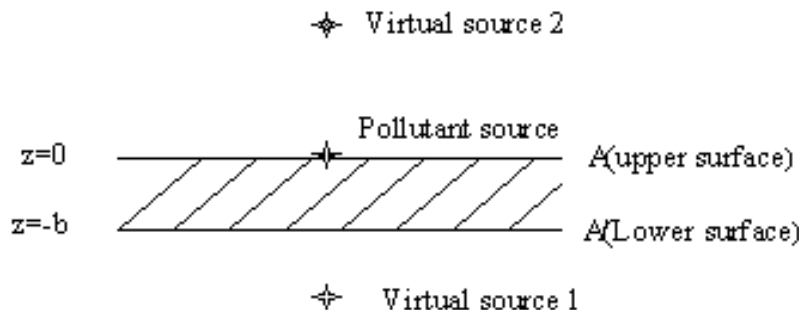


Figure 7. Pollution source on the aquifer .

Draw virtual source 1 symmetric to the pollutant source with the axis being A' (the lower surface). Thus, condition $\frac{\partial C}{\partial z}|_{z=-b} = 0$ is satisfied, while the condition $\frac{\partial C}{\partial z}|_{z=0}$ is not satisfied. In the same way, we draw virtual source 2 symmetric to virtual source 1 with A (the upper surface). Repeating this process, we get virtual source 3, and so on.

The concentration on the upper or lower surface can be considered as the result of accumulation of all the concentration values of all the sources (including the virtual sources). That is,

$$C_t(x, y, z) = 2 \sum_0^{\infty} C_m(x, y, z + 2(-1)^{i+1} \lfloor \frac{i+1}{2} \rfloor b, t).$$

Actually, we need to consider only the former three virtual sources, for the following reasons:

- The distances from these three sources to $A(A')$ are the smallest, so they have the most effect on C_t . Other virtual sources are very far away from $A(A')$ and generally the distance between them is larger than the value Height. Therefore, we neglect these virtual sources.
- The pollutant discharged from the virtual sources far from the surfaces of the aquifer needs a long time to reach the aquifer.

Finally, we transform (3) into

$$C_t(x, y, z) = 2 [C_m(x, y, z, t) + C_m(x, y, z + 2b, t) + C_m(x, y, z - 2b, t)].$$



关注数学模型
获取更多资讯

Thus, we get the final analytical solution of $C(x, y, z, t)$. Then we use the same computer-based method as in Problem One to calculate the approximate location and the time of the pollutant source.

3. In the last step, we draw a circle with center the approximate source point Q and diameter 25 m (or more). Inside this circle, we sample some soil from the surface and analyze its chemical constituents to find the maximum. Thus, we can accurately identify the location of the pollutant source.

Numerical Integration Scheme

To calculate leakage, it is necessary to integrate the values of the dependent variable (C) over space. Unfortunately, the integral of (3) does not possess an analytical representation and must therefore be integrated numerically. We employ a three-dimensional integration scheme for this model. The molar mass (M) of leaked liquid is computed as

$$M = \int \int \int C(x, y, z, t) dx dy dz \approx \sum_{i,j,k} C_{ijk} \delta x \delta y \delta z,$$

where C_{ijk} refers to the computed concentration in “differential” element (i, j, k) . We employ uniform spatial steps of $\delta x = \delta y = \delta z = 1$ m.

A Better Method for Mass Estimation

While processing the data by computer program, we minimize the variance to get a quasi-optimal solution. Meanwhile, we have estimated the m value, so we can compute the molar mass of leaked liquid more conveniently and efficiently as

$$M = mt.$$

Strengths and Weaknesses of the Model

Strengths

- The model has quite good practicality, and the given algorithm has little time complexity. For the given problem size, our C program for the grid-search algorithm runs in less than 2 min on a Pentium-166 computer.
- The model gives good agreement of predicted values and data. It is fast, efficient, and stable.
- As the given data are refined to simplify the computation, the accuracy does not decrease. For illustration, we list data for calcium in **Table 6**.



关注数学模型
获取更多资讯

Table 6.
Effect of refining to simplify computation.

Number of data points	x_0 (ft)	y_0 (ft)	t_0 (years since 1900)
60 (primitive)	7750	6060	93.70
36 (after refining)	7750	6040	93.75

Weaknesses

- If the detected area is not large enough, there is some error. As the distance between the pollution source and the monitoring well grows larger, computation accuracy increases, measurement accuracy decreases, and response time increases.
- To decrease the complexity of the computation, we simplify the groundwater flow net, which may affect the accuracy of the results.
- Not taking statistical factors into our model makes the result of our model not fit the crude data exactly.

References

- Abriola, Linda M., editor. 1989. *Groundwater Contamination*. Wallingford, U.K.: International Association of Hydrological Sciences.
- Barcelona, Michael, Allen Wehrhann, Joseph F. Keely, and Wayne A. Pettyjohn. 1990. *Contamination of Ground Water: Prevention, Assessment, Restoration*. Park Ridge, NJ: Noyes Data Corp.
- Guswa, J.H., W.J. Lyman, A.S. Donigian, T.Y.R. Lo, and E.W. Shanahan. 1984. *Groundwater Contamination and Emergency Response Guide*. Park Ridge, NJ: Noyes.
- Ward, C.H., W. Giger, and P.L. McCarty, editors. 1985. *Ground Water Quality*. New York: Wiley.



关注数学模型
获取更多资讯

Judge's Commentary: The Ground Pollution Papers

David L. Elliott

Visiting Senior Research Scientist
 Institute for Systems Research
 University of Maryland
 College Park, MD 20742
 dellioott@isr.umd.edu

Teams tended to expend more effort on Problem One, and these comments concern that problem. The top papers handled both problems well.

The papers that I saw broke Problem One into several subproblems; assumptions beyond the problem description were needed to attack these, and the best papers made these very explicit with as much justification as possible. The subproblems included:

1. list of “pollutant” species,
2. mathematical model of pollutant transport,
3. detection of time and number of spills, and
4. location of spill sources (using 1–3).

The answers varied greatly, even among the best papers, depending on the assumptions and on the interpretation of the spreadsheet data. The winners

- showed evidence of careful search and interpretation of relevant literature;
- posed the subproblems well, and found mathematical models capable of producing usable answers;
- presented their results in clear, convincing ways; and
- avoided major errors (these seemed often to be due to poor communication among team members!).

The UMAP Journal 20 (3) (1999) 369–370. ©Copyright 1999 by COMAP, Inc. All rights reserved. Permission to make digital or hard copies of part or all of this work for personal or classroom use is granted without fee provided that copies are not made or distributed for profit or commercial advantage and that copies bear this notice. Abstracting with credit is permitted, but copyrights for components of this work owned by others than COMAP must be honored. To copy otherwise, to republish, to post on servers, or to redistribute to lists requires prior permission from COMAP.



关注数学模型
获取更多资讯

The problem statement might well have given at the Web site some description of the site (dump? storage?), description of soil/aquifer types, and other qualitative information that a professional in this field would be given.

The spreadsheet columns are labeled according to assayed chemical species and contain their concentrations in the form of separate time series from several wells and depths. There was little agreement among the contestants as to which species were "pollutants": concentrations for most species (e.g., organochlorides) were negligible, others were non-increasing with time or likely to occur naturally (in rainfall or in soil), and some columns seem to use more than one unit of measurement.

The Outstanding entries are good examples of how different the models could be. The entry from Zhejiang University fits the data to solutions of a simple partial differential equation. Note that the "diffusion" mentioned here is mostly of dynamic origin (percolation, although I did not see that term in any paper I read). Some contestants seem to have considered thermal (Brownian) diffusion important, but it is far too small to be observable in most fluids. The team from Earlham College neglected diffusion but assumed that different species might travel at different rates; this team used time-series graphs to good effect in selecting species to look at and to estimate times.

Other papers had trouble in finding the direction of flow, in putting together diffusion and advection, or in finding a rationale for data selection. Some teams did not find relevant scientific literature that would help in modeling.

About the Author

David L. Elliott is Professor Emeritus of Mathematical Systems at Washington University in St. Louis, and since 1992 has been Visiting Senior Research Scientist at the Institute for Systems Research of the University of Maryland, College Park.

He took his B.A. (Pomona College, 1953) and M.A. (USC, 1959) in Mathematics, and his Ph.D. (UCLA, 1969) in Engineering. After working in control systems and oceanic acoustics at the U.S. Naval Ocean Systems Center, Prof. Elliott taught at UCLA, at Washington University, and as a visitor at Brown University and once more at UCLA. He also served as Program Director for System Theory at the National Science Foundation, 1987–1989. His research has been in nonlinear control theory and applied mathematics (including the kinetics of blood coagulation—he has hemophilia).

He is an IEEE Fellow and member of SIAM, AMS, MAA, and Sigma Xi. He was associate editor for several mathematical journals and edited *Neural Systems for Control* (Academic Press, 1997). His previous association with MCM was as faculty advisor in 1985 and 1986 for Outstanding MCM teams from Washington University.



关注数学模型
获取更多资讯

Author's Commentary: The Outstanding Ground Pollution Papers

Yves Nievergelt

Department of Mathematics, MS 32
 Eastern Washington University
 526 5th Street
 Cheney, WA 99004-2431
yves.nievergelt@mail.ewu.edu

Late on a November night, in the brew pub of an old logging and mining town somewhere in the Wild West, I happened to be sitting near a hydrogeologist. Besides the usual gossip typically heard in such a pub—about the taste of the local brew, the lack of fish in the river, cougars stalking deer in your back yard, and a bear trashing your garbage can in the front yard—the conversation turned to a discussion of a private or public agency that also monitors the geographic area from which the data come.

The data consist of a real, original, unaltered electronic spreadsheet listing measurements of pollutants in wells drilled through the aquifer in an area used by a private or public firm. The data are not only real, they are also significant, which means that someone could suffer or benefit from their analysis and interpretation.

After some discussion, the hydrogeologist granted permission to use the data in the MCM, provided no statement be made containing information that would identify the parties involved.

The two Outstanding teams used two fundamentally different approaches, but each demonstrated an effective understanding of the situation and a strong command of mathematical concepts. Both teams' understanding of the situation enabled them

- not to be overwhelmed by the size of the data file;
- not to be stopped by some of the data file's blank fields or repeated fields;
- not to be hampered by names of unfamiliar chemicals;

The UMAP Journal 20 (3) (1999) 371–372. ©Copyright 1999 by COMAP, Inc. All rights reserved. Permission to make digital or hard copies of part or all of this work for personal or classroom use is granted without fee provided that copies are not made or distributed for profit or commercial advantage and that copies bear this notice. Abstracting with credit is permitted, but copyrights for components of this work owned by others than COMAP must be honored. To copy otherwise, to republish, to post on servers, or to redistribute to lists requires prior permission from COMAP.



关注数学模型
获取更多资讯

- to recognize naturally occurring from potentially polluting chemicals;
- to sort out chemicals with concentrations that seemed nearly constant, nearly random, or potentially revealing of a trend; and
- to locate and use references from the literature and the World Wide Web.

Beyond such an understanding of the problem, the two teams adopted very different mathematical methods of solution.

The team from Zhejiang University used the method of least squares (minimum variance) to fit the parameters of a partial differential equation modeling the physics of advection, dispersion, and retardation: dispersion coefficients, ground water velocity, ground porosity, and the time and location of potential sources of pollution. Their result suggests four spills, near the points with coordinates (7077, 6538) and (6931, 5823) in 1991, and (7750, 6040) and (6423, 7461) near the end of 1993.

The team from Earlham College used Delaunay triangulations and Voronoi polytopes to interpolate concentration gradients and ultimately to detect sudden increases in pollutant concentrations and trace them back to a putative source. Their result suggests two spills, first about 1992 and again about 1996, near the point with coordinates (8000, 4500).

Though the two results differ from each other, they suggest an increase in pollution in the area corresponding to the upper right hand corner of the map $[0, 10000] \times [0, 7000]$. The two teams' papers also contain presentations of their assumptions, models, methods, and results that are quite impressive for a weekend's work.

About the Author

Yves Nievergelt graduated in mathematics from the École Polytechnique Fédérale de Lausanne (Switzerland) in 1976, with concentrations in functional and numerical analysis of PDEs. He obtained a Ph.D. from the University of Washington in 1984, with a dissertation in several complex variables under the guidance of James R. King. He now teaches complex and numerical analysis at Eastern Washington University.

Prof. Nievergelt is an associate editor of *The UMAP Journal*. He is the author of several UMAP Modules, a bibliography of case studies of applications of lower-division mathematics (*The UMAP Journal* 6 (2) (1985): 37–56), and *Mathematics in Business Administration* (Irwin, 1989). His new book is *Wavelets Made Easy* (Birkhäuser, 1999).



关注数学模型
获取更多资讯